MODELLING HYDROLOGICAL RESPONSE TO LAND USE LAND COVER CHANGE AND DEVELOPING BEST MANAGEMENT PRACTICES IN THE GIDABO WATERSHED

Kero Arigaw Adi

A Thesis Submitted to
The Department of Water Resources Engineering
School of Civil Engineering and Architecture

Presented in Partial Fulfillment of the Requirement for the Degree of Master's in Water Resources Engineering (Specialization in Irrigation Engineering)

Office of Graduate Studies
Adama Science and Technology University

August, 2021
Adama, Ethiopia

MODELLING HYDROLOGICAL RESPONSE TO LAND USE LAND COVER CHANGE AND DEVELOPING BEST MANAGEMENT PRACTICES IN THE GIDABO WATERSHED

Kero Arigaw Adi (ID: PGR/162/12)

Advisor
Abdulkerim B. Serur (Ph.D.)

A Thesis Submitted to
The Department of Water Resources Engineering
School of Civil Engineering and Architecture

Presented in Partial Fulfillment of the Requirement for the Degree of Master's in Water Resources Engineering (Specialization in Irrigation Engineering)

Office of Graduate Studies
Adama Science and Technology University

August, 2021
Adama, Ethiopia

APPROVAL SHEET FOR THESIS

I, the advisors of the thesis entitled **"Modelling Hydrological Response to Land Use Land Cover Change and Developing Best Management Practices in the Gidabo watershed"** and developed by Kero Argaw, hereby certify that the recommendation and suggestions made by the board of examiners are appropriately incorporated into the final version of the thesis.

Abdulkerim B. Serur (Ph.D.)		
Name of Advisor	Signature	Date

We, the undersigned, members of the Board of Examiners of the thesis by Kero Arigaw have read and evaluated the thesis entitled **"Modelling Hydrological Response to Land Use Land Cover Change and Developing Best Management Practices in the Gidabo watershed"** and examined the candidate during the open defense. This is, therefore, to certify that the thesis is accepted for partial fulfillment of the requirement of the degree of Master of Science in Water Resource Engineering (Specialization in Irrigation Engineering).

Chair Person	Signature	Date
Internal Examiner	Signature	Date
External Examiner	Signature	Date

Finally, approval and acceptance of the thesis is contingent upon submission of its final copy to the Office of Postgraduate Studies (OPGS) through the Department Graduate Council (DGC) and School Graduate Committee (SGC).

Department Head	Signature	Date
School Dean	Signature	Date
Postgraduate Studies Dean	Signature	Date

DECLARATION

I hereby declare that this Master Thesis entitled **'Modelling Hydrological Response to Land Use Land Cover Change and Developing Best Management Practices in the Gidabo watershed'** is my original work. That is, it has not been submitted for the award of any academic degree, diploma, or certificate in any other university. All sources of materials that are used for this thesis have been duly acknowledged through citation.

Kero Arigaw Adi		
Name of Student	Signature	Date

RECOMMENDATION OF THE ADVISOR

I, the advisor of this thesis, hereby certify that I have read the revised version of the thesis entitled **"Modelling Hydrological Response to Land Use Land Cover Change and Developing Best Management Practices in the Gidabo watershed"** prepared under my guidance by Kero Arigaw submitted in partial fulfillment of the requirements for the degree of Masters of Science in Water Resource Engineering (Specialization in Irrigation Engineering). Therefore, I recommend the submission of the revised version of the thesis to the department following the applicable procedures.

Abdulkerim B. Serur (Ph.D.)		
Name of Advisor	Signature	Date

ACKNOWLEDGMENTS

First and foremost, I would like to thank the Almighty God for his priceless mercy throughout my life and for providing the capability to accomplish this study.

Next, I would like to express my deep and sincere gratitude to my advisor Dr. Abdulkerim Bedewi for his excellent counsel, continuous support, motivation, and patience throughout my MSc. studies. His vast expertise and depth of knowledge helped in all the time of research and writing of this thesis. It was a great privilege and honor to work and study under his guidance. I would also want to express my gratitude to Dr. Dereje Berhanu for his kind technical assistance and support during using the SWAT model and SWAT-CUP.

I wish to extend my special thanks to Adama Science and Technology University (ASTU) for allowing me to take the Master's program in Water Resources Engineering and for financial support to complete this study. I am also very grateful to the National Metrological Agency (NMA) and the Ministry of Water, Irrigation, and Energy (MoWIE) for their support in providing necessary data.

Last but not the least, I would like to thank my family for their love, prayers, caring, and sacrifices for educating and preparing me for my future. It would have been difficult for me to finish my studies without their amazing understanding and encouragement throughout my academic career.

TABLE OF CONTENTS

TABLE OF CONTENTS

TABLE OF CONTENTS

TABLE OF CONTENTS

LIST OF TABLES

LIST OF FIGURES

LIST OF FIGURES

LIST OF TABLES IN THE APPENDIX

LIST OF FIGURES IN THE APPENDIX

ACRONYMS AND ABBREVIATIONS

BMPs	Best Management Practices
CN	Curve Number
DEM	Digital Elevation Model
ENVI	Environment for Visualizing Images
ERDAS	Earth Resource Data Analysis System
ETM	Thematic Mapper
ETM+	Enhanced Thematic Mapper Plus
FAO	Food and Agricultural Organization
GCP	Ground Control Point
GIS	Geographical Information System
GWQ	Groundwater Flow
HRUs	Hydrologic Response Units
LATQ	Lateral Flow
LULC	Land Use Land Cover
m.s.l	Mean Sea Level
MoWIE	Ministry of Water, Irrigation and Energy
MSS	Multispectral Scanner
MUSLE	Modified Universal Soil Loss Equation
NMA	National Meteorological Agency
NSE	Nash-Sutcliffe Efficiency
OLI	Operational Land Imager
PBIAS	Percent Bias
R^2	Coefficient of Determination
RS	Remote Sensing
SCS	Soil Conservation Service
SRTM	Shuttle Radar Topography Mission
SUFI-2	Sequential Uncertainty Fitting Version 2
SURQ	Surface Runoff
SWAT	Soil and Water Assessment Tool
UNESCO	United Nations Educational Scientific and Cultural Organization
UTM	Universal Transverse Mercator

ABSTRACT

Due to the increase in population and socio-economic development, land use land cover (LULC) change is a very important issue considering global dynamics and their responses to water resources. Water resources that can be used for agricultural production, domestic use, and hydropower generation have persistently been affected by both temporal and spatial changes of LULC. However, quantifying the impact of LULC on water resources and developing best management practices (BMPs) is very important for the sustainable use of these resources. The broad objective of this study was to investigate the potential impacts of LULC change on hydrological responses and developing the BMPs that have been paramount to alleviate sedimentation in the study area of the Gidabo watershed in the Rift Valley Lake basin. The LULC change analyses for three periods (1990, 2005, and 2019) were performed using ERDAS Imagine 2014 with a maximum likelihood classifier. The result has shown, the expansion of agricultural land by 8.9% and reduction of forest land and shrubland by 7.11% and 7.53% respectively during the study period. In this study, the Soil and Water Assessment Tool (SWAT) model was used to examine the effects of LULC change on streamflow and sediment yield. The model performance in simulating streamflow and sediment yield was evaluated through sensitivity analysis, calibration, and validation processes. Statistical model performance indicators namely coefficient of determination (R^2), Nash-Sutcliff efficiency (NSE), and percentage bias (PBIAS) were used, and the results indicates a good agreements between simulated and observed values during calibration and validation periods at three stations. Due to LULC changes, changes in streamflow and sediment yield were observed. Accordingly, average annual streamflow was increased by 1.16m^3/s (2.13%) and 2.04 m^3/s (3.62%), *and average annual sediment yield was increased up to 3.45 t/ha/yr (44%) and 7.06 t/ha/yr (47.38%) for the period 1990-2005 and 2005-2019 respectively. Based on the average annual simulated sediment yield using 2019 LULC, the 10 critical sub-watersheds whose annual sediment yield limit ranges above the tolerable limit were identified and prioritized for effective watershed management. Hence, three BMPs namely filter strips, terracing and reforestation were developed for critical sub-watersheds to reduce the sediment yield delivered to the Gidabo dam reservoir. The result revealed the terracing management option reduce the sediment yield up to 64.02%. Implementing filter strips with 5m, 3 m, and 1 m wide indicates 59.12%, 55.97%, and 50.73% reduction respectively whereas, reforestation has given the least reduction that is 40.98%. Therefore, applying terracing in critical sub-basins is the most effective practice for reducing sediment yield in Gidabo watershed.*

Keywords: LULC Change; SWAT Model; Streamflow; Sediment Yield; BMPs; Gidabo watershed

1. INTRODUCTION

1.1 Background

Land use and land cover (LULC) changes are a major concern considering global dynamics and their responses to environmental and socioeconomic factors (Koch et al., 2012). Hydrologic responses to LULC changes and land management practices are the integrated indicators of the watershed conditions (Shawul et al., 2019). LULC changes have potentially large impacts on catchment hydrology and ecological processes which include, evapotranspiration, surface runoff, groundwater flow, streamflow, and sediment yield over a range of temporal and spatial scales (Aghsaei et al., 2020). Due to natural causes as well as anthropogenic actions, the LULC of river basins has undergone multiple modifications and conversions. This change is a global issue in both extent and impacts but, its severity is more pronounced in developing countries in where their large number of human populations depends almost entirely on land and its resources for their daily activities (Moges and Bhat, 2018).

Ethiopia is a country with a high population number in the continent of Africa second to Nigeria, in which 85% of the population lives in rural areas that depend on agriculture and most of them are in highland areas (Bekele et al., 2019). According to Vanlauwe et al. (2014), the highland area of the country is characterized by land degradation and soil erosion with an estimated more than 1.9 billion tons of soil loss in each year with soil loss ranging from 5 to 300 t/ha/yr depending on the land use. The country is endowed with 12 river basins, but rapid population growth, lack of proper land management practice, and increasing conversion of vegetation into agricultural land face serious challenges in simultaneously meeting food requirements and dramatic water demands (Kassa, 2009). Additionally, socio-economic development, expansion of settlement land, and loss of vegetation in highland areas accelerate soil erosion in the watershed which leads the water resources under tremendous pressures and reducing the storage capacity of reservoirs (Adeba et al., 2015).

Soil erosion and sedimentation are sequential phenomena that first occurred upstream of the watershed. Then, due to one of the soil erosion agents that is water, after passing the erosion process, it is deposited at the plain or mouth of the stream channels as sedimentation that affect sustainable water resource planning and management and reservoir life (Abebe and Gebremariam, 2019). Besides, the life expectations of many reservoirs in Ethiopia built for irrigation are threatened by massive sedimentation (Vanmaercke et al., 2010). Gidabo River is passing through Gidabo dam before draining into the Lake Abayya that has been contributing water for Gidabo irrigation project available downstream of Gidabo dam. The dam has been built for the highest and urgent priority to increase food supply by improving and strengthening the agricultural production system in the country. The upstream watershed of the Gidabo reservoir is highly facing massive sedimentation that requires immediate action and integrated watershed management to reduce the siltation problem of the reservoir (MoWIE, 2019). Hence, quantification of LULC change impact at basin and sub-basin scale hydrology is vital to tackle these difficulties in water resources management (Shawul et al., 2019).

In assessing the impact of LULC change on water resource balance, the interaction of Remote Sensing (RS), Geographic Information System (GIS) and hydrologic modeling played a significant role. Hydrologic models can represent the watershed hydrologic process and depend significantly on the accuracy of the input data (Jin et al., 2019). From different hydrological models, physically-based distributed models are efficient in representing physical characteristics and spatial heterogeneity of the watershed (Dwarakish and Ganasri, 2015). Among those models, the Soil and Water Assessment Tool (SWAT) model is the most widely used model around over a long period efficiently for evaluating the impacts of different land management practices on water and sediment yield under complex watersheds with varying land uses, soils, and management conditions (Arnold et al., 2012; Gassman et al., 2007; Getachew and Melesse, 2012).

SWAT has been applied around the world to assess hydrological responses to LULC change with reasonable accuracy. For example, Aghsaei et al. (2020) applied the SWAT model to assess dynamic LULC impact on the hydrological response of a catchment in the Anzali wetland catchment, Gilan, Iran for the period from 1990-2013. They showed that the average annual evapotranspiration, water yield, and sedimentation increased due to the expansion of irrigation agriculture. Also, in Ethiopia Welde and Gebremariam (2017) apply SWAT in Tekeze Dam watershed in the northern part of Ethiopia for the period from 1986-2008. The results of their findings show that the conversion of forest, shrublands, and grassland into cultivated land resulted in an increase in average annual streamflow from 129.20 m^3/s to 137.74 m^3/s (6.20%) and Sediment yield from 12.54 to 15.17 t/ha (17.39%). For such sedimentation problems, Choto and Fetene (2019) designed best management practices for sediment reduction using the SWAT model on Gojeb watershed. They revealed reforestation is a more effective means of watershed management with 32.3% sediment reduction. Additionally, Filter strips have also shown 22.9% and stone bunds 29.4% sediment yield reduction efficiencies. Thus, this study aimed to analyze the impact of spatiotemporal variations of long-term LULC change on the streamflow and sediment yield considering multi-site calibration and validation and developing best management practices in Rift Valley river basin, Gidabo watershed using SWAT model.

1.2 Statement of the Problem

LULC changes have a great impact on natural resources, of which water is the most important one. Due to LULC change, there is an increase in the fluctuation of storage which leads to frequent high water scarcity during high water demand and frequent flooding in the rainy season. The impacts of land cover changes on water resource systems vary from place to place, depending on site-specific factors which are still continuous issues that need further research (Bewket and Sterk, 2005; Koch et al., 2012; Shawul et al., 2019). Hence, there is a need for empirical investigations into the problem.

Ethiopia is endowed with a substantial amount of water resources that can help for agricultural production, domestic use, and hydropower generation have persistently been affected by both temporal and spatial change of LULC. Previous studies on the effects of LULC dynamics Ethiopian on watershed hydrological responses summarized by Negese (2021) revealed a decreasing trend in dry average monthly flow, groundwater flow and recharge, and evapotranspiration and an increasing trend in surface runoff, mean wet monthly flow, mean annual streamflow and mean annual sediment yield due to significant loss of forest cover and shrublands and expansion of agricultural lands.

The Gidabo dam built across Gidabo river is 14.5 m tall and has a 15,000 ha irrigation potential but upstream of the watershed has been experiencing LULC change and land degradation over the past decades due to increasing population, conversion of forest, bushes, and shrubland into cultivation and settlements (MoWIE, 2019). Currently, the population of catchments is over 1.5 million and increased by 33.3% in the last decades (Wolde et al., 2021). Increased population and the socio-economic developments in the watershed exert pressure on LULC changes and consequently result in declining water and food potential in the catchment (Elias et al., 2019). The watershed is also facing high erosion and land degradation due to intense rainfall and anthropogenic activities in the watershed which resulting in a significant reduction of Gidabo dam capacity. This problem is supposed to be alleviated through developing best management practices in effective and efficient ways. Therefore, modeling LULC change impacts on hydrological responses and developing best management practices have been paramount to alleviate sedimentation issues in the study area of Gidabo watershed.

1.3 Objectives of the Study

1.3.1 General objective

The general objective of this study was to investigate the potential impacts of LULC change on hydrologic responses and developing best management practices in the study area of Gidabo watershed.

1.3.2 Specific objectives

To achieve the general objectives of this study, the following four specific objectives were formulated.

- ❖ To assess spatiotemporal variations of LULC change of Gidabo watershed (1990 to 2019)
- ❖ To evaluate the performance of the SWAT hydrologic model in simulating streamflow and sediment yield in the Gidabo watershed
- ❖ To assess the LULC impact on streamflow and sediment yield
- ❖ To develop best watershed management practices to alleviate sedimentation issues in the Gidabo dam

1.4 Research Questions

The following four research questions were formulated to achieve the specific objectives these study.

- ❖ How spatiotemporal variations of LULC change look like in the study area?
- ❖ How well SWAT hydrologic model performs in simulating streamflow and sediment yield in the Gidabo watershed?
- ❖ How streamflow and sediment yield responds under changing LULC over the study area?
- ❖ Which management practice is the best to alleviate sedimentation problem in the Gidabo watershed

1.5 Significance of the Study

LULC has a profound impact on the functioning of socioeconomic and environmental systems, with considerable tradeoffs for sustainability, food security, biodiversity, and people's and ecosystem's vulnerability to global change consequences (Kassa, 2009; Wolde et al., 2021). In Ethiopia, most parts of the regions face threats concerning food production that mostly affects the rural livelihood mainly due to an increase in population on one hand and inappropriate resource management on the other hand. However, there is no systematic research on techniques that deal with impact analysis of LULC and hydrological regime at a watershed level and sub-watershed level at the study area in particular. Hence, the knowledge of how LULC influences streamflow and sediment yield will enable policymakers and planners to formulate watershed management actions to minimize the adverse effect of future land-use changes on streamflow and sediment yield. Besides, it is important to have a good understanding of the effect of historic LULC on hydrologic response to predict the future LULC change effects on water resources. This study will play its role by providing important information on LULC change and its impact on the streamflow and sediment yield as well as the best watershed management practices to alleviate sediment yield entering into Gidabo dam.

1.6 Scope and Limitation of the Study

This study is focused on determining the impact of LULC on the streamflow and sediment yield due to historic LULC change in the Gidabo watershed. It also includes identifying the best management practice to minimize sediment production in the dam watershed. The catchment lies approximately between 38°10'00" to 38°40'00"E longitude and 6°10'00" to 6° 60' 00" N latitude with a drain area of about 2378 km^2. An approach, based on land surface features mainly responsible for erosion, which includes slope and soil type is also used in this study by dividing the catchment into sub-watersheds to assess the sub-watersheds contributing maximum sediments to the reservoir. This was achieved through a method that combines GIS and RS techniques to analyze the LULC change and hydrological model (SWAT) to simulate the hydrological processes. But, this study is limited from investigating future LULC changes on the hydrologic responses. The other limitation of this study is even though the LULC change significantly affects the hydrologic process but it is not the only factor. These factors are not taken into account.

1.7 Thesis Organization

This thesis was organized into five main chapters. The introduction is the first chapter that contains the background of the study that provides the overview of the study carried out. It also provides information on the problems experienced in the study area in light of the changing LULC (study problem). Furthermore, the objectives, significance, and scope/limitation of the study were discussed. The second chapter (literature review) emphasizes a detailed explanation of the LULC change concept and fundamental causes leading to LULC change. It also contains the application of RS and GIS on LULC change analysis and some of LULC change studies carried out globally as well as in Ethiopia. Additionally, the hydrological responses to LULC change, SWAT model theoretical concept and its application, and best management practices to alleviate sediment yield were reviewed in detail. The third chapter (materials and methods) describes a brief description of the study area, materials and software used, required data preparation as well as data quality analysis and step-by-step methodology adopted to accomplish the whole objectives of the study. The fourth chapter explains the results of the study focusing on the research objectives with the discussion of previous related works. Finally, in the under fifth chapter, conclusions and recommendations are provided.

2. LITERATURE REVIEW

In this chapter, important concepts of LULC change and fundamental causes leading to LULC change, RS and GIS application in LULC analysis, and previous research works related to LULC change were reviewed. Additionally, hydrological responses to LULC change, hydrological models especially the SWAT model concept and its application, and BMPs to alleviate sediment yield were explained in detail.

2.1 Land Use Land Cover Change

Land cover describes the physical properties of the earth's surface as expressed in the distribution of flora, water, soil, and other physical aspects, whereas land use describes how the land has been used by humans and their habitats, such as agriculture, settlements, and industry (Kaul and Sopan, 2012). Land use and land cover are two discrete terms that are often used by one another. For example, settlement is cover but if buildings are included whether it is being used for residence or industrial activity, it shows the land use component. The discrete depiction of land cover has advantages in terms of concision and clarity, but it has led to an overemphasis on land-cover conversions and neglect of land-cover modification. Land-cover conversions are defined as the total shift of one land-cover category to another due to agricultural increase, deforestation, or urban expansion. Land-cover modifications are more subtle changes that affect the character of the land cover without changing its overall classification (Lambin et al., 2003).

People's use of land resources varies depending on the applications for which it is used, such as food production, shelter, recreation, material extraction and processing, and the biophysical qualities of the land (Parveen et al., 2018). Land-use change is always caused by multiple interacting factors originating from different levels of organization of the coupled human-environment systems (Kassa, 2009). The mix of driving forces of land-use change varies in time and space, according to specific human-environment conditions. Lambin et al. (2003) described fundamental causes leading to land-use change as endogenous and exogenous. The fundamental causes leading to land-use change are mostly endogenous, such as resource scarcity, increased vulnerability, and changes in social organization, even though they may be influenced by exogenous factors as well. The other high-level causes, such as changing market opportunities and policy intervention, are mostly exogenous, even though the response of land managers to these external forces is strongly mediated by local factors.

Analyses of the causes of land-use change have moved from simplistic single-cause explanations to an understanding that integrates multiple causes and their complex interactions over the last years. Humans have always modified land to gain the necessities for living, but the rate of exploitation was not as high as it is today (Parveen et al., 2018). The estimated historical LULC changes at global scales from 1700 to 1990s revealed that cropland increased 300-400 million ha to 1500-1800 million ha, pasture increased from 500 million ha to around 3100 million ha, forest area decreased from 5000-6200 million ha to 4300-5300 million ha, and steppes, grassland, and shrubland experienced a decline around 3200 million ha to 1800-2700 million (Lambin et al., 2003).

Recently the LULC change is not the same as before. The 20th century has witnessed an acceleration of the pace and intensity of land-cover change. Since the 1960s, spurred in part by the Green Revolution, a shift in land-use practices toward agricultural intensification has been observed. Indeed, between 1961 and 2002, while cropland areas increased by only 15%, irrigated areas doubled, world fertilizer consumption increased 4.5 times, and the number of tractors used in agriculture increased 2.4 times. These drivers of land-cover change during the 20th century have been modulated by rapid and pervasive globalization (Ramankutty et al., 2006). Like the rest of the world, East Africa is not an exception to these dynamics. According to Guzha et al. (2018), natural forests have been lost to human settlements, urban areas, croplands, and grazing pastures in the East African region due to LULC. This forest cover has decreased annually by about 1% while the human population increased at an average annual rate of 2% between 1990 and 2015.

At global, regional, and local scales, the current high rate of LULC dynamics has resulted in unprecedented changes in ecosystems and environmental processes. LULC dynamics are a key landscape process that can affect water, sediment, pollutants, and energy flows. Furthermore, the impact of land use on water resource availability is high. According to Choubin et al. (2019), sediment detachment and transport tend to accelerate in degraded watersheds due to increasing overland flow by reducing soil moisture content and groundwater recharge. Recently, monitoring and mitigating the negative impact of LULC change has become a major priority of scholars, decision-makers, and policymakers around the world (Erle and Pontius, 2007).

2.2 Application of RS and GIS for Land Use Land Cover Analysis

Digital change detection is the process that helps in determining the changes associated with land use and land cover properties concerning geo-registered multi-temporal remote sensing data. From the mid-1970s to the present, remote sensing has played a significant role in tracking actual changes in land use and land cover on global and regional scales (Lambin et al., 2003). Remote sensing is a powerful tool in deriving and providing accurate and timely information on the spatial distribution of LULC dynamics over large areas. The use of satellite data in conjunction with GIS to aid in interpretation is a recent trend that aims to take advantage of the growing amount of accessible geographical data (Mallupattu and Reddy, 2013).

Remote sensing imagery is the most important data resource of GIS. For change detection, GIS provides a framework for gathering, storing, analyzing, and displaying digital data. The recognition of synoptic data of the earth's surface through time is done using satellite images (Maina et al., 2020). Since 1972, continual global coverage at moderate to high resolution the Landsat data such as Landsat Multispectral Scanner (MSS), Thematic Mapper (TM), Enhanced Thematic Mapper Plus (ETM+), and Landsat-8 Operational Land Imager (OLI) has been usually used for LULC change analysis. In general, the goal of the change detection procedure is to identify LULC changes using satellite images that occur between two or more dates (Muttitanon and Tripathi, 2005).

According to the modified United Nations Educational Scientific and Cultural Organization (UNESCO, 1976) classifications scheme, there are only about 157 different land cover types and no study site will have all of those different land cover types. Hence, it will be necessary to group pixels into a smaller number of closely related classes based on spectral similarity through the process known as Classification (Oumer, 2009). There are two major approaches (supervised and unsupervised classification) to the classification of remotely sensed images for various applications.

In supervised classification, the software is trained to recognize that certain types of pixels represent specific land cover types. In this approach, prior knowledge of the area and information gathered during fieldwork are important inputs used by the software to classify the pixels into similar groups based on sample signatures identified. In unsupervised classification, the desired number of groups or clusters will be inputted into the software (Oumer, 2009). The software then groups the pixels according to similar spectral characteristics in order of decreasing brightness. These groupings are not made based on land cover, but on the similarity in spectral characteristics of the pixels. It is also common to come across a third approach known to be a hybrid classification that combines both supervised and unsupervised classification techniques.

Following image classification, an accuracy assessment is conducted to determine the level of classification acceptance and the process of change detection. Accuracy assessment is a term used for comparing the classified to ground data that are believed to be correct to determine the classification process's accuracy. The accuracy of classification is commonly examined by comparing the classification with some reference data that reflects the true land cover at the ground. A standard accuracy assessment procedure for baseline land cover products involves the use of the error matrix and the standard procedure for one-point-in-time land cover products can be extremely difficult to apply to multi-temporal change analysis products. As a result, accuracy evaluation is usually analyzed to the most recent image that serves as a reference, with ground control points (ground truth) captured as part of the data required for change analysis (Maina et al., 2020).

2.3 Land Use Land Cover Change in Ethiopia

Change of land use land cover (LULC) is a dynamic and complex process that is influenced by several interconnected processes ranging from environmental variables to socioeconomic dynamics and has a significant impact on the functions, dynamics, and structures of most landscapes (Yesuph and Dagnew, 2019). In the highlands of Ethiopia, favorable agricultural and climatic conditions have attracted human settlers to occupy all suitable agricultural areas over the past several centuries. As a result, agriculture eventually moved from gently sloping lands in the highlands to steeper sloping lands on the plateau's swampy flat plains, with the removal of forests and other vegetation covers (Esa et al., 2018). Many studies that have been conducted in different parts of the Ethiopian highlands have shown that there were considerable LULC changes in the country.

Zeleke and Hurni (2001) in their study reported that natural forest cover was declined from 27% in 1957 to 2% in 1982 and 0.3% in 1995 in Northwestern Ethiopian Highlands. On the contrary, cultivated land increased from 39% in 1957 to 70% in 1982 and 77% in 1995. Oumer (2009) also conducted a comparative study on the LULC change in Lenche

Dima (Gubalafto district) and Kuhar Michael (Fogera district in the Lake Tana basin) of the Amhara National Regional State for the time frame between 1972/3 to 2005. The result shown in Kuhar Michael, dense shrub/bushland decreased at an annual rate of -0.1%, while open shrub/bushland increased at a rate of 0.3%. As opposed to this, dense shrub/bushland increased at a rate of 0.2% and open shrub/bushland declined at an annual rate of -0.2% in Lenche Dima. Grassland showed a net decrease at a rate of -0.3% in Kuhar Michael due to conversion into cultivated lands, while an increase with an annual rate of 0.1% is found in Lenche Dima as a result of the implementation of watershed management practices.

Yesuf et al. (2015) identified the spatiotemporal LULC changes across the lake Hayq closed drainage basin in northeast Ethiopia over 50 years from 1957-2007. They indicated that farmlands/settlements and shrublands/degraded lands increased by 43.1% and 136.9%, at an annual rate of 27.4 and 13.5 ha/yr respectively between 1957 and 2007. In contrast, bushlands, grasslands, forestlands, and lake surface area were diminished by 68.8%, 62.7%, 90.5%, and 7.6%, at a rate of 24.0, 7.6, 6.1, and 3.7 ha year/ respectively, over the five decades. Recently, Yesuph and Dagnew (2019) conducted their study at Beshillo watershed of the Blue Nile basin in the North-Eastern highlands of Ethiopia for the period 1973 to 2017. They identified seven major LULC classes, and the study's overall scenario indicates that the watershed has had highly noticeable LULC shifts in the past, which are likely to be continuing in the future due to ongoing anthropogenic activities and natural forces.

The study concludes that, while all land use types changed, the most significant shift was a constant increase of farmland/settlements regions, primarily at the expense of Afro/sub-Afro alpine vegetation areas. On the contrary, Afro/sub-Afro alpine vegetation showed a consistent net loss over the study of periods as it significantly shrank from 19.8% of the total watershed area in 1973 to 14.7% in 2017, mainly as the result of an expansion of the cropland, built-up area, and grazing land. Additionally, Dibaba et al. (2020) show that Finchaa Catchment in Northwestern Ethiopia has undergone significant LULC change since 1987. Between 1987 and 2017, cropland, urban and built-up areas increased while rangeland, grazing lands, and swampy area decreased.

According to many works of literature, LULC and socioeconomic dynamics have a strong relationship. As the population grows, so does the demand for cultivated land, grazing land, and fuelwood; settlement areas expand to meet the rising demand for food and energy, and livestock populations grow (Kassa, 2009). The interaction of biophysical, socioeconomic, and institutional forces ultimately drove LULC transformations, according to Yesuph and Dagnew (2019). Zeleke and Hurni (2001) also reported population pressure has been found to harm natural forest cover in Dembecha Woreda north-western Ethiopia. Bekele et al. (2019) pointed out that population pressure was the main cause for the expansion of farmland, settlements, and significant shrinking of grassland in Keleta watershed in Awash River basin. Hence, most of the empirical evidence indicated that population number increase has a paramount impact on the environment.

2.4 Impact of Land Use Land Cover Change on Streamflow

Many studies have found that land use land cover change has an undesirable and significant global ecological trend that impacts the quantity of water available. At the basin and sub-basin level, LULC has a significant impact on the streamflow response. These changes may have immediate and long-term effects on terrestrial hydrology. An annihilative land-use change can alter the long-term water balance between rainfall and runoff, as well as the hydrological cycle in the short term either by increasing water yield or in some cases by reducing or even eliminating low flow (Abraham and Nadew, 2018).

Mao and Cherkauer (2009) indicated in their study, water resource was affected through the conversion of forest land and grasslands to farmlands by human activities in the Upper Midwestern United States. Zhang and Ross (2015) also investigated the potential link between LULC and streamflow as a result of mining activities. The study elucidated that the mining-affected basins experienced a tremendous increase in streamflow; necessitates the implementation of reclamation schemes to improve the hydrological condition of the basin.

The impacts of land-use change on hydrological conditions of the Andassa watershed, Blue Nile Basin in Ethiopia were investigated by Gashaw et al. (2018) for the period 1985-2015. They reported the increase of annual streamflow (2.2%), wet seasonal streamflow (4.6%), surface runoff (9.3%), and water yield (2.4%) while the decrease of dry season streamflow (2.8%), lateral flow (5.7%), ground water flow (7.8%) and ET (0.3%) due to a continuous expansion of cultivated land and built-up area, and reduction of forest, shrubland, and grassland during their study period. In the Upper Awash Basin, Shawul et al. (2019) found the transition from indigenous forest, shrubland, and pasture to cultivation and urban land resulted in a relatively significant increase in surface runoff and total water yield, but also a decreasing trend in evapotranspiration, lateral flow, and groundwater flow. A better understanding of basin hydrology and the relationship between land-use change and relative variation in water balance and associated water distribution is helpful to watershed planners and decision-makers (Wang et al., 2012).

2.5 Impact of Land Use Land Cover Change on Sediment Yield

Natural weathering of rocks and soils, agricultural and urban development-induced increased erosion of lands, streams, and shorelines, and suspension of previously eroded particles deposited in stream corridors are all sources of sediment. Vegetation cover is well recognized as a key factor in drainage basin erosion and sediment production. Vegetation and land use are important factors in respect to the hydrology and sediment production of catchments because they are more dynamic than many other factors, with short seasonal changes as well as long-term land use management changes (Thornes, 1990).

In Gojeb Watershed Omo-Gibe basin, Choto and Fetene (2019) shown a significant land use cover change implied a change in the amount of sediment yield in the watershed. As a result, the sediment yield was increased from year to year during the 31 years due to the conversion of shrublands and grasslands to agricultural. Over 31 years period (1985-2015) an increase of cultivated land by 14.97% resulted in an increase of sediment yield by 41.07 t/km^2. Similarly in the Guder subwatershed, Blue Nile basin of Ethiopia, Kidane et al. (2019) reported the expansion of cultivated land at the expense of forest and shrubland increased the mean rate of soil erosion from 25.8 t/ha/yr in 1973 to 28.7 t/ha/yr in 1995 and 30.3 t/ha/yr in 2015, as well as total soil loss from 198 million t/yr in 1973 to 221 million t/yr in 2015. Hence, sediment yield has shown a direct relationship with reduction of vegetation cover and expansion of cultivated land as a result it increased from year to year.

2.6 Hydrologic Models

2.6.1 Hydrologic model concepts

Modeling is the process of organizing, synthesizing, and integrating parts into a realistic representation of the prototype. Hydrological models are tools that integrate our knowledge of hydrologic systems to simulate real-world hydrologic processes. These models comprise a set of mathematical descriptions of portions of the hydrologic cycle and they are based on a set of interrelated equations that try to convert the physical laws which govern extremely complex natural phenomena to abstract mathematical forms (Kassa, 2009).

Watershed hydrologic models have been developed for many different reasons and therefore have many different forms. They are, however, primarily intended to achieve one of the two basic goals. The one aim of watershed modeling is to get a better understanding of a watershed's hydrologic processes and how changes in the watershed may affect these phenomena. Another aim of watershed modeling is to create synthetic hydrologic data sequences for facility design or forecasts. They are also providing valuable information for studying the potential impacts of changes in land use or climate. The variety of uses and the rapid increase both in scientific understanding and in technical support, from data collection systems and computer technology, have produced an enormous range in levels of sophistication.

2.6.2 Classification of hydrologic models

Hydrological models vary in ways of the time step, spatial scale, whether the model simulates single events or continuously, and how different hydrological components are computed. According to Dwarakish and Ganasri (2015), watershed-scale models are further divided into lumped, semi-distributed, and fully distributed models based on their spatial distribution. The lumped modeling approach treats a watershed as a single unit for computations by averaging watershed parameters and variables over a single unit. Semi-distributed models divide the entire watershed into HRUs or sub-basins, whereas spatially variability is represented by grids in distributed models. Comparatively, semi-distributed and distributed models account for the spatial variability of hydrologic processes, input, boundary conditions, and watershed characteristics better than lumped models (Elfert and Bormann, 2010).

The models can be characterized as stochastic, deterministic, and mixed depending on how the hydrological processes are represented. The outcome of a deterministic model is exactly specified by known relationships between states and events with leaving no space for random variation. In such models, two equal sets of model input run always yield the same output under identical conditions. On the other hand, if a model has at least one component of random character which is not explicit in the model input, but only implicit or hidden it is called a stochastic model. If the model components are described by a mix of deterministic and stochastic components, the model is called a stochastic-deterministic or hybrid model (Kassa, 2009).

The hydrological models can also be classified according to whether the hydrological processes are described as conceptual, empirical, or fully physically based. Empirical models are used to establish a relationship between rainfall and runoff to predict runoff in different catchments (Chen et al., 2013; Shirke et al., 2012). Empirical models contain no physical transformation function to relate input to output; such models usually build a relationship between input and output based on hydro-meteorological data (Sarkar and Kumar, 2012). Physical processes such as subsurface flow, surface runoff, and infiltration in the watershed are not explicitly considered in empirical models, which is a major limitation. Furthermore, these numerical models are incapable of modeling the impact of vegetation changes on various hydrological components (Dwarakish and Ganasri, 2015).

Conceptual models are used for simplifications of the complex processes of a catchment. The particular components of these models often have to be described by empirical functions based on the observation of certain processes. Physically-based distributed models, on the other hand, can explicitly represent the spatial variability of important land surface characteristics including topographic elevation, slope, aspect, vegetation, and soil, as well as climatic parameters such as precipitation, temperature, and evapotranspiration distribution (Akbari and Singh, 2012).

2.6.3 Guidelines for model selection

While choosing a model for a specific application, it is important to consider its applicability to simulate and also prediction performance. The model functionality and complexity can become major criteria in model selection. In terms of hydrologic process representation, the model functionality differs due to the equations adopted to simulate the processes and model discretization. On other hand, the estimated data, resources, time, and cost required to parameterize and calibrate a model, as well as the professional judgment and experience required to operate these models, can be used to describe model complexity (Dwarakish and Ganasri, 2015).

In particular, it’s necessary to identify the simplest model that will yield adequate accuracy, bearing in mind that model complexity is not synonymous with the accuracy of the results, that the model has to be characterized by flexibility, by the possibility of making it applicable under various spatial and temporal conditions and that increased accuracy has to be worth the increased effort (Kassa, 2009). The selection of a model is a key aspect in obtaining satisfactory answers to a given problem. Numerous hydrological models are currently being used to simulate the hydrological process at various geographical and temporal dimensions.

Because each project has its own set of objectives and needs, the majority of the criteria are project-specific. According to Cunderlik (2003), four fundamental selection criteria must be considered based on the specific purpose of the project. These are (i) required model outputs relevant for the required purpose and thus to be estimated by the model, which questions whether the model forecasts the variables required by the project, such as peak flow, event volume, and hydrograph, long-term flows, (ii) hydrologic processes that needed to accurately predict the intended outputs using the model, raising the question of whether the model can simulate controlled reservoir operation, single event, or continuous processes, (iii) availability of input data, which questions if all of the model's inputs can be available within the project's time and cost limits, (iv) cost of the project, which questions the investment is justifiable in the context of the project's objectives or not.

2.7 Soil and Water Assessment Tool Model

The Soil and Water Assessment Tool (SWAT) model was developed by the US Department of Agriculture Research Service (USDA-ARS). SWAT is a physically-based, semi-distributed, basin-scale, daily time step, and conceptual model that operates on a continuous-time step. Furthermore, it is a watershed scale physically-based model that functions on a daily time step (Neitsch et al., 2011). SWAT is designed to predict the impact of climate, land use, and management practices on water, sediment, and agricultural chemical yields in gauged and ungauged watersheds on a daily time step. The model is process-oriented, computationally efficient, and has capable of long-term simulation which has acquired widespread popularity in recent years as a reliable transdisciplinary watershed modeling tool (Neitsch et al., 2012).

SWAT has become recognized as a multifunctional model that can be used to integrate various environmental processes to enable more effective watershed management and the generation of better-informed policy decisions all over the world (Gassman et al., 2007). An interesting aspect of SWAT is the ongoing development that is taking place, with contributions coming from different groups, in different parts of the world. SWAT also provides several options for calculating runoff and evapotranspiration, each with its own set of input data requirements. Many studies approve that the SWAT model's applicability to Ethiopian situations at different topography, watersheds, and basin-scale, as well as evaluation of the impact of climate change on hydrology. The review of studies (for instance, Kassa, 2009; Getachew and Melesse, 2012; Welde and Gebremariam, 2017; Shawul et al., 2019; Choto and Fetene, 2019) indicated that the model is capable of simulating hydrological processes with reasonable accuracy.

A watershed is divided into multiple sub-watersheds in SWAT, which are subsequently subdivided into hydrologic response units (HRUs) with homogenous land use, management, topographical, and soil characteristics. Within a SWAT simulation, the HRUs are represented as a percentage of the sub-watershed area and may or may not be contiguous or physically identifiable. Alternatively, a watershed can be subdivided into sub-watersheds that are characterized by dominant land use, soil type, and management.

2.8 Best Management Practices to Alleviate Sediment Yield

Assessing sediment yield and identifying hotspot areas play a significant role in reducing sediment loadings to the dam watershed and implementing sustainable watershed management of the watershed (Tesema and Leta, 2020). The absence of such management in watersheds can lead to widespread soil erosion and siltation of the reservoir that can reduce the useful life of the dam scheme (Nadew et al., 2019). For effective and efficient implementation of watershed management practices, identification of sediment-prone areas is important. Watershed prioritization is thus the ranking of different critical sub-basins of a watershed according to the order in which they have to be taken up for treatment and soil conservation measures (Choto and Fetene, 2019). Implementing a suite of best management practices (BMPs) is needed to mitigate significant erosion from the upper catchment and reduce the sediment delivered to the reservoir to extend the reservoir's life span.

Agricultural and structural-based BMPs are commonly used for reducing soil loss within the critical sediment parts of the watershed (Uniyal et al., 2020). Agricultural BMPs are referred to as the practices that are implemented within the agricultural field by the farmers. Contour farming is one of the many soil solutions that are considered agricultural BMPs to reduce surface runoff by intercepting and reducing the runoff velocity. It consists of performing field operations like tilling, planting, and harvesting, etc. along the contour.

This BMP effectively reduces the erosive power of surface runoff and prevents or minimizes the development of rills and sheet erosion. Conservational tillage is another agricultural BMP that facilitates sediment setting by reducing runoff velocity and helps in soil moisture conservation. Structural BMPs are land-based infrastructures that are either natural or man-made structure that is built on the edges of the land/field and considered as permanent BMPs with a life span greater than 3 years. Various structural BMPs can be employed to mitigate soil loss at the contour depending on the slope of the landscape. These structures aid in the reduction of slope length which reduces soil erosion.

Several studies have been evaluated the effectiveness of various BMPs on hot spot areas of a watershed to reduce sediment yield and soil erosion around the world including our country Ethiopia. For example, Uniyal et al. (2020) shown structural BMPs (0.66-70%) and agricultural BMPs (2-7%) in minimizing sediment yields at watershed level in the Upper Baitarani River basin in Eastern India. Also in Ethiopia Nadew et al. (2019) shown, applying filter strips and parallel terrace/stone bunds scenarios reduced the existing sediment yields by 48% and 53% respectively from the existing condition scenario both at the sub-basins and the basin outlet in Guder watershed, Blue Nile Basin in Ethiopia.

Moreover, Tesema and Leta (2020) treated high sediment yield areas with three management options namely vegetative filter strips, grass waterway, and terracing in Kesem dam watershed, Awash basin, Ethiopia. Overall, while these three management practices substantially reduced sediment yield at a high level but the highest reduction was obtained under filter strips. When high sediment yield sub-basins were treated with filter strips up to 80% sediment yield reduction was obtained, indicating the high sediment trap efficiency of filter strips compared to the rest. Though such BMPs have been proven individually effective, their applicability to a watershed understudy must be assessed.

3. MATERIALS AND METHODS

This chapter describes the study area, materials and software used, required data and preparation, and data quality analysis. Moreover, detailed methodology of SWAT model simulation, sensitivity analysis, model calibration and validation, and developing BMPs were described. Finally, the framework of the overall methodology was designed.

3.1 Description of the Study Area

3.1.1 Location

The Gidabo dam is located in Oromia Regional States, 377 km from the capital city of Ethiopia. The Gidabo River is located in the Abaya-Chamo sub-basin of the Rift Valley Lakes basin situated in the southern part of Ethiopia. It originates from the highland area of Aletawendo escarpment, joining numerous large streams and finally passing through Gidabo dam before draining into Lake Abaya. It has been contributing water for Gidabo irrigation project available downstream of Gidabo dam. The Gidabo dam catchment is found in Borena zone in Oromia Region, Sidama Region, and Gedeo Zone in SNNP Region. The upstream of Gidabo dam catchment lies approximately between 38°10'00" to 38°40'00"E longitude and 6°10'00" to 6° 60' 00" N latitude (Figure 3.1). The drain area up to Gidabo dam location is about 2378 km^2.

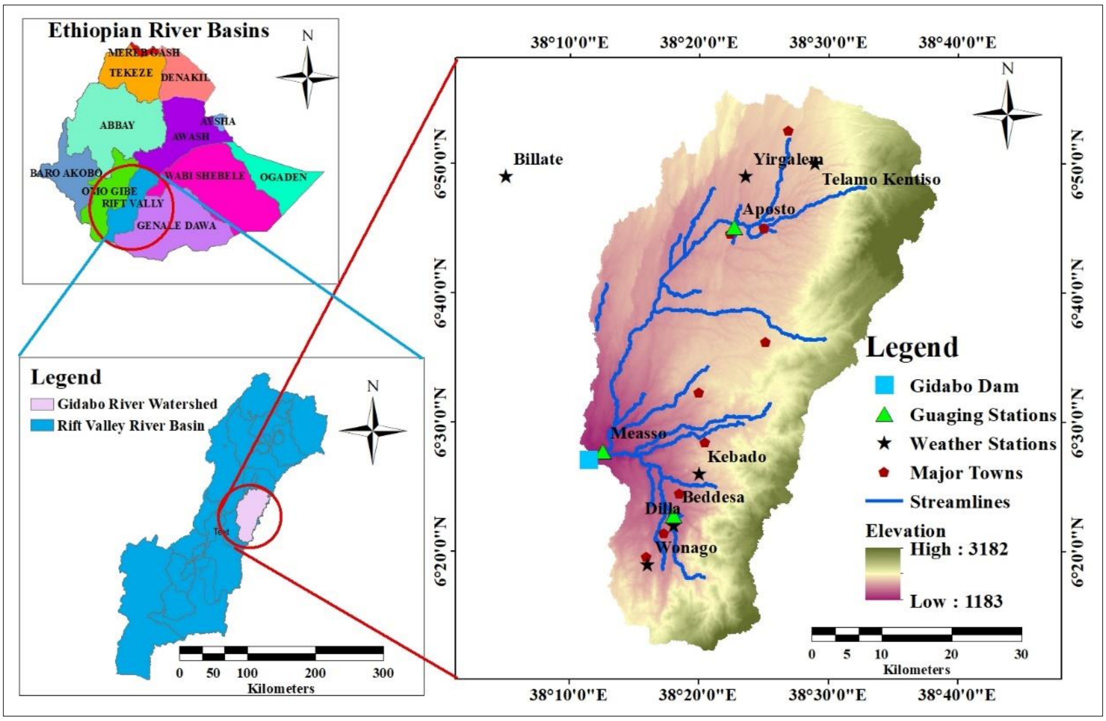

Figure 3.1. Location of the study area

3.1.2 Climate characteristics of the study area

Ethiopia is classified under five climate zones namely Bereha (hot and hyper-arid type of climate), Kola (hot and arid type of climate and the altitude is less than 1500 m), Woina-Dega (warm climate the altitude is between 1500-2500 m), Dega (temperate climate of high land and the altitude is between 2500-3000 m), Wurch (cold climate and the altitude is more than 3000 m) based on the altitude and temperature (NMA, 2001). Since the Gidabo watershed is located between the elevations 1183 to 3182 m above mean sea level (m.s.l), which is characterized under all five climate zones.

There are rainy and dry seasons in the Gidabo watershed. The main rainy season is from April to October with a peak rainy season from April to May and a second peak rainy season from September to October. These two peak seasons are separated by the relatively small rainy season in June to August while the rest seasons from November to February are dry. The mean monthly rainfall of the watershed varies between 36.82 mm to 187.93 mm (Figure 3.2) and mean annual rainfall is varied from 954.98 mm to 1843.70 mm. As recorded at different stations, the temperature of the study area varies with the altitude of the area from place to place. The monthly average maximum temperature of the watershed varies between 24.2°C and 33.06°C and similarly, the average monthly minimum temperature of the watershed varies between 10.7°C and 17.43°C (Figure 3.3).

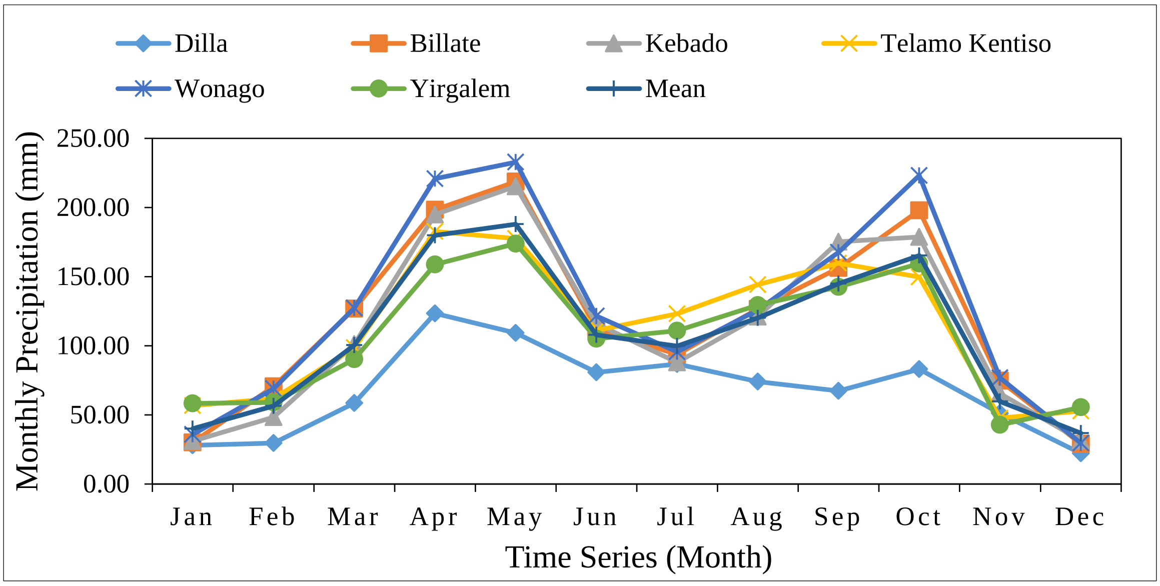

Figure 3.2. Mean monthly precipitation characteristics of the study area

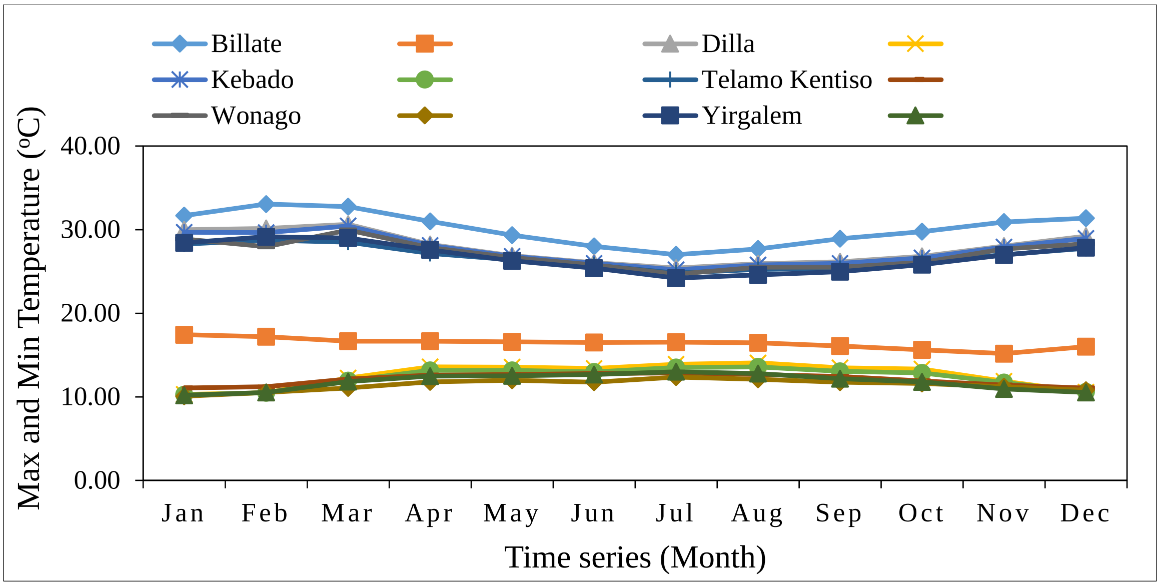

Figure 3.3. Mean monthly maximum and minimum temperature characteristics of the study area

3.1.3 Topography

The altitude of the catchment area ranges from 1183 to 3182 m above mean sea level (m.s.l). The major physiographic units in this area are undulating plains, valleys, steep stream banks, and major escarpment at the eastern part of the watershed (Tedla, 2011). The Gidabo watershed elevation varies from 1182 m above m.s.l at the dam site to 3183 m above m.s.l at the peak of the watershed, which is located at the western part of the watershed as shown in Figure 3.1.

3.2 Materials and Software's

Many Software were used for this study to achieve the goal of the objectives. These software's includes RAINBOW, Geographical Information system (GIS), Earth Resources Data Analysis System (ERDAS) Imagine 2014, Environment for Visualizing Images 5.3 (ENVI 5.3), ArcGIS interfaced Soil and Water Assessment Tool (ArcSWAT-2012), and Sequential Uncertainty Fitting version 2 (SUFI-2) algorithm in SWAT calibration and uncertainty program (SWAT-CUP) software package was used. RAINBOW was used for the homogeneity test of rainfall data. ArcGIS and ERDAS Imagine 2014 were used for the preparation of spatial data including LULC image classifications. For radiometric and atmospheric correction images were calibrated using the radiometric correction and atmospheric correction tool respectively in ENVI 5.3 software. Also, land gap filling was performed using ENVI 5.3 software. The SWAT model was used for the assessment of land management activities on streamflow and sediment yield. Sequential Uncertainty Fitting version 2 (SUFI-2) algorithm in SWAT calibration and uncertainty program (SWAT-CUP) software package was used for model sensitivity, calibration, and validation.

3.3 Model Input and Data Sources

3.3.1 Weather data

The climate of the watershed provides the moisture and energy inputs that control the water balance and determine the relative importance of the different components of the hydrologic components (Neitsch et al., 2011). The climate variables required by SWAT consist of daily precipitation, maximum and minimum temperature, solar radiation, wind speed, and relative humidity to be input from records of measured data or generated during simulation. For this study, these data were obtained from Ethiopian National Meteorological Agency (NMA). The weather data used were represented from six stations (Dilla, Kebado, Telamo Kentiso, Wonago, and Yirgalem) located in the watershed and one station (Billate) located around the watershed for the period 1988-2018. Table 3.1 shows weather stations used in this study located in and around the Gidabo watershed.

Table 3.1. Weather stations used in and around the study area

No.	station Name	Lat	Long	Elev (m)	Elements					
					PCP	Tmin	Tmax	RH	SR	WS
1	Billate	6.82	38.08	1361	yes	yes	yes	no	no	no
2	Dilla	6.37	38.30	1579	yes	yes	yes	yes	yes	yes
3	Kebado	6.43	38.33	1807	yes	yes	yes	no	no	no
4	Telamo Kentiso	6.83	38.48	1911	yes	yes	yes	no	no	no
5	Wonago	6.32	38.27	1748	yes	yes	yes	no	no	no
6	Yirgalem	6.81	38.39	1786	yes	yes	yes	no	no	no

Where PCP is Precipitation, Tmin is Minimum Temperature, Tmax is Maximum Temperature, RH is Relative Humidity, SR is Solar Radiation, and WS is Wind Speed.

3.3.2 Hydrological data

3.3.2.1 Streamflow data

Daily or monthly flow data is required for calibration and validation for SWAT simulated results. Daily streamflow records of the major streamflow gauging stations of the watershed at Aposto, Bedessa, and Measso (located near dam outlet) for the years 1988-2014 were obtained from the Ministry of Water, Irrigation and Energy of Ethiopia (MoWIE). Figure 3.4 indicates the peak flow occurs from April to October and minimum flow occurs from November to March three gauging stations. This is highly related to the temporal pattern of rain fall in the study area.

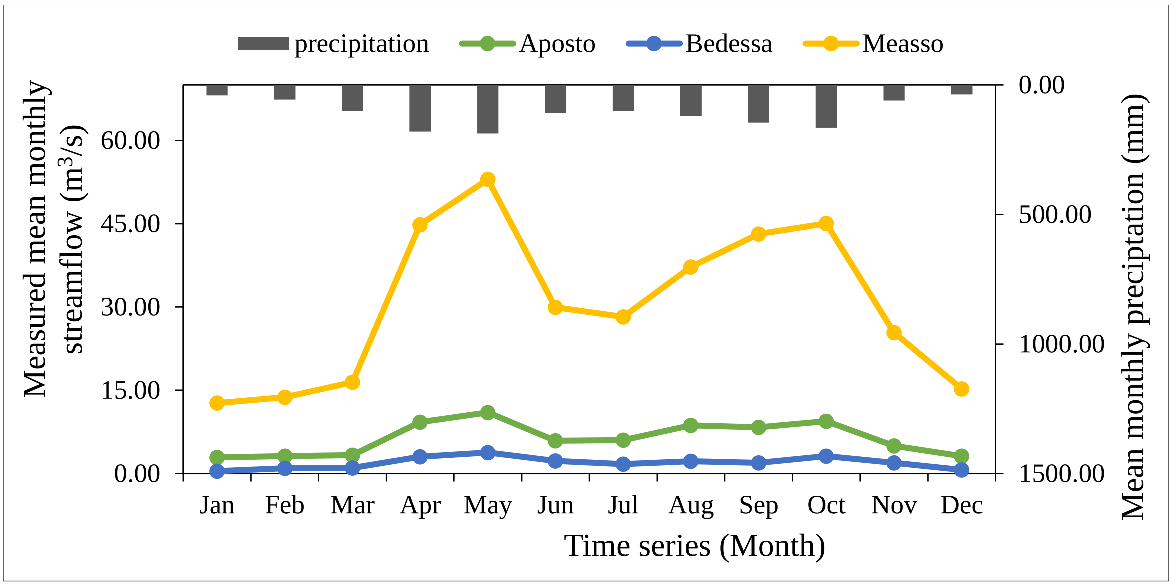

Figure 3.4. Mean monthly flow of Aposto, Bedessa, and Measso stations (1990-2014)

3.3.2.2 Sediment yield data

The sediment yield records were a challenge to obtain since the measured sediment concentration taken from the MoWIE was not in a continuous-time step. When these records are unavailable, estimates are often derived from empirical relations between stream flows and sediment yield called rating curve equations (Jung et al., 2020). First, sediment concentrations at the gauging stations of Aposto and Bedessa were converted into suspended sediment yield using Equation 3.1 (Morris and Fan, 1998). Hence, the sediment yield data was prepared through a sediment rating curve using a serious data record available at Aposto and Bedessa gauging station as shown in Figures 3.5 and 3.6 respectively. Rating curve Equations 3.2 and 3.3 developed from streamflow and sediment yield relationships are correlated with an R^2 value of 0.96 and 0.91 at Aposto and Bedessa respectably.

$$S_y = 0.086C * Q \tag{3.1}$$

$$S_y = 11.76Q^{1.15} \tag{3.2}$$

$$S_y = 18.91Q^{1.33} \tag{3.3}$$

Where S_y is suspended sediment yield (ton/day), C is sediment concentration in mg/l, Q is streamflow (m^3/s), and 0.086 is a conversion factor.

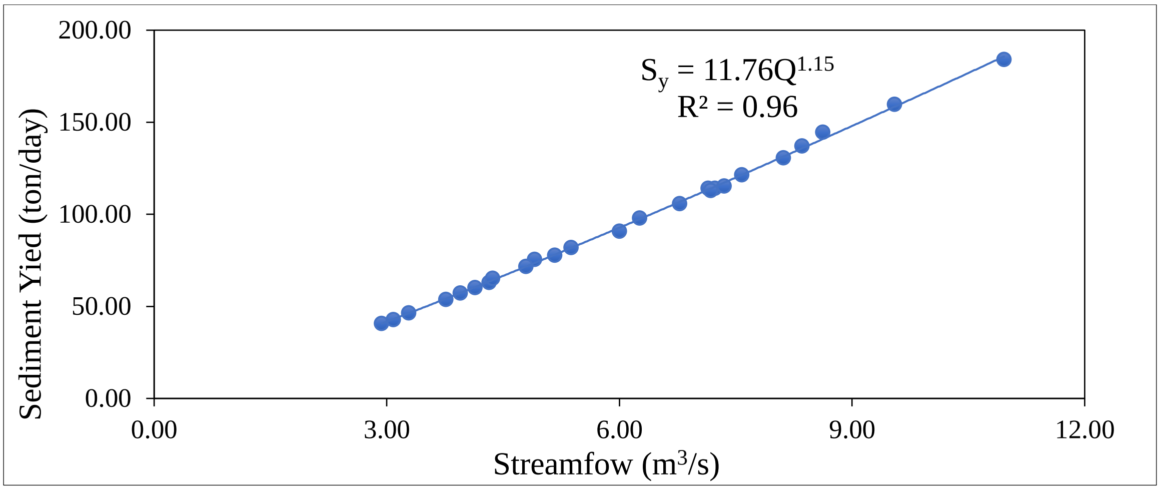

Figure 3.5. Sediment rating curve for Aposto station

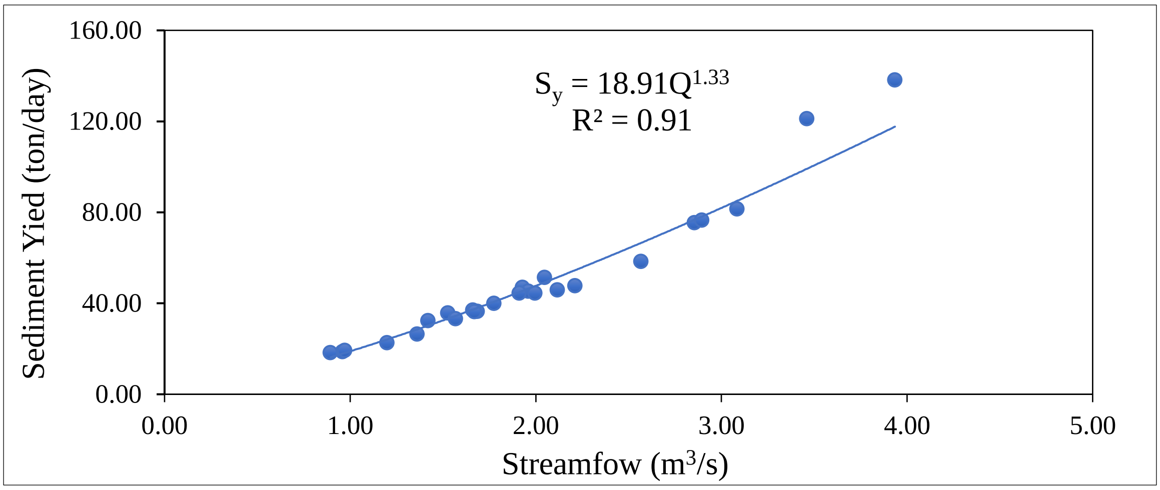

Figure 3.6. Sediment rating curve for Bedessa station

For Measo station at the outlet of the dam, the data prepared from Aposto and Bedessa gauging station were summed up and transformed to the outlet of the dam site by using the watershed area ratio method because the Gidabo watershed has more or less similar characteristics as explained in Tedla (2011). This area ratio method estimates flow at an ungauged location by multiplying the measured data at the gaged sites by the area ratio of the ungauged to gaged watersheds (Gianfagna et al., 2015). Scholars (for instance, Gianfagna et al. (2015); Choto and Fetene (2019); Tesema and Leta (2020)) used area ratio method for the watershed with similar watershed characteristics to transform measured data from gauged to the ungauged station.

3.3.3 Digital elevation model data

Topography is characterized by a digital elevation model (DEM) that depicts the elevation of any point in a given area at a specific spatial resolution. A 30 m × 30 m resolution of DEM of the study area obtained from Shuttle Radar Topography Mission (SRTM) was extracted using the GIS software by masking the shapefile of the Gidabo watershed which was used later to delineate the watershed. Additionally, it is used for the land slope class classification which was the basic parameter for the Hydrological Response Unit (HRU) definition. The different land slope classes as shown in Figure 3.7, the slope class found between 5-10% and 10-20% is the majority of land slope class of the watershed which covers 34.46% and 33.17% respectively. The remaining land slope classes 0-5%, 20-40%, and greater than 40% cover 22%, 10%, and 0.24% of the watershed respectively. These different land slope classes showing a variation of higher topography in Gidabo watershed.

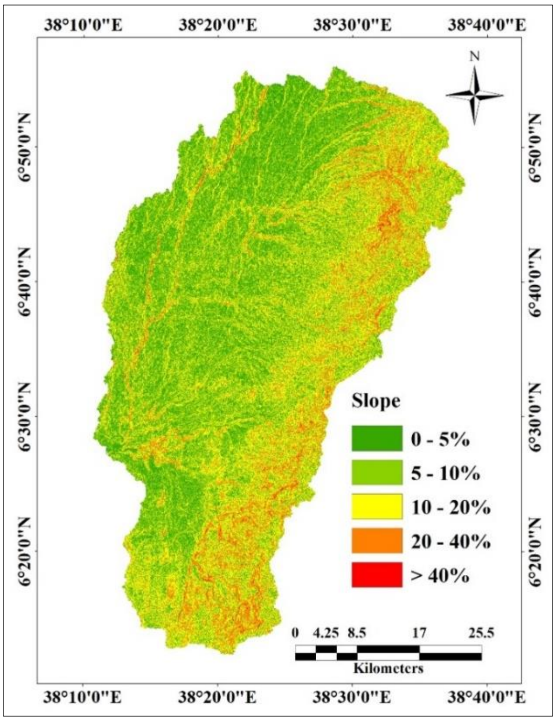

Figure 3.7. Slope class of the study area

3.3.4 Soil data

Soil is one of the dominant watershed characteristics and has a great influence on surface runoff generation. The FAO soil classification was used to define the soil type and eleven different soil types were classified. As a result, 22.98% of Pellic Vertisols, 22.37% of Eutric Cambisols, 19.33% Chromic Vertisols, and 13.81 % Orthic Luvisols are the majority of soil types in the watershed. The other soil types such as Calcaric Flubisols, Calcic Fluvisols, Chromic Luvisols, Dystric Gleysols, Dystric Nitisols, Eutric Nitisols, and Orthic Acrisols covers 22.51% of the watershed. The physical and chemical characteristics of the soil data play a large role in determining the movement of water and air within the HRU. The soil properties such as depth of soil layer, soil texture, hydraulic conductivity, bulk density, and organic carbon content are required by SWAT for each layer of each soil type. These soil data were obtained from major world soils of the Food and Agricultural Organization (FAO, 2002). To integrate the soil map with the SWAT model, a user soil database that contains textural and chemical properties of soils was prepared for each soil layer and added to the SWAT user soil databases. The soil map of the study is presented in Figure 3.8.

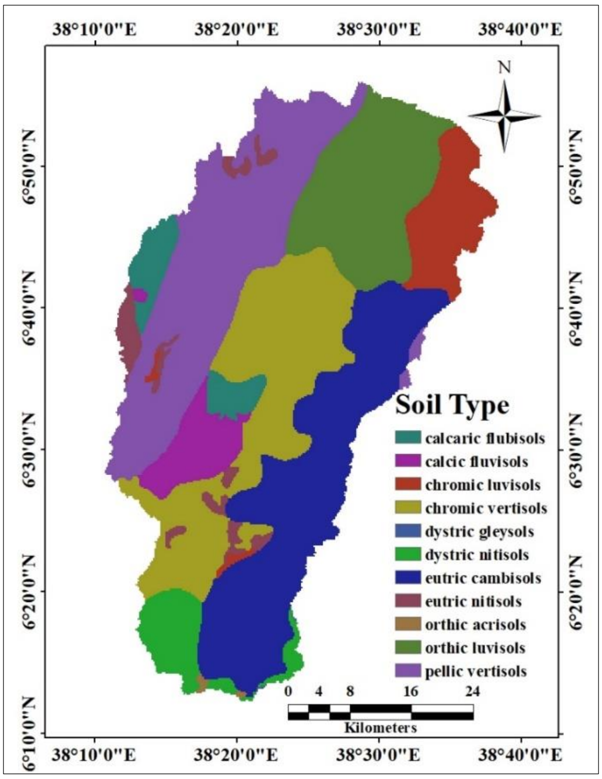

Figure 3.8. Soil map of the study area

3.3.5 Land use land cover data

Land use land cover was used to examine spatiotemporal variations of LULC change of the Gidabo watershed. LULC is also one of the inputs for the SWAT model to describe the Hydrological Response Units (HRUs) of the watershed along with slope and soil map.

3.3.5.1 Data acquisition and preprocessing

The land use land cover (LULC) data sets for the three historical periods were derived from multi-temporal series Landsat images. Landsat 5 Thematic Mapper (L5-TM) images of 1990, Landsat 7 Enhanced Thematic Mapper Plus (L7-ETM+) of 2005, and Landsat-8 Operational Land Imager and Thermal Infrared Sensor (L8-OLI/TRS) of 2019 at 30 m resolution (Table 3.2) were obtained from the United States Geological Survey (USGS) earth explorer website (http://earthexplorer.usgs.gov/). These images were selected as they are cloud-free and acquired in the same season to avoid seasonal variation in vegetation pattern and distribution throughout the year.

Table 3.2. Source and characteristics of satellite imagery used in this study

Satellite Data	Path/Row	Image Date	Number of Bands	Cloud Cover (%)	Spatial Resolution
L5-TM	168/55	16/01/1990	7	0	30 m
	168/56	16/01/1990	7	0	30 m
L7-ETM+	168/55	01/01/2005	8	0	30 m
	168/56	01/01/2005	8	0	30 m
L8-OLI	168/55	18/12/2019	11	0	30 m
	168/56	18/12/2019	11	0	30 m

Preprocessing satellite imagery before conducting image classification and change detection is very vital to minimize instrumental errors and to build a more thorough association between the obtained data and surface features on the ground (Alawamy et al., 2020). In this study, sequential preprocessing steps were performed using ArcGIS 10.4, ERDAS Imagine 2014, and ENVI 5.3 software packages. These steps comprised radiometric and atmospheric corrections in addition to layer stacking, mosaicking, image gap-filling, and sub-setting. To improve the clarity and visualization of the Landsat images used in this study, appropriate band compositions (layer stacking) were carried out. The layer stacked images in path/row 168/55 and 168/56 were merged into a single image by mosaicking them together. In performing layer stacking, mosaicking and sub-setting ERDAS Imagine 2014 software was used.

For radiometric and atmospheric correction images were calibrated using the radiometric correction and atmospheric correction tool respectively in ENVI 5.3 software. Because of scan line corrector (SLC) failure (SLC-Off problem) that occurred on May 31, 2003, till 2013 for ETM+ sensor of Landsat 7 images has had line gaps, resulting in a loss of about 22% of data. The Landsat 7 image dated January 1, 2005, was affected by the SLC-Off error where line gaps covered a portion of the study area on both sides. Therefore, the image was corrected in such a way that the missing data caused by the failure of the SLC were filled by applying for the Landsat gap fill extension in ENVI 5.3 using the single file gap-fill (triangulation) method. This procedure uses geostatistical interpolation techniques to perform correlations between pixels in an image by using data from the same image where empty pixels are replaced by the mean of their neighbors in the nearest two lines (Alawamy et al., 2020).

3.3.5.2 LULC classification and accuracy assessment

Classification of the image is a process conducted to catalog all pixels in an image or raw remotely sensed data into a finite number of individual LULC classes to produce beneficial thematic maps and information. This process is performed by assigning different spectral signatures from the dataset to several classes based on reflectance attributes of the diverse types of LULC. Six major LULC classes such as agricultural land, bare land, built-up land, forest land (dense forest), shrubland (open forest), and water bodies as shown in Table 3.3 were chosen for mapping the entire Gidabo watershed area. Due to the similar spectral response of tree cover in agroforestry systems to open forests, the region under agroforestry was classified as shrubland.

In this study, supervised classification was applied for LULC classification using ERDAS Imagine 2014 software. The most important step in this procedure was selecting over 500 training samples for each Landsat image by drawing polygons around representative regions of each LULC class. For the classes (agriculture land, forest land, and shrubland), a minimum number of training samples were 100 because these classes have been major LULC classes in the watershed. Training sites for the predefined LULC classes (Table 3.3) were developed by the visual interpretation of the Landsat images (1990, 2005, 2019) based on prior knowledge of some of the study areas, information from the previous studies, and using Google earth pro 7.3.3 software. Google Earth represents a powerful and attractive source of positional data that can be used for investigation and preliminary studies with suitable accuracy and low cost. Since Google Earth images with the high spatial resolution are free for the public, they are used directly in land use land cover mapping in small geographical extend (Tilahun and Teferie, 2015). Once the training sites were developed, the maximum likelihood classifier was applied to create spectral signatures and then used to classify all pixels in the image.

Table 3.3. Land use and land cover categories identified at the study area

LULC Class	SWAT Code	Description
Agricultural Land	AGRL	Land areas used for crop cultivation area currently under crop, fallow, and land under preparation and the scattered rural settlement that is closely associated with the cultivated fields.
Bare Land	BARR	Land areas with low or no vegetation including rocky areas
Built-up Area	URBN	Land areas where most land is covered with structures including urban and rural residential and roads
Forest Land	FRSE	The land area covered with highly dense trees
Shrubland	FRST	Land areas with scattered trees mixed with short bushes, grasses, and areas under agroforestry
Water Body	WATR	Land areas which are waterlogged, swampy throughout the year, reservoir and rivers.

The accuracy of the classification was assessed for the three supervised classifications based on the ground truth in ERDAS Imagine 2014. The accuracy assessment was done using historical high-resolution google imagery captured January 16, 1990, January 1, 2005, and December 18, 2019, obtained from Google Earth Pro 7.3.3 software were used to carry out the accuracy validation for LULC maps of 1990, 2005, and 2019 respectively. The random sampling technique was used to identify verification points based on the distribution area of each LULC class. A total number of 180 verification points were randomly selected with a minimum sample number of at least 20 for each class. Classification accuracy was assessed using measures derived from the error matrices which include user, producer, and overall accuracy and kappa coefficient (Equation 3.4). If $K \leq 0.5$ shows rare agreement, $0.5 \leq K \leq 0.75$ shows a medium level of agreement, $0.75 \leq K \leq 1$ shows a high level of agreement, and $K = 1$ for perfect agreement (Dibaba et al., 2020).

$$K = \frac{P_0 - P_C}{1 - P_C} \tag{3.4}$$

Where K is the Kappa coefficient, P_o is the proportion of correctly predicted cells and P_c is the expected proportion correction by chance between the observed and predicted map.

3.3.5.3 LULC change detection Analysis

LULC detection is the process of identifying differences in geographical surface phenomena over time. LULC change detection involves the ability to quantify spatiotemporal effects using multi-temporal data sets. The Post-classification comparison technique was chosen in this study to be employed for LULC change detection. This classification technique involves the classification of multiple date images separately to generate thematic maps, which are then compared pixel-by-pixel of corresponding classes to produce tables. This approach was selected for its advantage to minimize the possible effects of sensor and atmospheric and environmental differences between images as they are independently classified and provides more detailed information obtained from a complete matrix of LULC change (Adepoju et al., 2006). Pairs of the produced classified thematic maps (1990, 2005, and 2019) were compared in ArcGIS 10.4 software. Change detection of LULC was performed to understand the changing status and its magnitude of change rate for the study periods. The magnitude of change (MC) and the percentage of change (PC) for each LULC class during each period was computed based on Equations 3.5 and 3.6.

$$\text{MC (ha)} = A_i - A_f \tag{3.5}$$

$$\text{PC (\%)} = \frac{A_i - A_f}{A_i} \times 100 \tag{3.6}$$

Where A_i is the class area at the initial time and A_f is the class area at the final time

3.4 Data Analysis

3.4.1 Filling missing data

Missing data occur when no data value is stored for the variable in an observation. Missing data are a common occurrence and can have a significant effect on the conclusions that can be drawn from the data. To fill the gaps (missing observations) in data, several interpolation techniques are currently used. Spatial interpolation techniques are commonly used to fill in gaps in daily rainfall series by estimating the unknown rainfall amount at a point based on known data from nearby stations (Burrough and McDonnell, 1998). Among that, the Inverse Distance Weighted technique was employed to estimate missing data for this study. This method weights for each sample are inversely proportionate to its distance from the point being estimated and it is reliable if the weather stations are situated within a 100 km radius (Lam, 1983). This method uses the observed values at other stations for estimating the missing value of an observation, which is determined by Equation 3.7. The method is fast, easy to implement, and easily tailored for specific needs.

$$P_x = \frac{\sum_{i=1}^{N} \frac{1}{{d_i}^2} P_i}{\sum_{i=1}^{N} \frac{1}{{d_i}^2}} \tag{3.7}$$

Where P_x is the estimated value, P_i is the observed value of the i^{th} neighboring station, d_i is the distance from each location the point being estimated and N is the number of neighboring stations.

3.4.2 Consistency test

The continuous daily rainfall series of each station were subjected to quality control to detect outliers caused by instrumental and human errors. A Double Mass Curve (DMC) was used to check the consistency of rainfall. A DMC is a plot of one variable's arithmetic cumulative figures against the cumulative figures of another variable or the cumulative computed values of the same variable for the same period. The DMC theory is based on the concept that a graph of one quantity's accumulation against the accumulation of the others over the same period plots a straight line since the data are proportional and the slope of the line shows the constant of proportionality between the quantities (Searcy and Hardison, 1960). In other words, a significant break in the slope of the double-mass curve means that the proportionality is not a constant at all rates of accumulation. Graphical inspection of the double mass curves for this study (Appendix B.1) indicated no significant inconsistency in most of the stations used in this study.

3.4.3 Homogeneity test

Using non-homogeneous data may be increased or decreased the real representation. To know the collected data either is homogenous or non-homogenous the data should be checked. For this study, the homogeneity test was evaluated using RAINBOW (Raes et al., 2006) software employing frequency analysis. RAINBOW offers a test of homogeneity which is based on the cumulative deviations from the mean. By evaluating the maximum and the range of the cumulative deviations from the mean, the homogeneity of the data of a time series was tested. One of the tests of homogeneity is based on the cumulative deviations from the mean using Equation 3.8 (Raes et al., 2006).

$$S_k = \sum_{i=1}^{k}(X_i - \overline{X}) \tag{3.8}$$

Where X_i is the records from the series X_1, $X_{2\ldots}$ X_n and $\overline{X}$ is the mean. The initial value of $S_K = 0$ and the last value $S_K = n$ is equal to zero. For a record X_i above normal, the $S_k = i$ increases while for a record below normal $S_k = i$ decreases.

For a homogenous record, one may expect that the S_k's fluctuate around zero since there is no systematic pattern in the deviations of the X_i's from their average value X. If the cumulative deviation crosses one of the horizontal lines, the homogeneity of the data set is rejected with 90, 95, and 99% probability. For this study, the probabilities of rejecting the homogeneity of the datasets were evaluated in the homogeneity statistics menu. Appendix B.2 shows, the homogeneity of rainfall stations plotted in the homogeneity plot menu.

3.5 Hydrologic Model Setup and Simulation

3.5.1 SWAT model setup

The Soil and Water Assessment Tool (SWAT) model was developed by the United States Department of Agriculture Research Service. This model is semi-distributed, physically-based, computationally efficient, and capable of continuous simulation over long periods. The SWAT model requires input data of topography, soil, and land use along with hydro-meteorological data to simulate hydrological processes (Arnold et al., 2012). The SWAT model interfaced with GIS that integrates various spatial data (DEM, LULC, and soil) and climate data which is currently embedded in an ArcGIS interface called ArcSWAT. In this study, the GIS interfaced ArcSWAT-2012 was used to set up a SWAT model for the Gidabo watershed.

3.5.1.1 Watershed delineation

Watershed delineation is used to divide the watershed into discrete land areas and stream reaches that drain into a single outlet. SWAT model allows the user to delineate the watershed and sub-watershed using DEM by expanding the spatial analyst extension function in ArcGIS. Before starting watershed delineation, 30 m resolution DEM data prepared was projected into Ethiopian projection parameter UTM Zone 37. There are various steps including DEM setup, stream definition, inlet-outlet definition, watershed outlet selection, and definition and calculation of sub-basin parameters in the watershed delineation process. By default, the ArcSWAT model interface proposes the minimum and maximum watershed area and allows the size of the sub-basin in hectares to define the minimum drainage area required to form the origin of the stream because the smaller the threshold area gives more detail of the drainage network, large numbers of the sub-basin, HRUs, and vice versa. For stream definition, the minimum threshold area proposed by the model was used. As a result, the watershed was subdivided into 39 sub-basins using the default 5000 ha threshold area by selecting the outlet manually at the outlet of Gidabo dam (Figure 3.9).

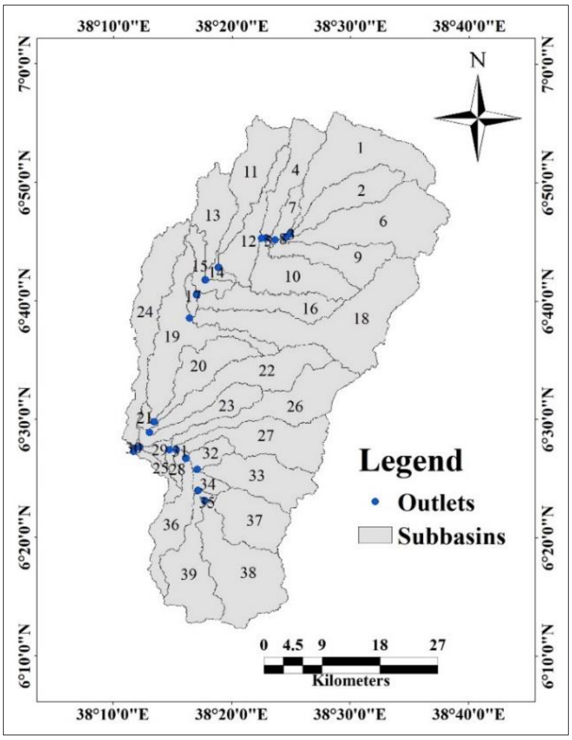

Figure 3.9. Sub-basins of the study area

3.5.1.2 Hydrologic response unit's determination

In SWAT, a watershed divided into multiple sub-basins is sub-divided into hydrologic response units (HRUs) that consist of homogenous LULC, soil, and slopes. The HRU analysis tool in ArcSWAT allows the user to load LULC, soil, and slope maps for the project. The HRU analysis in SWAT includes the delineation of HRUs by overlaying the spatial map of slope classes, land use, and soil data. In this study, the delineated watershed by ArcSWAT with prepared land use and soil layers were overlapped 100%. In addition to land use and soil, the HRU analysis in SWAT includes divisions of HRUs by slope classes. The multiple slope options that consider different slope classes were selected. LULC, soil, and slope were reclassified to correspond with parameters in the SWAT database. For HRU definition, the reclassified LULC, soil, and slope in the SWAT database were overlaid. To define the distribution of HRUs, multiple HRU definition option of 5% LULC, 10% soil and 10% slope threshold was used. This means the minor LULC, soil, and slope less than the percentage was removed. As a result, the Gidabo watershed was divided into 592, 652, and 769 sub-watersheds for LULC of 1990, 2005, and 2019 respectably.

3.5.1.3 Weather data

SWAT requires daily values of precipitation, maximum and minimum temperature, solar radiation, relative humidity, and wind speed. The user may choose to read these inputs from a file or generate the values using monthly average data summarized over several years. Since relative humidity, wind speed, and solar radiation data records were limited for all the stations except for Dilla station. For such challenges, SWAT includes the weather generator (WGN) model to generate or to fill gaps in measured records. This Weather generator model needs different weather parameters (Appendix A.6). Dilla station was used to generate the limited data records for the rest stations using the weather generator capabilities of SWAT models. The missed data were filled by assigning a missing data identifier of -99 which allows the SWAT model to generate weather data for that day from average monthly values. After the weather parameters were prepared by using WGN, it was imported into the SWAT database to generate automatically the weather records for the rest stations.

3.5.2 Hydrological component of SWAT

No matter what type of problem is studied with SWAT, water balance is the driving force behind everything that happens in the watershed. The simulation of hydrology in the watershed can be separated into two major divisions. The first division is the land phase of the hydrological cycle that controls the amount of water, sediment, nutrient, and pesticide loadings to the main channel in each sub-basin. The second division is the water or routing phase of the hydrologic cycle which can be defined as the movement of water, sediments, etc. through the channel network of the watershed to the outlet.

3.5.2.1 Land phase

In the land phase of the hydrological cycle, SWAT simulates the hydrological cycle based on the water balance Equation 3.9.

$$SW_t = SW_0 + \sum_{i=0}^{t}\left(R_{day} - Q_{surf} - E_a - W_{sweep} - Q_{gw}\right) \tag{3.9}$$

Where SW_t is the final soil water content (mm), SWo is the initial soil water content on day i (mm), t is the time (days), R_{day} is the amount of precipitation on day i (mm), Q_{surf} is the amount of surface runoff on day i (mm), E_a is the amount of evapotranspiration on day i (mm), W_{sweep} is the amount of water entering the vadose zone from the soil profile on day i (mm), and Q_{gw} is the amount of return flow on day i (mm) (Neitsch et al., 2012).

i. Surface runoff

Surface runoff or overland flow is a flow that occurs whenever the rate of water application to the ground surface exceeds the rate of infiltration. Using daily or sub-daily rainfall amounts, SWAT simulates surface runoff volumes for each HRU. SWAT provides two methods for estimating surface runoff: the SCS curve number method (SCS, 1972) and the Green and Ampt infiltration method (Heber Green and Ampt, 1911). Even though the SCS curve number method is better in estimating runoff volume accurately. Hence, the SCS curve number method was adopted in this study. The method is an empirical model, which is based on the following Equation 3.10.

$$Q_{surf} = \frac{[(R_{day} - 0.2S)]^2}{(R_{day} + 0.8S)} \tag{3.10}$$

Where Q_{surf} is the accumulated runoff or rainfall excess (mm), R_{day} is the rainfall depth for the day (mm), S is the retention parameter (mm). The retention parameter is defined by Equation 3.11.

$$S = 25.4\left[\left(100\,\frac{1000}{CN}\right) - 10\right] \tag{3.11}$$

Where CN is the curve number for the day

SCS defines three antecedent moisture conditions: I-dry (wilting point), II-average moisture, and III-wet (field capacity). The moisture condition I curve number is the lowest value the daily curve number can assume in dry conditions. The curve numbers for moisture conditions I and III are calculated with Equations 3.12 and 3.13.

$$CN_1 = CN_2 - \frac{CN_2 - 20(100 - CN_2)CN_1}{[100 - CN_2 + \exp(2.533 - 0.0636(100 - CN_1))]} \tag{3.12}$$

$$CN_3 = CN_2[\exp(0.00673(100 - CN_2))] \tag{3.13}$$

Where CN_1 is the curve number for antecedent moisture condition-I, CN_2 is the curve number for antecedent moisture condition-II, and CN_3 is the curve number for antecedent moisture condition-III.

ii. Peak runoff rate

The peak runoff rate is the maximum runoff flow rate that occurs with a given rainfall event. The peak runoff rate is an indicator of the erosive power of a storm and is used to predict sediment loss. SWAT estimates the peak runoff rate with a modified rational method (Chow et al., 1998) as expressed in Equation 3.14. The rational method mainly assumes that if rainfall of intensity begins at time t = 0 and continues indefinitely, the rate of runoff will increase until the time of concentration ($t = t_{conc.}$). The time of concentration is the time for a drop of water to flow from the remotest point in the sub-basin to the sub-basin outlet. It is calculated as the sum of the time it takes for flow from the remotest point in the sub-basin to reach the channel and the time it takes for flow in the upstream channels to reach the outlet.

$$Q_{peak} = \frac{\alpha_{tc} * Q_{surf} * A}{3.6 * t_{conc}} \tag{3.14}$$

Where Q_{peak} is peak runoff rate (m^3/s), α_{tc} is the fraction of daily rainfall that occurs during the time of concentration, Q_{surf} is the surface runoff (mm H_2O), A is the sub-basin area (km^2), t_{conc} is the time of concentration (hr), and 3.6 is a unit conversion factor.

iii. Potential evapotranspiration

Potential evapotranspiration (PET) is the rate at which evapotranspiration would occur from a large area uniformly covered with growing vegetation that has access to an unlimited supply of soil water and that was not exposed to advection or heat storage effects. If the actual evapotranspiration is considered the net result of atmospheric demand for moisture from a surface and the ability of the surface to supply moisture, then PET is a measure of the demand side. To estimate PET, the Priestley-Taylor method, Penman-Monteith method, and the Hargreaves method have been incorporated in SWAT. Depending upon the availability of input data, the user may select one of the three methods. The Penman-Monteith method was selected for this study and it requires air temperature, relative humidity, solar radiation, and wind speed. The PenmanMonteith Equation (Monteith, 1965) combines components that account for energy needed to sustain evaporation, the strength of the mechanism required to remove the water vapor, and aerodynamic and surface resistance terms and expressed by Equation 3.15.

$$\lambda \mathrm{E} = \frac{\Delta.(\mathrm{H_{net}} - \mathrm{G}) + \rho_{\mathrm{air}}.\mathrm{C_\rho} \, [\mathrm{e_z}^0 - \mathrm{e_z}]/\gamma_\mathrm{a}}{\Delta + \gamma.(1 + \gamma_\mathrm{c}/\gamma_\mathrm{a})} \tag{3.15}$$

Where, λE is the latent heat flux density (MJ m^{-2} d^{-1}), E is the rate of evaporation (mm d^{-1}), Δ is the slope of the saturation vapor pressure-temperature curve, H_{net} is the net radiation (MJ m^{-2} d^{-1}), G is the heat flux density to the ground (MJ m^{-2} d^{-1}), ρ_{air} is the air density (kg m^{-3}), C_ρ is the specific heat at constant pressure (MJ kg^{-1} $^oC^{-1}$), e_z^0 is the saturation vapor pressure of air at height z (kPa), e_z is the water vapor pressure of air at height z (kPa), γ is the psychrometric constant (kPa $^oC^{-1}$), γ_a is the diffusion resistance of the air layer (aerodynamic resistance) (s m^{-1}) and γ_c is the plant canopy resistance (s m^{-1}).

3.5.2.2 Routing phase

Once SWAT determines the loadings of water and sediment to the main channel, the loadings are routed through the stream network of the watershed. SWAT incorporated Muskingum storage routing (river routing) and variable storage routing methods to rout the water through the channel network. Where, variable storage method uses a simple continuity Equation in routing the storage volume, and the Muskingum routing method models the storage volume in the channel length as the combination of wedge and prism storages. In the variable storage method, inflow exceeds outflow and a wedge of storage is produced when a flood wave advances into a reach segment. This method was developed by (Williams, 1969) and later recommended (Williams and Hann, 1972) as reported in (Arnold et al., 1995). Therefore this routing method was adopted in this study as expressed in Equation 3.16.

$$\Delta V_{stored=} V_{in-} V_{out} \tag{3.16}$$

Where, ΔV_{stored} is the change in volume of storage during the time step (m^3 H_2O), V_{in} is the volume of inflow during the time step (m_3 H_2O)and V_{out} is the volume of outflow during the time step (m^3 H_2O).

3.5.2.3 Soil erosion and sediment simulation

Erosion is the wearing down of landscape over time that includes the detachment, transport, and deposition of soil particles by the erosive forces of raindrops and surface flow of water. The Modified Universal Soil Loss Equation (MUSLE) (Williams, 1975) is used in the SWAT model to estimate erosion produced by rainfall and runoff. The rainfall energy factor is replaced with a runoff factor in MUSLE, which improves sediment yield prediction, eliminates the need for delivery ratios, and allows the Equation to be applied to single storm events. Sediment yield prediction is improved because runoff is a function of antecedent moisture conditions as well as rainfall energy. In this study, SWAT estimates sediment yield with the Modified Universal Soil Loss Equation (MUSLE) shown in Equation 3.17.

$$\mathrm{Sed} = 11.8\left(Q_{surf} * Q_{peak} * A_{hru}\right)^{0.56} * K_{USLE} * C_{USLE} * P_{USLE} * LS_{USLE} * CFRG \tag{3.17}$$

Where Sed is the sediment yield on a given day (metric tons), Q_{surf} is the surface runoff volume (mm), Q_{peak} is the peak runoff rate (m^3/s), A_{hru} is the area of the HRU (ha), K_{USLE}

is the USLE soil erodibility factor (0.013 metric ton m^2 hr/ (m^3-metric ton cm)), C_{USLE} is the USLE cover and management factor, P_{USLE} is the USLE support practice factor, LS_{USLE} is the USLE topographic factor and CFRG is the coarse fragment factor.

3.6 Sensitivity Analysis, Calibration, and Validation

Computer-based models can perform long-term simulations of the effects of watershed processes and management activities on water quality and quantity. To use model outputs for specific purposes, models should be scientifically sound, rigorous, and defensible scientific research to guide policy, regulatory, and management decision-making (Moriasi et al., 2007). Therefore, process-based SWAT input parameters must be held within a realistic uncertainty range. Sequential Uncertainty Fitting version 2 (SUFI-2) algorithm in SWAT calibration and uncertainty program (SWAT-CUP) software package (Abbaspour et al., 2007) was used for model sensitivity, calibration, and validation.

3.6.1 Sensitivity analysis

The first step in the calibration and validation process in SWAT is the determination of the most sensitive parameters for a given watershed or sub-watershed (Arnold et al., 2012). Sensitivity analysis is the process of determining the rate of change in model output concerning changes in model inputs (parameters). In parametrization, the parameters to be used and how to regionalize the parameters are the two important issues. This is because not all SWAT parameters are relevant to all sub-basins and not all should be used simultaneously to calibrate the model.

Usually, one-at-a-time (OAT) or local sensitivity analysis and all-at-a-time (OAT) or global sensitivity analysis are performed. In OAT, all parameters are held constant while changing one to identify its effect on some model output or objective functions. The limitation of OAT is that the sensitivity of one parameter is often dependent on the values of other parameters, which are all fixed to values whose accuracy is not known. In AAT, however, all parameters are changing; hence, a larger number of simulations (500-1000 or more) are required depending on the number of parameters to see the impact of each parameter on the objective function. But, AAT takes advantage of OAT by producing more reliable results.

In this study, the global sensitivity analysis method in the SWAT calibration and uncertainty program (SWAT-CUP) software package (Abbaspour et al., 2007) was used for sensitivity analysis. In this analysis, the larger value of the t-stat and the smaller p-value was taken as a more sensitive parameter (Abbaspour et al., 2017). The sensitivity analysis of streamflow was performed first followed by sediment yield. The inputs are the observed data, simulated data, and most sensitive parameters regarding streamflow and sediment with the absolute lower and upper bound parameters value.

3.6.2 Model calibration and validation

Predictive watershed models are required to be calibrated using measured data to better parameterize a model to a given set of local conditions thereby reducing the prediction uncertainty. This is performed carefully by selecting values for model input parameters (within their respective certainty ranges) by comparing model predictions for a given set of assumed conditions with observed data for the same conditions. This means, modification of those selected sensitive input parameter values and comparison of the predicted output of interest to measured data until a defined objective function is achieved.

In this study, the SWAT model was calibrated and validated for streamflow and sediment yield of the watershed for each of the three stations namely Aposto, Bedessa, and Measso (near dam outlet) using SWAT-CUP which provides a decision-making framework that incorporates a semi-automated Sequential Uncertainty Fitting version 2 (SUFI-2). For calibration, the most sensitive parameters were used, and their values were changed iteratively within the allowed upper and lower ranges until the acceptable agreement between measured and simulated streamflow was attained.

After successful calibration, model validation was involved by running a model using input parameters determined during the calibration process for the component of interest (streamflow and sediment yield). Validation involves running a model using parameters that were identified during the calibration process and comparing the predictions to observed data which are not used in the calibration. Calibration and validation were carried out by splitting the available observed data into a range of datasets for each of the three stations. The selection of observed data periods for calibration and validation was based on the availability of relatively consistent observed data. First, the model was set to run for 1988-2014 with the initial 2 years (1988-89) as a model warm-up period that allows the model to stabilize for further simulations. Then, the consequent phases were established as calibration (1990-2006) and validation (2007- 2014) periods.

3.6.3 Model performance evaluation

After running the model for analysis of results, simulated streamflow and sediment yield were evaluated to determine the reliability of prediction compared to the measured data using graphical inspection and quantitative statistics measures during the calibration and validation periods. The graphical technique is the first overview of model performance which provides a visual comparison of simulated and measured constituent data. In terms of quantitative statistics, the model performance was assessed using three statistical performance ratings namely coefficient of determination (R^2), Nash-Sutcliffe efficiency (NSE), and percent bias (PBIAS) recommended by Moriasi et al. (2007).

The R^2 describes the degree of collinearity between simulated and measured data. The value of R^2 ranges between 0 and 1. Where R^2 value closer to 1, the higher is the agreement between the simulated and the measured values. It is estimated based on Equation 3.18. The NSE determines the relative magnitude of the residual variance compared to the measured data variance that is calculated by Equation 3.19 (Nash and Sutcliffe, 1970). The value of NSE ranges from 1 to $-\infty$ (negative infinity) with values less than or very close to zero indicating poor model performance and values equal to one indicating perfect performance. The PBIAS measures the average tendency of simulated values to be lower or larger than their observed values for a specific quantity during the calibration and validation period. PBIAS is computed using Equation 3.20 in which a value approximate to 0 is ideal (Moriasi et al., 2007). The general model performance ratings (Moriasi et al., 2007) are indicated in Table 3.4.

$$R^2 = \frac{\left(\sum_{i=1}^{n}[X_i - X_{av}][Y_i - Y_{av}]\right)^2}{\sum_{i=1}^{n}[X_i - X_{av}]^2[Y_i - Y_{av}]^2} \tag{3.18}$$

$$NS = 1 - \frac{\sum_{i=1}^{n}(X_i - Y_i)^2}{\sum_{i=1}^{n}(X_i - X_{av})^2} \tag{3.19}$$

$$PBIAS = 100\left(\frac{\sum_{i=1}^{n} X_i - \sum_{i=1}^{n} Y_i}{\sum_{i=1}^{n} X_i}\right) \tag{3.20}$$

Where X_i is the measured value, X_{av} is the average measured value, Y_i is the simulated value and Y_{av} is the average simulated value.

Table 3.4. Overall recommended performance ratings (Moriasi et al., 2007)

Performances	R^2	NS	PBIAS
Very good	$0.70 < R^2 \leq 1.00$	$0.75 < NS \leq 1.00$	$PBIAS < \pm 10$
Good	$0.60 < R^2 \leq 0.70$	$0.65 < NS \leq 0.75$	$\pm 10 \leq PBIAS < \pm 15$
Satisfactory	$0.50 < R^2 \leq 0.60$	$0.50 < NS \leq 0.65$	$\pm 15 \leq PBAS < \pm 25$
Unsatisfactory	$R^2 < 0.50$	$NS < 0.50$	$PBIAS \geq \pm 25$

3.7 Analysis of Streamflow and Sediment Yield Responses under Changing LULC

Simulating the impacts of LULC change on streamflow and sediment yield in Gidabo watershed is one of the most important parts of this study. The calibrated and validated SWAT model was used to evaluate the impacts of LULC change on the hydrological responses based on 1990, 2005, and 2019 LULC inputs. Three independent simulation runs were performed on monthly basis for the period 1988-2014 keeping other input parameters unchanged. Seasonal streamflow variability and water balance component responses to LULC change at different spatiotemporal scales were evaluated. Additionally, the impact of LULC change on sediment yield variability was also carried out at different spatiotemporal scales. The change between different historical LULC categories was analyzed by considering the relative difference between two consecutive periods of LULC and the corresponding simulated hydrological responses.

3.8 Identification of Critical Sub-Watersheds

All reservoirs located downstream of the watershed formed by constructing dams across natural watercourses are subject to some level of sediment inflow and deposition (Bhatia and Thawait, 2015). The sediment deposition lowers the reservoir's active capacity over time, which has an impact on the reservoir's regulating capacity to provide outflows with time. Critical areas are those within a watershed that contribute a large amount of sediment yield to the downstream outlet. They are generally considered to be high-level sediment sources that interact with high sediment transport potentials.

To implement watershed management, constraints like finance and land availability are always considerable factors that limit best management practices (BMPs) implication at the same time in whole watersheds. In a large watershed, a few sub-watersheds are might be more critical and responsible for a high amount of runoff and soil losses. Therefore, critical parts of the watershed must be identified for implementing soil and water conservation measures. In this study, critical sub-watersheds (high sediment source sub-basins) to reduce sediment yield to Gidabo dam were identified and prioritized based on annual sediment yield simulated using current 2019 LULC in the SWAT model from the sub-watersheds.

3.9 Developing Best Management Practices

To reduce soil erosion and sediment transport, the implementation of best management practices (BMPs) in watersheds has been recognized as an effective method (Betrie et al., 2010). According to spatial variability of sediment yield, the source-level identified by SWAT model was applied to simulate the effectiveness of BMPs to reduce sediment yield. The best management practices were represented in the SWAT model by modifying SWAT parameters to reflect the effects of practices on the process simulated within the SWAT model (Waidler et al., 2011). However, the selection of these best management practices and the values of their parameters are site-specific and should reflect the reality of the study area (Nadew et al., 2019).

In this study, three different management scenarios (filter strips, terracing, and reforestation) were selected and implemented in the SWAT model based on the Ministry of Agriculture and Rural Development guideline (Desta et al., 2005), and documented local research experience in the Ethiopian highlands (Hurni, 1985). The effectiveness of these BMPs scenarios was quantified by comparing each one with the baseline scenario to obtain a percent of the reduction. This effectiveness was computed using Equation 3.21.

$$\text{Effectiveness } (\%) = \frac{(\mathrm{Y_{baseline}} - \mathrm{Y_{BMP}})}{\mathrm{Y_{baseline}}} \times 100 \tag{3.21}$$

Where $Y_{baseline}$ and Y_{BMP} are the average annual sediment yields in the baseline scenario and the BMP scenario respectively.

3.9.1 Baseline scenario

In the baseline scenario, the existing watershed condition was considered. The baseline scenario corresponds to the current land management practice without conservation measures. The baseline scenario was obtained by running the SWAT model using the 2019 LULC.

3.9.2 Filter strip

Filter strips are vegetated areas that are situated between surface water bodies and cropland, grazing land, forest land, or disturbed land. Filter strips are also called vegetative filters or buffer filters. They are generally placed where runoff water leaves a field with the aim of removing larger soil particles. Larger particles including soil loss can settle out as a result of delayed runoff water leaving a field. In this scenario, 1, 3, and 5 m wide filter strips were assigned in agricultural lands of all selected critical sub-basin. This filter width value was assigned based on local research experience in Ethiopian highlands (Betrie et al., 2010; Nadew et al., 2019; Choto and Fetene, 2019). SWAT provides a specific method to incorporate filter strips through the FILTREW parameter defined in MGT (.mgt) of SWAT input table which reflects the width of the strip. The SWAT model calculates trapping efficiency for sediment using Equation 3.22 (Neitsch et al., 2012).

$$\mathrm{trap_{eff}} = 0.367 * \ \mathrm{FILTREW}^{0.2967} \qquad (3.22)$$

Where $\mathrm{trap_{eff}}$ is trapping efficiency and FILTERW is the width of the vegetation strips.

3.9.3 Parallel terrace

Terraces are an earthen embankment or combination of ridge and channel constructed across the field slope in which designed to reduce erosion by reducing slope length and retaining runoff for moisture conservation. This conservation practice is applied in where soil erosion caused by water and excessive slope length is the problem. Implementing terracing in a field reduces surface runoff by trapping water in small depressions, reduces the peak flow rate by shortening the slope, and reduces sheet and gully erosion by increasing the amount of sediment settling in the runoff.

In this study, terracing was simulated by activating the terracing option in the scheduled management operations tool (.ops) in the SWAT. The model parameters that are appropriate for the representation of the effect of parallel terraces are the USLE support practice factor (USLE_P) along with average slope length (SLSUBBSN). The values of SLSUBBSN for the average slope of the HRU were set based on Equation 3.23 (Arabi et al., 2006) whereas USLE_P were assigned from the SWAT user’s manual version 2012 for terraced conditions (Neitsch et al., 2012).

$$\text{SLSUBBSN} = (0.21 * \text{S} + 0.9)\frac{100}{\text{S}} \qquad (3.23)$$

Where SLSUBBSN is the average slope length of the sub-basin and S is the average slope of the HRU.

3.9.4 Reforestation

Reforestation requires the conversion of land to its historical natural vegetation conditions. In this study, reforestation of high sediment yield prone areas of agricultural land, shrubland, and bare land were considered and compared with the above two scenarios. These were performed by activating the Land Use Update (.LUP) tool in the SWAT model which allows the existing land use update can be deleted and the new one can be added.

3.10 Flow Chart of the Methodology

In this study, the hydrologic model SWAT was used to analyze hydrological responses under LULC change and to develop BMPs. Figure 3.10 describes sequential steps of the methodologies with the data required by the SWAT model to achieve the objectives this study. The following framework illustrates the general workflow of the study.

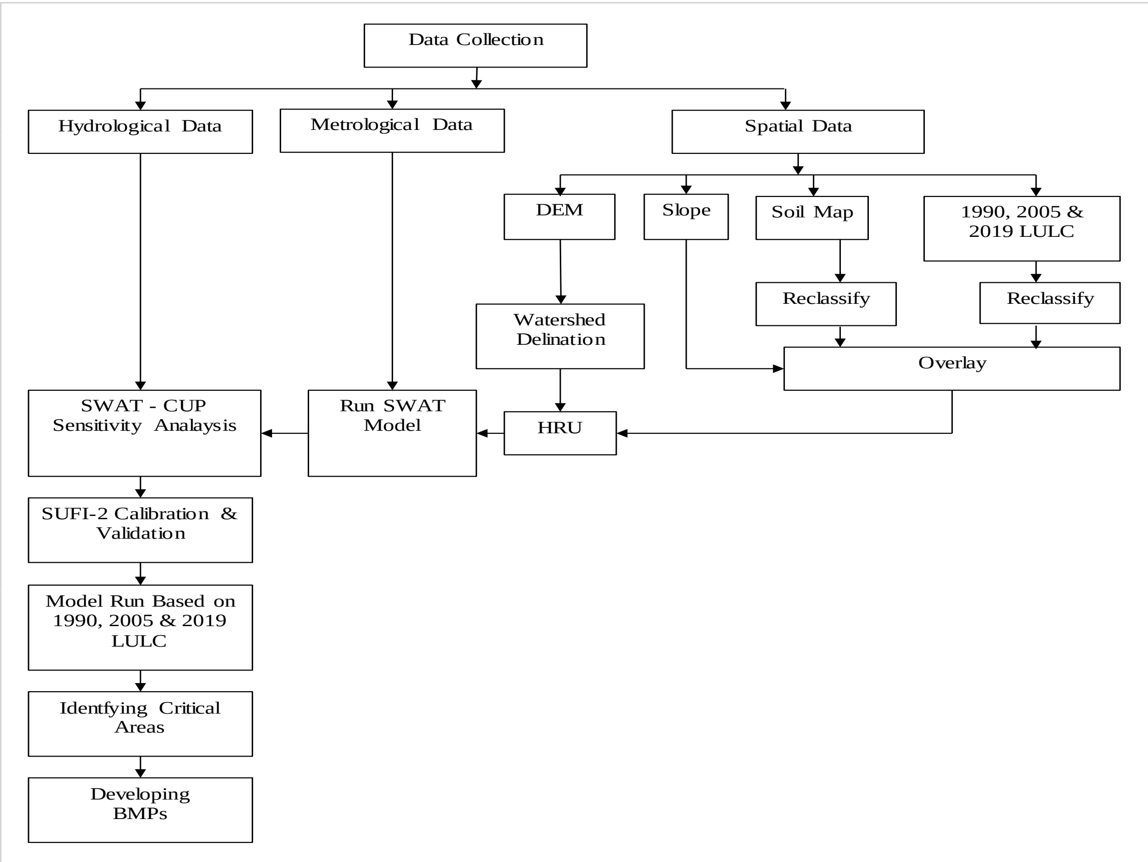

Figure 3.10. Flow chart of the overall methodology

4. RESULTS AND DISCUSSIONS

This chapter provides the results of the LULC classification accuracy and changes detection analysis in Gidabo watershed. The most sensitive streamflow and sediment yield parameters and the performance of the SWAT model in simulating streamflow and sediment yield during validation and calibration were also discussed. Furthermore, streamflow and sediment yield responses to LULC change were analyzed and discussed in detail. Finally, the spatial distribution of sediment yield, identification of critical sediment source, and the effectiveness of different BMPs were analyzed and discussed.

4.1 Land Use Land Cover Change

4.1.1 Land use land cover classification accuracy assessment

To categorize the Landsat images (TM, ETM+, and OLI-8), the maximum likelihood classifier used has shown the distribution of six dominant LULC classes for the years 1990, 2005, and 2019 in the study area. For these LULC images, accuracy assessments were carried out to examine the agreement between the produced map and the actual condition that exist on the ground. Accordingly, the overall accuracy of classified maps of 1990, 2005, and 2019 were 90.56%, 88.9%, and 91.11% which indicated acceptable values for map quality and accuracy standard as compared to the study made by Mather (1995) which indicates the value of overall accuracy greater than 70% is regarded as acceptable classification accuracy. Additionally, the calculated kappa coefficient for the maps 1990, 2005, and 2019 were 0.88, 0.86, and 0.89 respectively which indicated a high level of agreement because the values were greater than 0.75. The user, producer, overall accuracy assessment, and kappa coefficient for the 2019 LULC classification are presented in Table 4.1. The rest of the accuracy assessments for 1990 and 2005 LULC classifications are illustrated in Appendix A.3.

4.1.2 Land use land cover classification

Based on the supervised classification of 1990, 2005, and 2019 Landsat images, six prevalent LULC types (agricultural land, shrubland, forest land, built-up area, bare land, and water body) were obtained as shown in Figure 4.1. Among these LULC types, shrubland (land areas with scattered trees mixed with short bushes, grasses, and area under agroforestry) was the most dominant land use in the Gidabo watershed followed by agricultural and forest land for the study periods. Especially, the northern and central part of the watershed was dominantly covered by shrubland whereas the eastern and southern part was dominantly covered by agricultural and forest land respectively but, the LULC types of built-up area, bare land, and water body were distributed over different parts of the study area.

Table 4.1. 2019 land use land cover classification accuracy assessment

LULC Class	Agricultural	Bare Land	Built-up	Forest Land	Shrubland	Water Body	Total	User Accuracy (%)
Agricultural	33	2	0	0	2	0	37	89.19
Bare Land	1	22	1	0	0	0	24	91.67
Built-up	0	2	23	0	0	0	25	92.00
Forest Land	0	0	0	28	3	1	32	87.50
Shrubland	0	0	0	2	38	0	42	90.48
Water Body	0	0	0	0	0	20	20	100.00
Total	36	26	24	30	43	21	180	
Producer Accuracy (%)	91.67	84.62	95.83	93.33	88.37	95.24		
Overall Classification Accuracy = 91.11%								
Overall Kappa Statistics = 0.89								

4.1.3 Land use land cover change detection

The areal LULC change analysis in the past decades from the year 1990-2019 was visible and occurred as either an expansion or a decline between consecutive study periods. The LULC change detection depicted a continuous expansion in the spatial extent of agricultural land, built-up area, and bare land while shrubland, forest land, and water body revealed a continuous declined between sequential study periods. In the year 1990, the Gidabo watershed was dominated by shrubland (42.79%) followed by forest land (24.89%) and agricultural land (23.09%) while built-up area, water body, and bare land accounted for 5.48%, 2.67%, and 1.08% of the watershed respectively. In the years 2005 and 2019, the shrubland was also dominant with area coverage of 40.07% and 35.25% followed by agricultural (28.88% and 32.00%) and forest land (19.46% and 17.78%) in the watershed respectively whereas built-up, bare land and water body are minor as compared with shrubland, agricultural and forest lands. The temporal distribution of the major LULC classes in 1990, 2005, and 2019 is shown in Table 4.2.

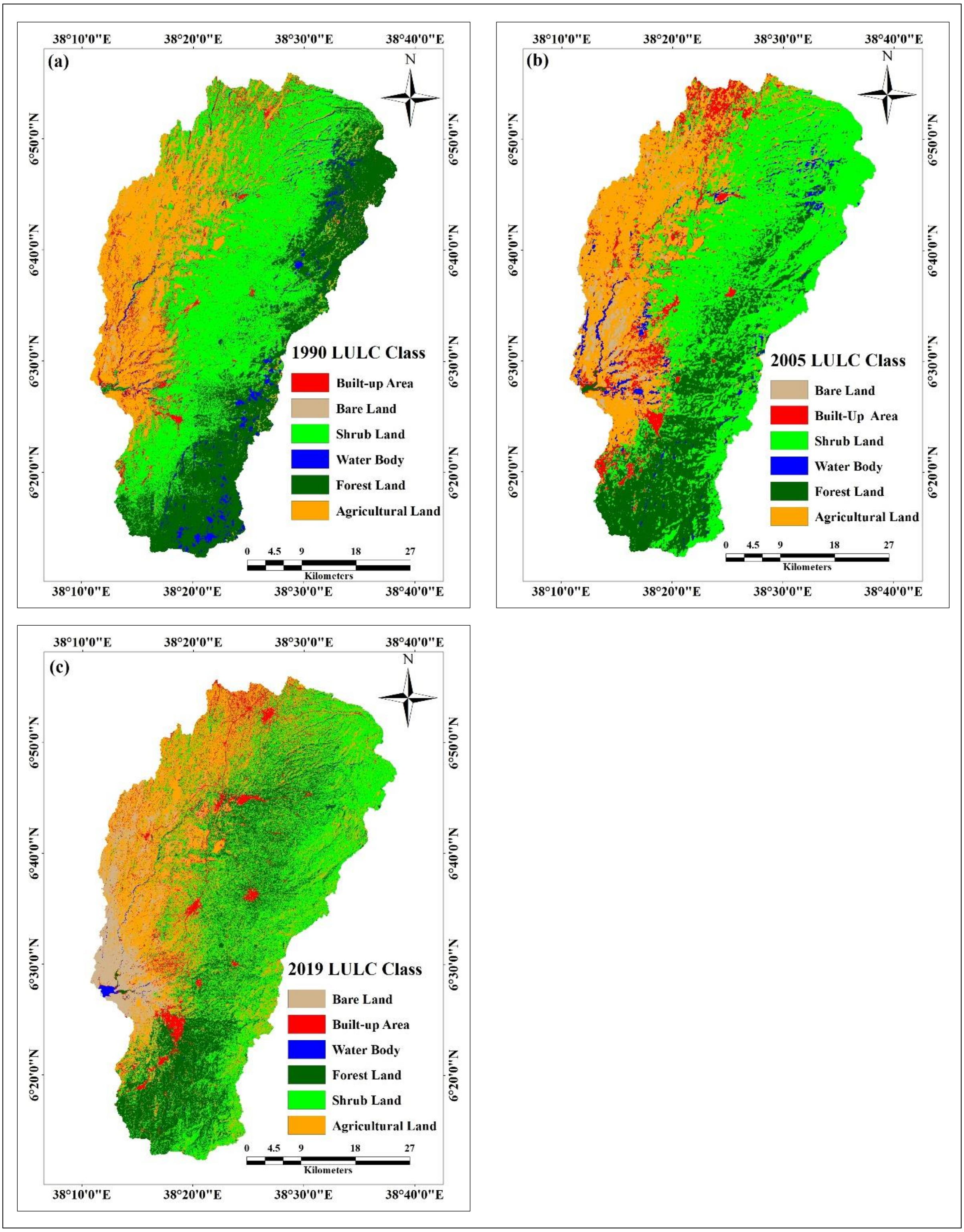

Figure 4.1. Land use land cover type map of (a) 1990, (b) 2005, and (c) 2019

Comparing the LULC data of the years 1990, 2005, and 2019, the most LULC changes were obtained in the agricultural, shrubland, and forest land use types as shown in Table 4.3. During the 15 year time interval from 1990-2005, the area coverage of agriculture, built-up and bare land increased by 137.76 km^2 (5.79%), 25.84 km^2 (1.09%), and 34.32 km^2 (1.44%) with an average increase of about 9.18, 1.72 and 2.29 km^2/yr respectively. In this time frame, the areal coverage of shrubland, forest land, and water body was decreased by 129.16 km^2 (5.43%), 64.64 km^2 (2.72%), and 4.08 km^2 (0.17%) with an average decline of about 7.11, 7.53, and 1.36 km^2/yr. Most forest areas lost were converted to shrubland (8.88%) and about 5.33% to agricultural land. The decline in shrubland areal coverage was observed because of the conversion of shrubland to agricultural land (10.41%) and built-up area (3.22%).

In the year between 2005 and 2019, more shrubland, bare land, built-up area, and water body change, and less agricultural and forest change was observed compared with the time frame between 1990 and 2005. The agricultural land areas which amounted to 686.84 km^2 in 2005 was increased to 761.01 km^2 which shows 74.09 km^2 (3.11%) expansion with an annual increase rate of 4.94 km^2/yr. Approximately with the same rate of expansion, bare land, and the built-up area were increased to 54.01 km^2 (2.27%) and 54.68 km^2 (2.30 %) with an annual increasing rate of 3.60 and 3.65 km^2/yr. The LULC change analysis of shrubland, forest land, and water body depicted a decline with 114.45 km^2 (4.81%), 39.87 km^2 (1.68%), and 28.29 km^2 (1.19%) with an annual decreasing rate of 4.31, 8.61, and 0.27 km^2/yr. An agricultural expansion observed in the year 2019 was because of 2.5% forest land and 11.27% of shrubland was converted to agricultural land. In the same manner, agricultural land of 3.33% and 2.6%, shrubland of 0.22% and 4.11% was converted to bare land and built-up area respectively.

Table 4.2. The spatial distribution of the major LULC classes in 1990, 2005 and 2019

LULC Class	1990 Coverage		2005 Coverage		2019 Coverage	
	Area (km^2)	Area (%)	Area (km^2)	Area (%)	Area (km^2)	Area (%)
Agricultural	549.16	23.09	686.64	28.88	761.01	32.00
Bare Land	25.47	1.08	60.05	2.52	114.06	4.80
Built-up	130.23	5.48	156.07	6.56	210.75	8.86
Forest Land	592.00	24.89	462.83	19.46	422.51	17.78
Shrubland	1017.55	42.79	952.91	40.07	838.46	35.25
Water Body	63.58	2.67	59.50	2.50	31.22	1.31
Total	2378.00	100.00	2378.00	100.00	2378.00	100.00

In the study period between 1990 and 2019 expansion of the agricultural, built-up area, and bare land whereas, the decline of shrubland, forest land, and water body was seen. A great amount of change was observed in agricultural land, shrubland, and forest land. Agricultural land was increased by 211.85 km^2 (8.90%) with an average annual change rate of 7.06 km^2/yr whereas shrubland and forest land was decreased 179.04 km^2 (7.53%) and 169.09 km^2 (7.11%) with an annual rate change of 5.97 and 5.63 km^2/yr respectively. A change in bare land, built-up area, and water body was also seen as other land uses with different amount of rates of change. Bare land and the built-up area were increased with an amount of 88.33 km^2 (3.71%) and 80.52 km^2 (3.38%) with an annual rate change of 2.94 and 2.68 km^2/yr while water body was declined with 32.33 (1.36%) with an annual rate of change of 1.08 km^2/yr. Comparing the two sub-periods (1990-2005 and 2005-2019), the LULC changes follow a similar trend in both sub-periods.

In the study period, a rise in the agricultural land and built-up area was due to the higher population influx and the rapid socio-economic development in the watershed leads to reduce in natural vegetation and expansion of agricultural land and built-up area to the nearest possible regions. Bewket and Sterk (2005), Shawul et al. (2019), Choto and Fetene (2019), and many other researchers reported the conversion of large areas of forest and shrubland to agricultural land and also indicated the conversion of some amounts of agricultural and shrubland to built-up areas due to the higher rate of population growth in the highlands regions of Ethiopia. Therefore, population growth is the driving factor to LULC change in Gidabo watershed which leads to significant alteration of streamflow and sediment yield LULC.

Table 4.3. Land use land cover change detection

LULC Class	1990-2005 Change		2005-2019 Change		1990-2019 Change	
	Area (km^2)	Area (%)	Area (km^2)	Area (%)	Area (km^2)	Area (%)
Agricultural	+137.76	+5.79	+74.09	+3.11	+211.85	+8.90
Bare Land	+34.32	+1.44	+54.01	+2.27	+88.33	+3.71
Built-up	+25.84	+1.09	+54.68	+2.30	+80.52	+3.38
Forest Land	-129.16	-5.43	-39.87	-1.68	-169.04	-7.11
Shrubland	-64.64	-2.72	-114.45	-4.81	-179.09	-7.53
Water Body	-4.08	-0.17	-28.29	-1.19	-32.37	-1.36

4.2 Streamflow Modelling

4.2.1 Streamflow sensitivity analysis

The sensitivities to the model performance give insight into parameter identifiability using the available information daily streamflow data (Kassa, 2009). The global sensitivity analysis was performed using monthly observed data in the Sequential Uncertainty Fitting (SUFI-2) algorithm that is linked with the SWAT Calibration Uncertainty Program known as SWAT-CUP. Accordingly, twenty parameters were selected for sensitivity based on manual training in ArcSWAT and reviewing different works of literature. The ranges of variation of these parameters are based on absolute SWAT value which is illustrated in Appendix A.4. After conducting a series of simulations, SWAT-CUP provides the sensitivity of parameters in rank order based on its t-stat and p-value. The highest value of t-stat indicates the ratio of the high parameter coefficient to standard error and lower the p-value related to the rejection of the hypothesis that an addition in the value of the parameter provides a significant increase in the variable response (Abbaspour et al., 2017). The fifteen most sensitive hydrologic flow parameters during calibration and validation in the watershed are given below in Figure 4.2.

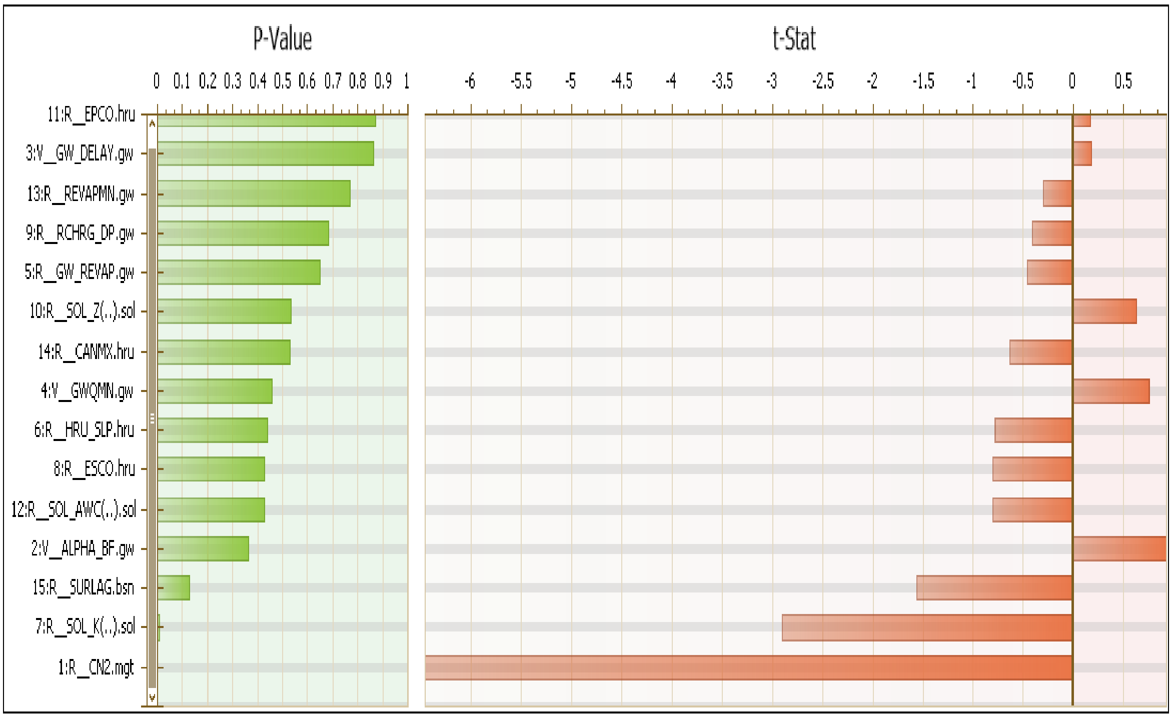

Figure 4.2. Streamflow sensitive parameters

As shown in Figure 4.2, the surface runoff response parameters SCS CN II value (CN2) was found to be the most sensitive flow parameter in Gidabo watershed followed by saturated hydraulic conductivity of the soil layer (SOL_K), surface runoff lag time in the HRU (SURLUG), base flow alpha-factor (ALPHA_BF) and available water capacity of the soil layer (SOL_AWC). Soil evaporation compensation factor (ESCO), average slope steepness (HRU_SLP), threshold depth of water in the shallow aquifer required for return flow to occur (GWQMN), maximum canopy storage (CANMX), and depth from the soil surface to bottom of the layer (SOL_Z) also have the highest influence in controlling the streamflow. Table 4.4 shows the best optimized fitted parameters value during calibration.

Table 4.4. Streamflow parameters sensitivity rank

Parameter Name	Min Value	Max Value	Fitted Value	Rank
R_CN2	-25%	25%	-16.87	1
R_SOL_K	87.84	1117.84	459.74	2
R_SURLAG	6.36	21.28	17.47	3
V_ALPHA_BF	0.41	0.56	0.51	4
R_SOL_AWC	0.12	0.73	0.32	5
R_ESCO	0.19	0.64	0.36	6
R_HRU_SLP	0.14	0.59	0.44	7
V_GWQMN	2192.61	7057.39	4454.73	8
R_CANMX	11.26	73.74	39.06	9
R_SOL_Z	0.42	1.33	0.57	10
R_GW_REVAP	0.10	0.27	0.26	11
R_RCHRG_DP	0.11	0.74	0.69	12
R_REVAPMN	17.04	342.04	131.98	13
V_GW_DELAY	20.43	354.57	119.00	14
R_EPCO	0.36	1.19	0.71	15

4.2.2 Streamflow calibration and Validation

Multi-site streamflow calibration was done in three gauging stations namely Aposto, Bedessa, and Measso (near at dam outlet) using a semi-automated SUFI-2 algorithm in monthly time setup. The model was calibrated for 1990-2006 at each gauging station and the two years from 1988-1989 were used as a warm-up period. The performance of the model at each gauging station was tested at every stage of the model simulation with the parameters printed out at the respective stage. The parameter values were changed repeatedly within the allowed ranges until independent agreements between measured and simulated streamflow were obtained for each gauged sub-basin.

The SWAT model performance was evaluated using performance indicators such as coefficient of determination (R^2), Nash-Sutcliffe coefficient of efficiency (NSE), and percentage of bias (PBIAS) at stations. Accordingly, the model performs well at Aposto with 0.74, 0.66, and 14.9 values of R^2, NSE, and PBIAS respectively. At Bedessa gauged station, the performance of the model was good with R^2 of 0.64 and NSE value of 0.61 and satisfactory of PBIAS value 19.7. The model performs very well at Measso (near at dam outlet) with R^2 of 0.80 and PBIAS of -3.2 and performs well with an NSE value of 0.74 during the calibration period.

Calibrated parameters were used to evaluate the model performance of reproducing simulated results related to the measured value of streamflow. Without further adjustment of calibrated flow parameters, validation of the model was performed using an independent set of measured flow data. Similar to the calibration process multi-site validation was carried out at Aposto, Bedessa, and Measso (near dam outlet) with a monthly time setup. Monthly based data from the year 2007-2014 was used for model validation without further adjustment of best fitted calibrated parameters value for each gauged sub-basins.

The performance indicator result shows the model performs well during validation in all three gauged sub-basins. The value of R^2, NSE, and PBIAS at Aposto was 0.72, 0.65, and 18.1 respectively while at the value of R^2, NSE and PBIAS at Bedessa were 0.74, 0.65, 1.2 and Measso (near dam outlet) was 0.74, 0.71 and 8.0 respectively. In Bedessa gauged station, performance rating during the validation period performs better than calibration due to good measured data quality in the validation period than calibration. Observed and simulated streamflow hydrograph and scatter plot at three stations during calibration and validation are illustrated in Figures 4.3, 4.4, and 4.5.

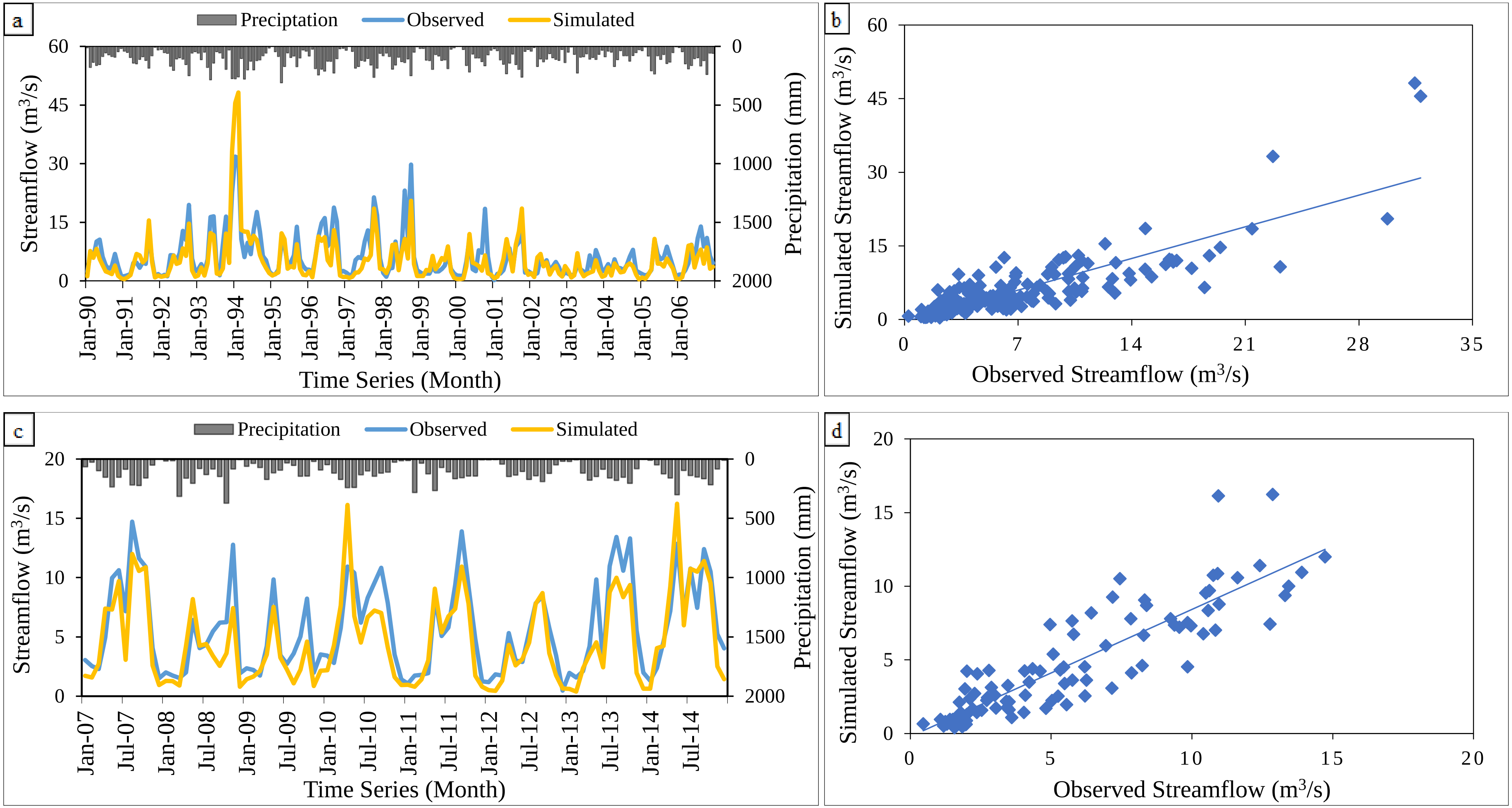

Figure 4.3. Observed and simulated streamflow hydrograph and scatter plot at Aposto hydrometric station: (a) hydrograph during calibration period, (b) scatter plot during calibration period, (c) hydrograph during validation, (d) scatter plot during validation period

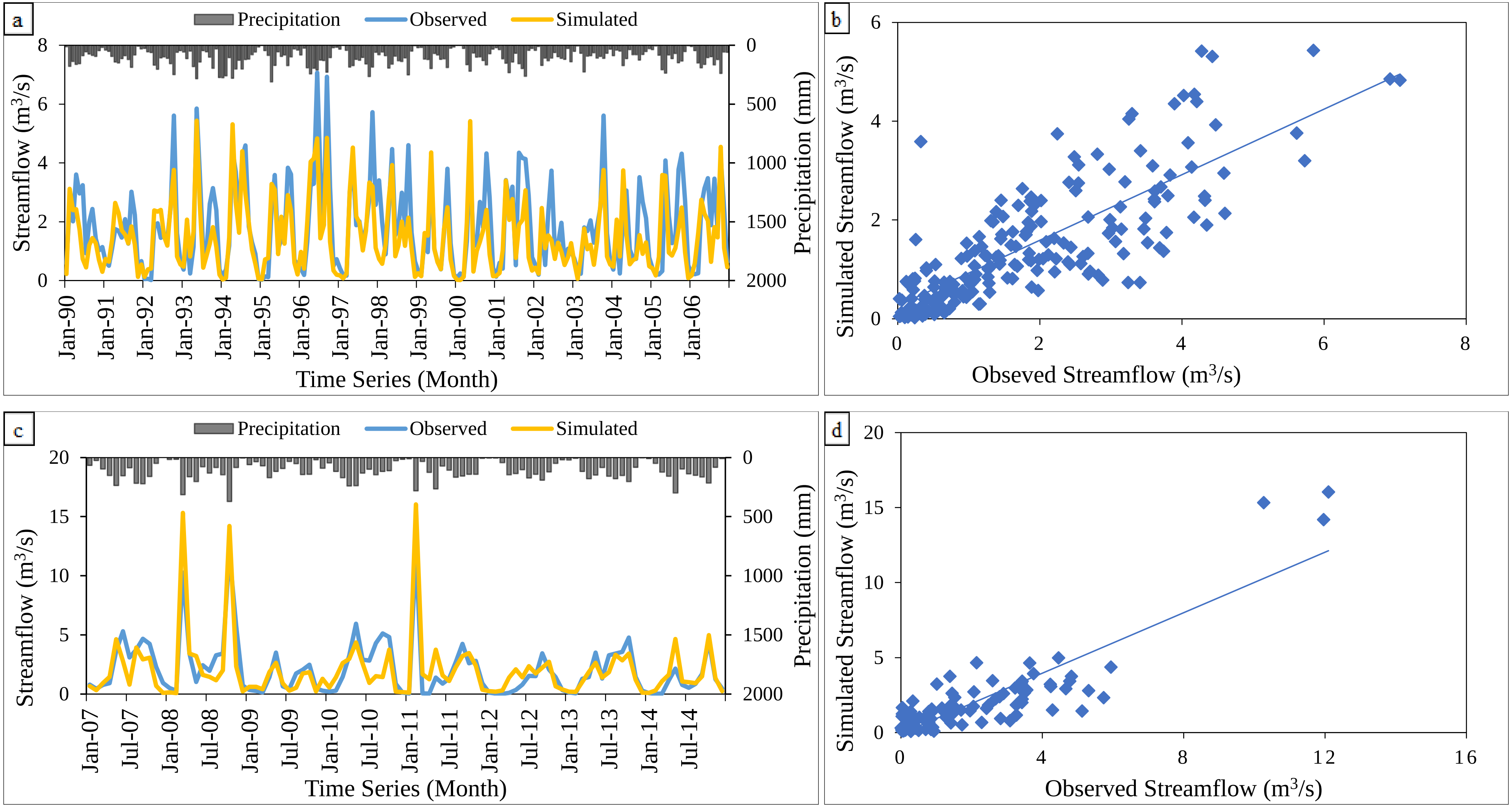

Figure 4.4. Observed and simulated streamflow hydrograph and scatter plot at Bedessa hydrometric station: (a) hydrograph during calibration period, (b) scatter plot during calibration period, (c) hydrograph during validation period, (d) scatter plot during validation period

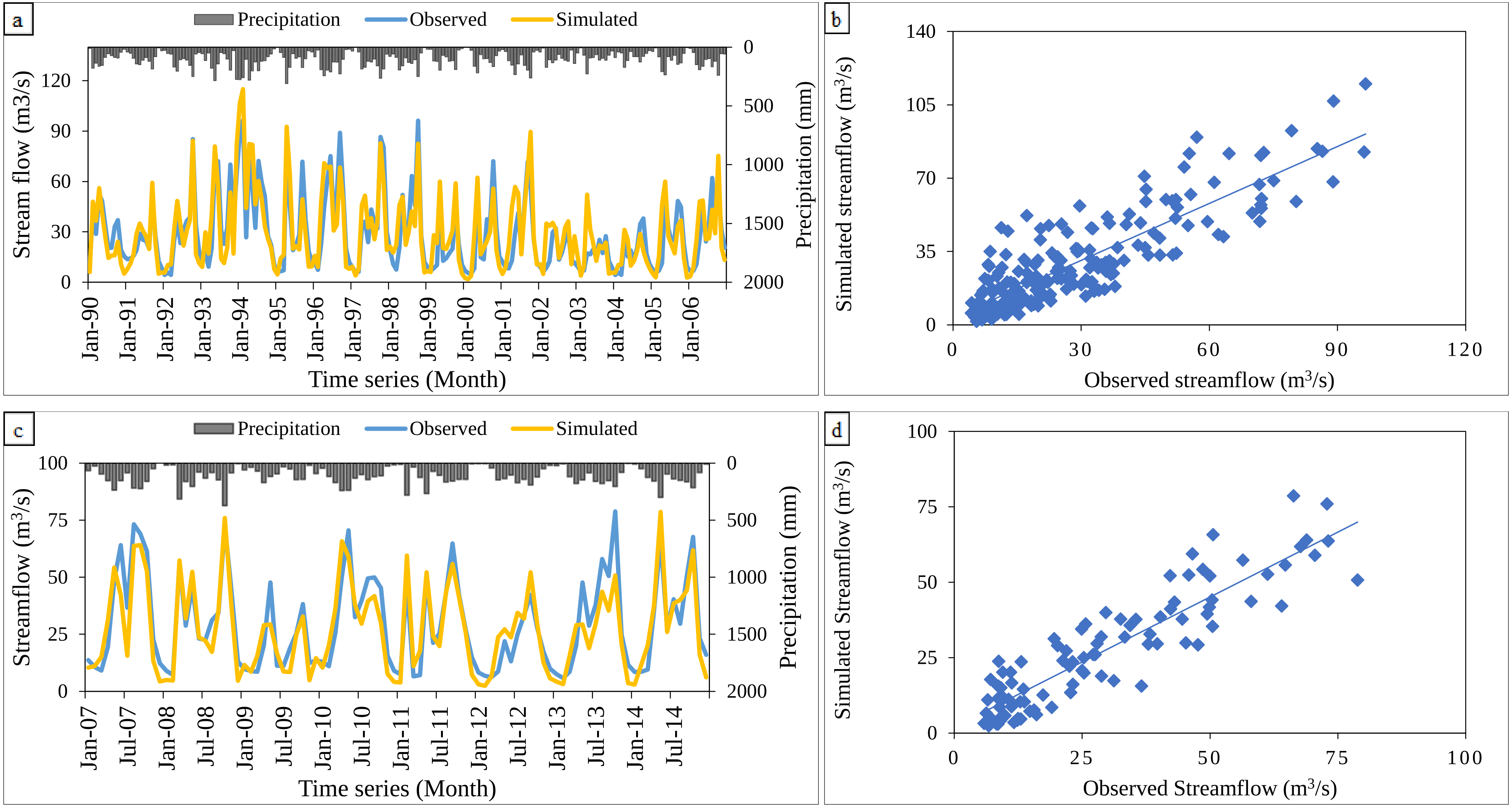

Figure 4.5. Observed and simulated streamflow hydrograph and scatter plot at Measso hydrometric station: (a) hydrograph during calibration period, (b) scatter plot during calibration period, (c) hydrograph during validation, (d) scatter plot during validation period

The possible explanation for the uncertainty of model simulation might arise from some of the model parameters considered to have negligible influence on streamflow. In addition to this, the lack of consistent hydro-metrological data and spatiotemporal data including soil and LULC data can also result in a slight discrepancy in the model simulation. But, the graphical interpretation together with the statistical measures given in Table 4.5 between measured and simulated data meets the criteria recommended (Moriasi et al., 2007). Therefore, the SWAT model performance evaluation by comparing the observed and simulated streamflow at calibration and validation period proved the SWAT model to be capable of simulating the streamflow in Gidabo watershed.

Table 4.5. Statistical analysis for streamflow calibration and validation periods

Performance Indicators	Aposto		Bedessa		Measso	
	Calibration	Validation	Calibration	Validation	Calibration	Validation
R^2	0.74	0.72	0.64	0.74	0.80	0.74
NSE	0.66	0.65	0.61	0.65	0.74	0.71
PBIAS	14.9	18.1	19.7	1.2	-3.2	8.0

4.3 Sediment Yield Modelling

4.3.1 Sediment yield sensitivity analysis

Sediment yield sensitivity analysis was carried out with ten sediment yield-related parameters obtained from a different piece of literature works using monthly observed sediment yield data in the SUFI-2 algorithm that linked with SWAT-CUP. The ranges of variation of these sediment yield parameters were based on absolute SWAT values which are illustrated in Appendix A.5. In the end, six parameters with the highest sensitive values were used for the calibration and validation process of the sediment. The six most sensitive sediment yield parameters during calibration and validation in the watershed are given in Figure 4.6 and the best optimized fitted parameters values during calibration are given in Table 4.6.

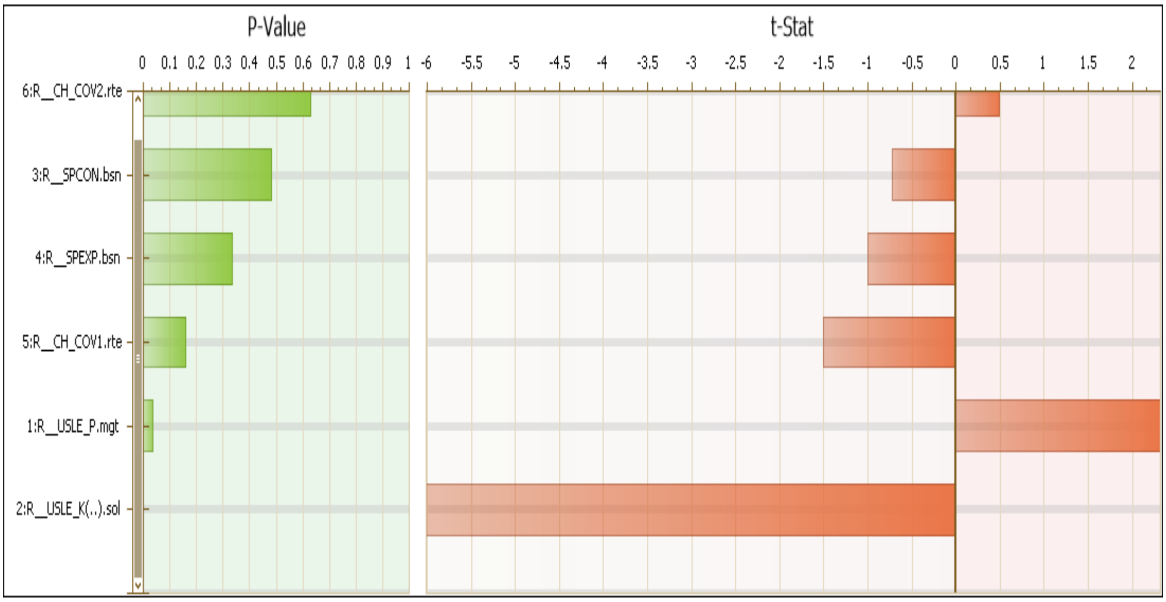

Figure 4.6. Sediment yield sensitive parameters

Among the parameters, the USLE soil erodibility factor (USLE_K) was the most sensitive parameter followed by the USLE support practice factor (USLE_P) and Channel erodibility factor (CH_COV1). USLE_K and USLE_P were found to be the most sensitive parameter which is in agreement with several other studies (example, Aghsaei et al., 2020; Kidane et al., 2019; Choto and Fetene, 2019). Exponent parameter for calculating sediment retrained in channel sediment routing (SPEX), the linear parameter for calculating the maximum amount of sediment that can be retrained during channel sediment routing (SPCON), and channel cover factor (CH_COV2) are also important parameters in sediment transport in Gidabo watershed.

Table 4.6. Sediment yield parameters sensitivity rank

Name	Min value	Max value	Fitted value	Rank
R_USLE_K	0.16	0.45	0.26	1
R_USLE_P	0.41	0.68	0.56	2
R_CH_COV1	0.05	0.36	0.13	3
R_SPEXP	1.30	1.42	1.34	4
R_SPCON	0.004	0.0096	0.009	5
R_CH_COV2	0.45	0.76	0.46	6

4.3.2 Sediment yield calibration and validation

SWAT-CUP calibration and validation for monthly sediment yield were conducted after the model was calibrated and validated for streamflow. Like streamflow calibration, the model was also calibrated for sediment yield at three gauged sub-basins for the period 1990-2006 with two year warmup period from the year 1988-1989. The sediment calibration was done with calibration in monthly time setup based on the sensitive sediment parameters identified after sediment sensitivity analysis. The SWAT model was found to simulate very well in Aposto, Bedessa, and Measso (near dam outlet) stations with statistical measures computed between the simulated and observed monthly sediment loads for the calibration periods. The performance indicator R^2 of 0.84, 0.77, and 0.87, NSE of 0.79, 0.71, and 0.85 whereas PBIAS of 12.8, 17.9, and 12.5 at Aposto, Bedessa, and Measso (near dam outlet) gauged stations were obtained respectively.

After successful calibration of the sediment, the SWAT model was validated to sediment yield with the same calibrated parameter without adjusting their fitted values. The sediment yield was validated using a different group of monthly measured data observed at Aposto, Bedessa, and Measso (near dam outlet) from the period 2007-2014. The performance of the model was also checked by performance indicators with R^2, NSE, and PBIAS. The performance of the model for sediment yield validation was R^2 of 0.80, 0.82, and 0.85, NSE of 0.68, 0.78, and 0.81, and PBIAS of 12.5, -0.9, and -6.8 at Aposto, Bedessa, and Measso (near dam outlet) respectively. Observed and simulated sediment yield hydrograph and scatter plot at three stations during calibration and validation are presented in Figures 4.7, 4.8, and 4.9.

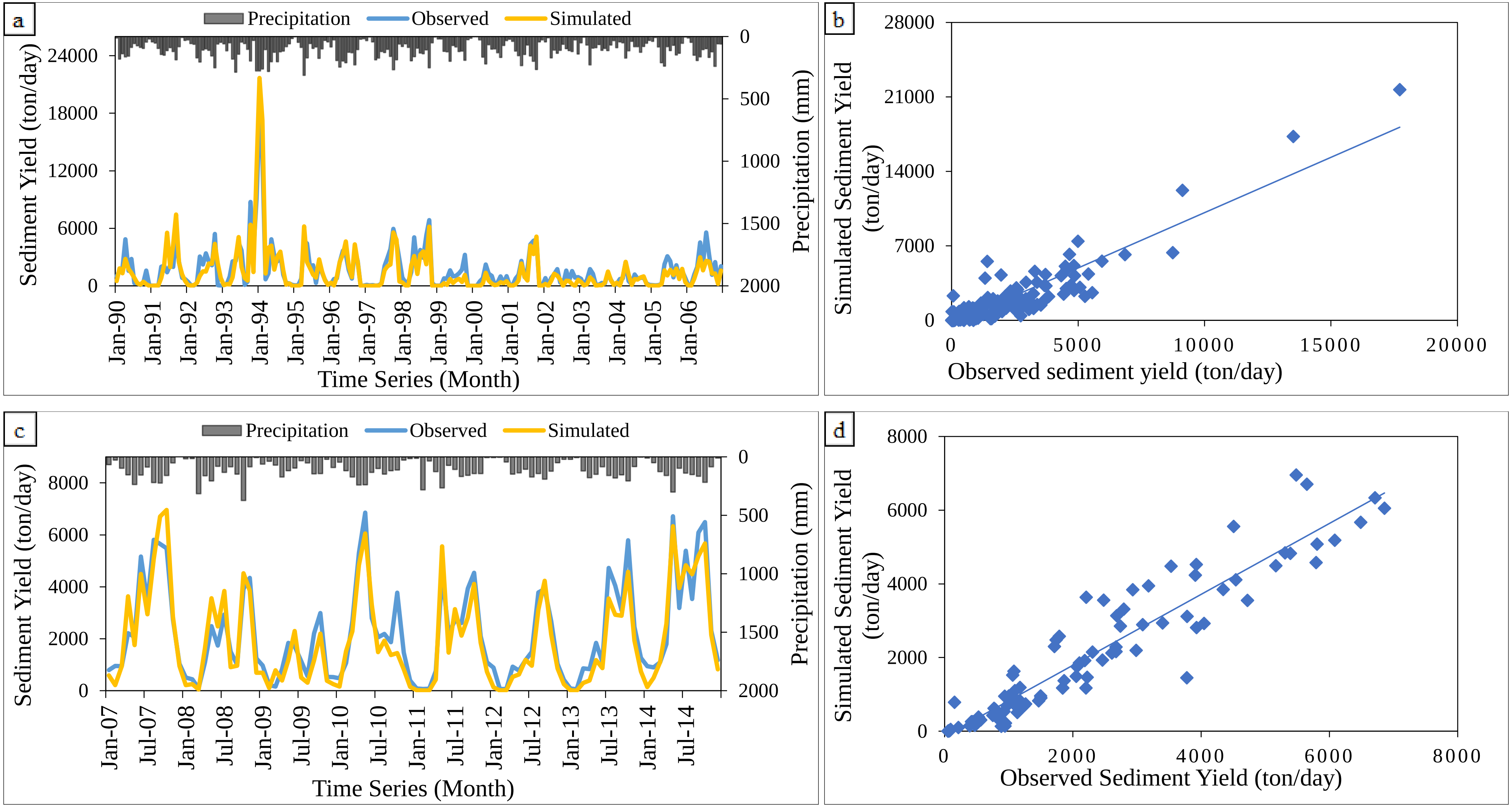

Figure 4.7. Observed and simulated sediment yield hydrograph and scatter plot at Aposto hydrometric station: (a) hydrograph during calibration period, (b) scatter plot during calibration period, (c) hydrograph during validation, (d) scatter plot during validation period

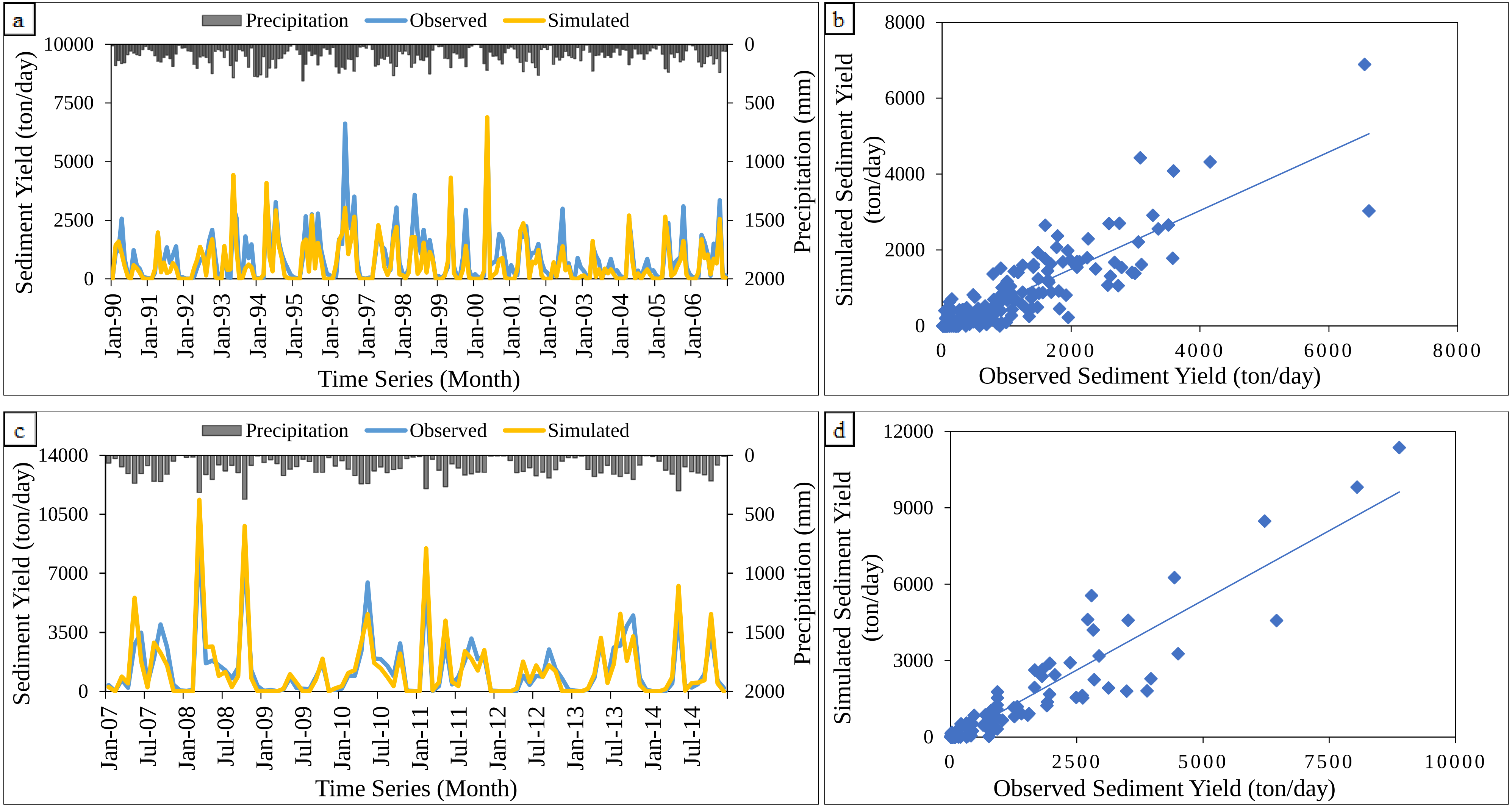

Figure 4.8. Observed and simulated sediment yield hydrograph and scatter plot at Bedessa hydrometric station: (a) hydrograph during calibration period, (b) scatter plot during calibration period, (c) hydrograph during validation period, (d) scatter plot during validation period

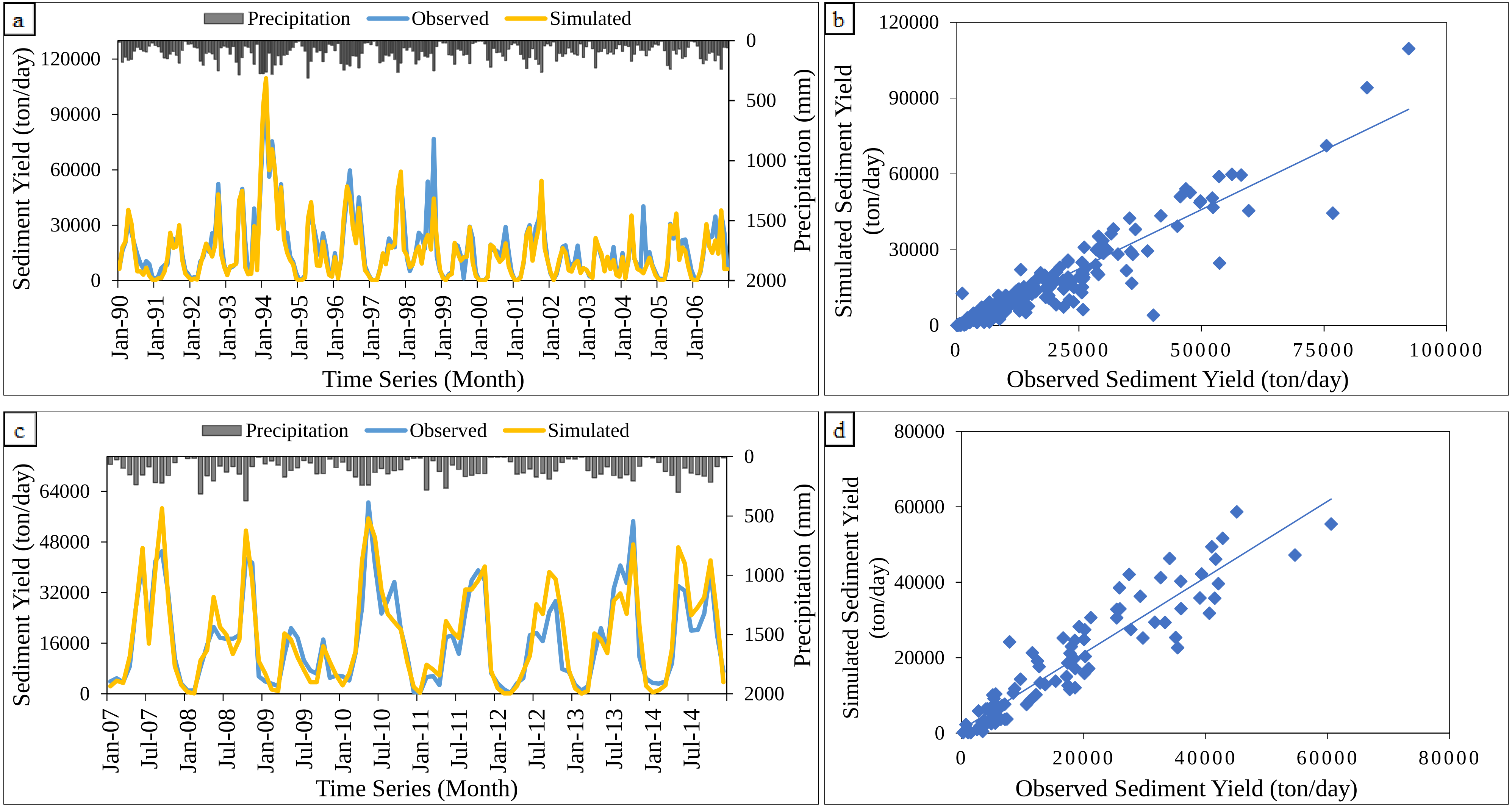

Figure 4.9. Observed and simulated sediment yield hydrograph and scatter plot at Measso hydrometric station: (a) hydrograph during calibration period, (b) scatter plot during calibration period, (c) hydrograph during validation period, (d) scatter plot during validation period

All values of the statistical indicators are between acceptable ranges during both calibration and validation periods. These indicate SWAT model has also capable of simulating sediment yield in the study area. During validation, a slight underestimation of sediment yield at Bedessa and Measso (near dam outlet) was obtained compared with calibration but still, the values are in recommended range both in calibration and validation. The R^2, NSE, and PBIAS values for the monthly calibration and validation sediment yield at three stations are shown in Table 4.7 below.

Table 4.7. Statistical analysis for sediment yield calibration and validation periods.

Performance Indicators	Aposto		Bedessa		Measso	
	Calibration	Validation	Calibration	Validation	Calibration	Validation
R^2	0.84	0.80	0.77	0.82	0.87	0.85
NSE	0.79	0.68	0.71	0.78	085	0.81
PBIAS	12.8	12.5	17.9	-0.9	12.5	-6.8

4.4 Streamflow and Sediment Yield Responses to Land Use Land Cover Change

The calibrated and validated SWAT model was used to evaluate the impact of the land use land cover (LULC) on the streamflow and sediment yield based on historical LULC of 1990, 2005, and 2019. The long-term hydrologic simulation from the year 1988-2014 was performed on monthly basis to analyze the impact of LULC change on streamflow and sediment yield at a particular watershed and sub-basins.

4.4.1 Streamflow responses to land use land cover change

The change of streamflow relative to LULC indicated that the mean annual stream value had increased by 1.16m^3/s (2.13%) and 2.04 m^3/s (3.62%) during the periods 1990-2005 and 2005-2019 respectively due to the LULC change. But, the mean monthly streamflow was increased for wet months (April-November) while decreased in dry months (October-March) in all three gauged stations as shown in Table 4.8. Streamflow from Aposto where a conversion of shrubland to agricultural land was observed, the mean monthly streamflow was increased up to 5.96% and 4.96% during wet months while decreased up to 7.59% and 5.78% during dry months from the period 1990-2005 and 2005-2019 respectively. In Bedessa sub-basins where forest land was converted to shrubland and agricultural land, the mean monthly streamflow was increased by 9.94 % and 12.46 % in wet months and decreased by 16.85 % and 5.97 % in dry months from 1990 to 2005 and 2005 to 2019, respectively.

The result of streamflow change at Measso near the dam outlet from the period 1990-2005 and 2005-2019 indicated that the streamflow was increased up to 6% and 4.45% in wet months and decreased by 8.51% and 5.04% in dry months respectively. The conversion of shrubland to agricultural and built-up land and the decline of forest land to shrubland in the study were highly responsible for the increment of streamflow during wet months and decrement during dry months. The expansion of agricultural land and built-up area over forest land shrubland results in the reduction of lateral flow (downward infiltration) that flows into the shallow aquifer. Hence, the streamflow during dry months that mostly comes from baseflow decreases whereas streamflow during the wet months increases. Because of this reason, streamflow responses to LULC are more sensitive in dry seasons in comparison with wet seasons. The streamflow change was high during the period 1990-2005 as compared with the period 2005-2019 due to LULC change. This is because of less expansion of agricultural land and less reduction of forest land in the second period (2005-2019) than the first period (1990-2005).

Table 4.8. Multi-site seasonal streamflow variation during 1990, 2005, and 2019 LULC

	Aposto			Bedessa			Measso		
Season	1990	2005	2019	1990	2005	2019	1990	2005	2019
Wet (m^3/s)	13.23	14.02	14.69	2.24	2.52	2.85	62.45	66.20	69.15
Dry (m^3/s)	8.65	7.99	7.53	1.53	1.28	1.20	36.32	33.23	31.56

The annual streamflow components such as surface runoff (SURQ), groundwater flow (GWQ), lateral flow (LATQ), and evapotranspiration (ET) based on three independent LULC indicated temporal variability in the watershed (Table 4.9). The streamflow component SURQ indicated increasing up to 8.12% and 14.60% for the period 1990-2005 and 2005-2019 respectively while GWQ, LATQ, and ET indicated decreasing trends. In other words, GWQ, LATQ, and ET contribution to streamflow was decreased by 0.90%, 2.15%, and 0.95% for the year 1990-2005 and decreased by 2.00%, 3.17%, and 2.90% respectively during 2005-2019. The increasing of SURQ and decreasing trend of GWQ, LATQ, and ET is directly attributed to the intensification of agricultural land, bare land,

and built-up area over forest land and shrubland. This expansion causes the increase of SURQ following rainfall and variation in lateral flow and groundwater storage.

Table 4.9. Average annual basin water balance value

LULC	RF (mm)	SURQ (mm)	LAT Q (mm)	GWQ (mm)	ET (mm)	WY (mm)
1990	1366.20	124.40	107.14	498.65	643.90	703.35
2005	1366.20	135.40	104.00	494.21	637.80	718.71
2019	1366.20	158.55	101.37	484.21	619.80	745.77

The result of previous studies in Ethiopia on the impact of LULC on watershed hydrological response has shown a decreasing trend in average monthly flow, GWQ, LATQ, and ET while the increasing trend in the wet average monthly flow, SURQ mean annual streamflow with a considerable expansion of agricultural over shrubland and forest land. Choto and Fetene (2019), Shawul et al. (2019), Gashaw et al. (2018), and Kassa (2009) in their studies reported that the expansion of agricultural land, bare land, and built-up area over forest and shrubland results in increasing of surface runoff and wet season streamflow while decreasing dry season streamflow, lateral flow, and groundwater storage. Therefore, the result revealed the change of land use land cover has a significant impact on stream as well as water balance components.

4.4.2 Sediment yield Responses to land use land cover change

The land use land cover change impact on the annual average sediment yield in Gidabo watershed is much greater than its effect on the streamflow of the watershed. The annual sediment yield of Gidabo watershed indicated high temporal variation due to LULC. Sediment yield was increased by 44% during 1990-2005 and increased up to 47.38% during 2005-2019. The watershed was contributed the total annual sediment yield of 4.39 t/ha, 7.84 t/ha, and 14.89 t/ha with simulated LULC of 1990, 2005, and 2019 respectively. This increasing trend of sediment yield was also similar in Aposto and Bedessa stations due to LULC change.

The amount of annual average sediment yield was increased up to 32.2% and 31.3% during 1990-2005 and also increased by 1.96% and 86.65% during 2005-2019 at Apost and Bedessa respectively. During the period 2005-2019, the increasing rate was very low in Aposto due to the less reduction in vegetation cover while very high in Bedessa due to a series reduction of forest land in sub-basins compared with the period 1990-2005. The high impact of LULC change on sediment yield obtained was due to the increasing trend of agricultural, bare land, built-up area over shrubland and forest land in the watershed which increases surface runoff and sediment yield following rainfall events in the watershed. The increase of cultivation land and bare land over forest and shrubland during the study period facilitates the looseness and movement of soil particles easily especially during high peak flow since soil erosion has a direct relationship with the surface runoff and streamflow.

The increase of surface runoff by 11 mm and 23.15 mm for two consecutive periods contributes to the increasing of the sediment yield. The high amount of soil erosion and sedimentation in the study area happens during the heavy rainfall period (April and May) in which much of the precipitation becomes surface runoff generating higher peak flow which in turn causes higher sediment yield as shown in Figure 4.10. Similarly in the Ethiopian highlands, Zeleke and Hurni (2001), Welde and Gebremariam (2017), Moges and Bhat (2018), Kidane et al. (2019), and Choto and Fetene (2019) reported the continuous expansion of agricultural, bare land, and built-up areas at the expense of vegetation cover in their study area have increased the rate of soil erosion and sediment yield. Hence, the land use land cover dynamics have a great impact on catchment soil erosion and sediment yield.

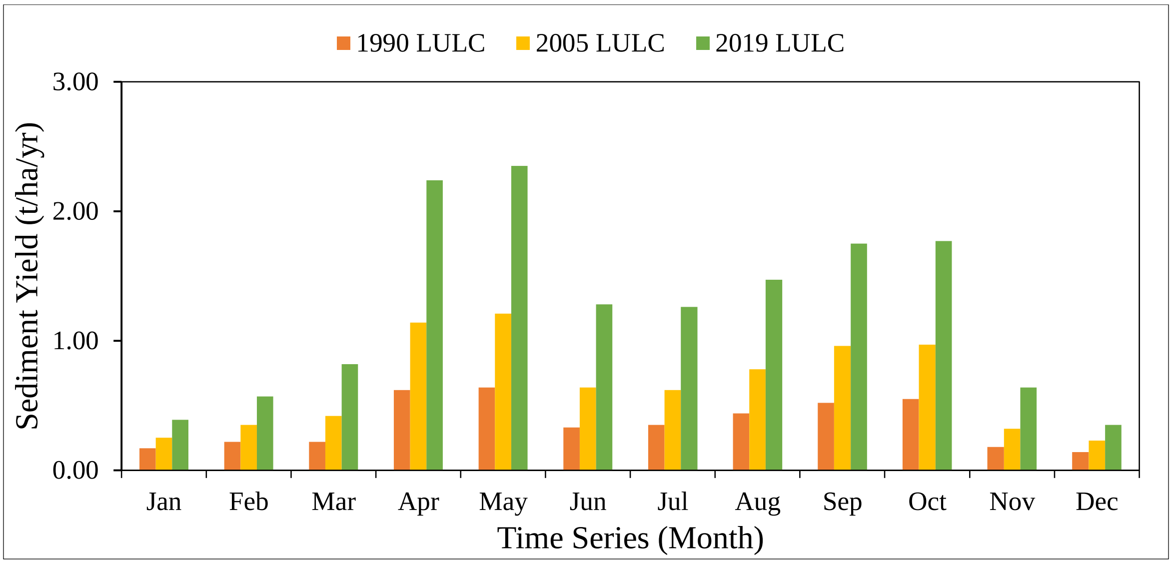

Figure 4.10. Monthly average sediment yield during 1990, 2005, and 2019 LULC

4.5 Spatial Distribution of Sediment Yield and Prioritization of Critical Sub-Basins

Variation in topography, soil type, and land use land cover, rainfall characteristics, and management conditions over the watershed results in spatial variability in surface runoff and sediment yield. The SWAT model simulated with 2019 LULC indicated the total annual amount of sediment yield from the watershed that entering to Gidabo dam reservoir estimated was 3,540,842 t/yr. This large amount of sediment yield has a great impact on the reservoir life and sustainable water supply for irrigation located downstream of Gidabo dam. A few sub-watersheds in a large watershed are more critical and responsible for a high amount of runoff and soil losses.

The contribution of average annual surface runoff and sediment yield from each sub-basins are varied from 26.9 mm to 584.4 mm and 0.0001 t/ha/yr to 97.01 t/ha/yr respectively. The highest amount of sediment yield is observed mainly in sub-basins dominated by agricultural and bare lands while low sediment yield is observed in the sub-basins covered mainly with dense forest followed by shrublands. Hence, to control the soil loss entering into the reservoir assessment of the spatial variability of sediment yield and identifying the most critical sediment source is very important for watershed management and planning.

The research worked to estimate soil erosion in Ethiopia by Hurni (1985), the range of the tolerable soil loss level for various agro-ecological zones of Ethiopia was found from 2 to 18 t/ha/yr. Accordingly, the simulated soil loss rate of 10 sub-basins from 39 sub-basins in the Gidabo watershed exceeds the maximum tolerable soil loss rate (18 t/ha/yr) which indicates sedimentation is a serious threat to the study area. From the spatial distribution of sediment yield (Figure 4.11), 10 sub-basins (19, 20, 21, 23, 24, 25 28, 29, 32, and 36) are identified most critical sediment source which produces average annual sediment yields above 41.97 t/ha/yr. The HRU distribution of the identified sub-basins indicates agricultural and bare land is the major controlling factor for runoff and sediment potential areas.

Surface runoff and sediment yield had a direct relationship since surface runoff influences detaching and moving soil particles. Most of the sub-watersheds that generate a high amount of surface runoff produce a high amount of sediment yield as illustrated in Figure 4.11. However, some sub-basins like 10, 16, 22, 27, 34, and 39 generate relatively high annual average surface runoff but produce tolerable annual average sediment yield, and sub-basins like 6, 24, and 31 generate low annual average surface runoff and produces a high annual average amount of sediment yields as compared with other sub-watersheds. This indicates, surface runoff alone is not the only major factor on sediment yield production but also land use land cover, topography, soil characteristics, and management practices are major factors on sediment yield.

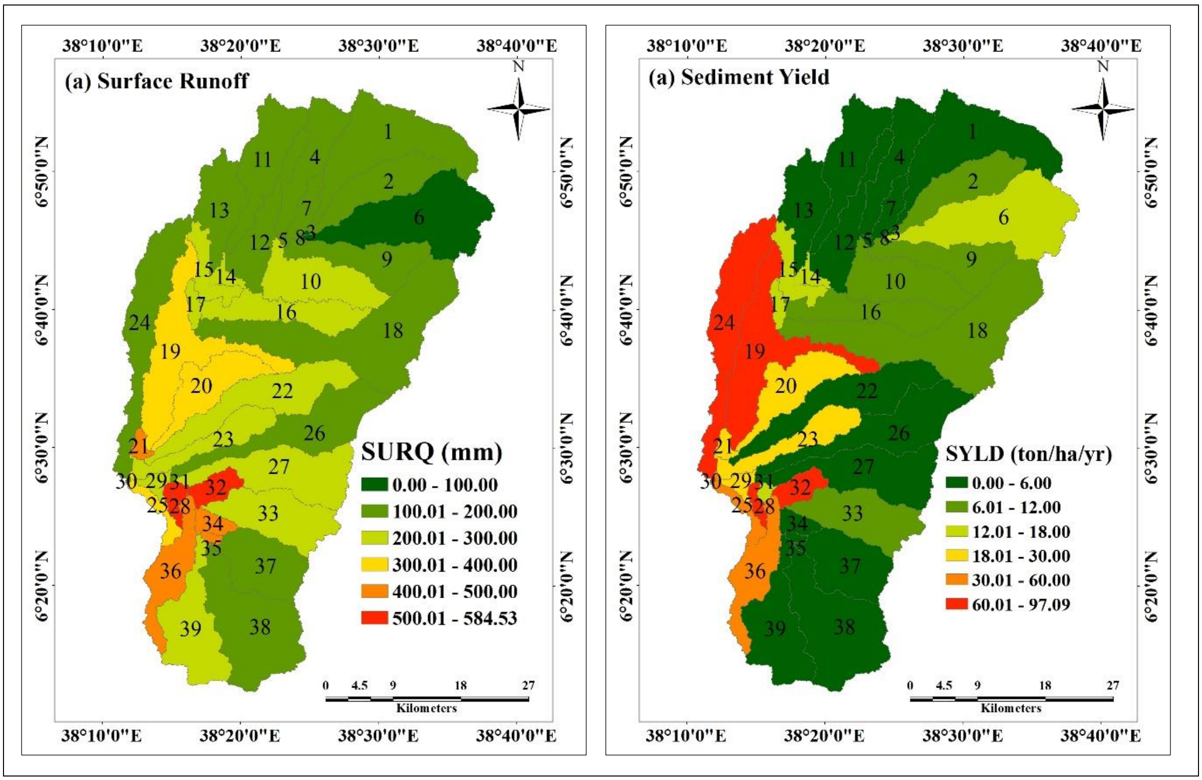

Figure 4.11. Spatial distribution of (a) surface runoff and (b) sediment yield in the study area

For instance, sub-basin 24 generates relatively low surface runoff but the sub-basin is covered with 51.9% agricultural land and 39.8% bare land with 47.1% Pellic vertisols soil types. In this sub-basin slope class, 10-20% is dominant with 41.7% area coverage. On another hand, sub-basin 39 generates a relatively high amount of surface runoff and produces a low amount of sediment yield because the sub-basin is covered with 65% forest land and 74.2% Dystric cambisols with 39% of 10-20% slope class. It can be concluded that land use land cover is the dominant factor for high sediment yield production rather than surface runoff in sub-basin while in sub-basin 39 land use land cover and topography are a factor for low sediment yield production.

Tesema and Leta (2020) in Kesem dam watershed and Nadew et al. (2019) in Guder watershed also identified the sub-basins that generates a high amount of surface runoff but produce a low amount of sediment yield and finally, they concluded that surface runoff in alone has not to impact on sediment yield. Therefore, high surface runoff does not give always result in high sediment production in alone but land use land cover, slope and soil type is the factors for sedimentation. In this study, 10 sub-basins (19, 20, 21, 23, 24, 25 28, 29, 32, and 36) identified as critical sediment source for watershed management purpose to reduce the severity of sedimentation in Gidabo dam reservoir.

4.6 Effectiveness of Best Management Practices

According to spatial variability of sediment source and sediment yield rate, best management practices (BMPs) scenarios were considered and developed. The selected BMPs were simulated in the SWAT model to identify the effectiveness in reducing surface runoff as well as sediment yield of the Gidabo watersheds. In this study, three different BMPs scenarios were developed and compared with the existing condition (baseline scenario). A simulation was performed for each scenario individually after changing appropriate parameter values with corresponding management practices. The scenario used and the stated parameters are illustrated in Table 4.10.

Table 4.10. Modified SWAT parameters

Scenarios	Description	Parameter Name		Calibrated Value	Modified Value
S0	Baseline	-		-	-
S1	Filter strip	FILTERW		0	1 m 3 m 5 m
S2	Terracing	SLSUBBSN	Slope 0-5%	91.46	60 m
			Slope 5-10%	60.97	35 m
			Slope 10-20%	24.39	15 m
			Slope > 20%	9.14	8 m
		USLE_P		0.56	0.18
S3	Reforestation	10% AGRL, 20% FRST, and 50% BARR			

Scenario-0 (Baseline) was implemented without best management practices to reflect the existing conditions. The baseline scenario reflects the current land management practices (2019 LULC) without conservation.

Scenario-1 (Filter strip) was implemented on all agricultural HRUs that are along with all soil types and slope classes to filter the runoff and traps the sediment in a given agricultural plot of identified critical sub-basins. The impact of the filter strip on sediment trapping was evaluated by assigning a FILTERW value of 1, 3, and 5 m that reflects the width of the filter strip. Accordingly, treating the soil erosion and sediment yield prone sub-basins with a 5 m wide filter strip reduced their sediment yield by 54.27% to 93.97%. It also reduced the average annual sediment yield to 6.09 t/ha/yr which is 59.06% of the average annual baseline value.

Implementing a 3 m and 1 m wide filter strip in critical sub-basins reduced annual sediment yield by 29.11% to 90.20% and 44.93% to 92.27% with an annual sediment reduction of 50.74% and 55.97% of the baseline value which is 6.56 t/ha/yr and 7.34 t/ha/yr respectively. These results are consistent and similar with the previous research work in Ethiopian highlands by Nadew et al. (2019) and Tesema and Leta (2020) at Guder watershed and Kessem dam watershed respectively. Nadew et al. (2019) reported 48% of annual average sediment yield reduction by applying a 5 m wide filter strip in Guder watershed. Similarly, Tesema and Leta (2020) reported 59.2% and 72.7% of annual average sediment yield reduction compared with baseline value by implementing 5 m and 10 m wide filter strip in Kessem dam watershed.

Scenario-2 (Parallel terraces) were applied on agricultural and bare land HRUs combined with all soil types, and slope classes of 0-5%, 5-10%, 10-20%, and greater than 20% to reduce overland flow, sheet erosion, and slope length. To represent the effect of parallel terrace and stone bund, appropriate SWAT parameters such as average slope length (SLSUBBSN) and USLE support practice (USLE_P) were modified. Based on the slope classes, the assigned SLSUBBSN parameter values by SWAT were 91.46 m, 60.98 m, 24.39 m, and 9.14 m for slope class 0-5%, 5-10%, 10-20%, and over 20% respectively. The SLSUBBSN represents the spacing between successive traces at field conditions that were modified to 60 m, 35 m, 15 m, and 8 m for the above slope classes based on Equation 3.23. USLE support practice (USLE_P) was obtained from the SWAT user's manual version 2012 for terraced conditions (Neitsch et al., 2012).

Implementing the terracing management option reduced the average annual sediment yields from critical sediment yielding sub-basins by 64.06% to 95.72%. This reduction of sediment yield from the critical sub-basins caused in reduction to average annual sediment yield to 5.36 t/ha/yr by 64.02% from the Gidabo watershed. Similarly, Betrie et al. (2010) and Tesema and Leta (2020) reported applying terracing management helps in average annual watershed sediment yield reduction 41% and 63% in the Blue Nile basin and Kessem dam watershed respectively. Therefore, applying terracing management on the watershed is one of the options to reduce considerable sediment yield by reducing runoff and soil erosion.

In scenario-3 (Reforestation), the impact of reforestation on sediment yield reduction was simulated. A good vegetative cover provides the best, least cost, and long-term protection against erosion by insulating the soil against direct raindrop impact and enhancing infiltration (Morris and Fan, 1998). It is difficult and impractical to change agricultural land into evergreen forest land due to increasing population growth and food demand. Thus, reforestation of 10% of agricultural land, 20% shrubland, and complete reforestation of bare land on sediment-prone areas from the recent (2019) LULC were considered and the amount of sediment yield reduction in Gidabo watershed was estimated.

The evergreen forest was selected because it provides adequate cover against rainfall throughout the year. The reforestation scenario has reduced the average sediment annual yield by 27.12% to 89.33% in sediment yield critical sub-basins. Reforestation reduced the annual average Gidabo watershed sediment yield to 8.84 t/ha/yr by 40.67% of the baseline value. Betrie et al. (2010) and Choto and Fetene (2019) also shown the reduction of sediment yield by 11% in the Blue Nile basin and 32.3% in the Gojeb watershed of Ethiopian highlands respectively by applying reforestation.

4.6.1 Comparison of best management practices

The result of sediment yield reduction by applying conservation measures was compared with the simulation result of the existing conditions (baseline scenario). In comparison with the baseline scenario, the implemented watershed management options (Filter strips, Terracing, and Reforestation) indicated a high influence on the sediment yield reduction of the critical sub-basins as shown in Figures 4.12 and 4.13. Table 4.11 summarizes the impact of each management option in sediment yield reduction.

Table 4.11. Comparison best management practices in the study area

Scenario	BMPs		Sediment yield (t/ha/yr)	Reduction (%)
S0	Baseline		14.9	-
		1 m	7.34	50.73
S1	Filter strip	3 m	6.56	55.97
		5 m	6.09	59.12
S2	Terracing		5.36	64.02
S3	Reforestation		8.84	40.67

From implemented management options, applying of terracing management option in critical sub-basins shown the highest sediment reduction in critical sub-watershed as well as watershed-level followed by filter strips and reforestation. This indicates that the use of terracing can potentially make improvements marked by the control and limitation of soil erosion. This is consistent with previous research (Bracmort et al., 2006; Briak et al., 2019; Betrie et al., 2010; Nadew et al., 2019; Tesema and Leta, 2020). Hence, the selection of sediment management options has a great implication on the downstream system of the watershed, amount of sedimentation and life span of the Gidabo dam, irrigation project infrastructures such as canal, and irrigation project sustainability. The results would provide useful information for policymakers, practitioners, and water resource engineers to implement the most effective BMPs with in the watershed or in other similar watersheds.

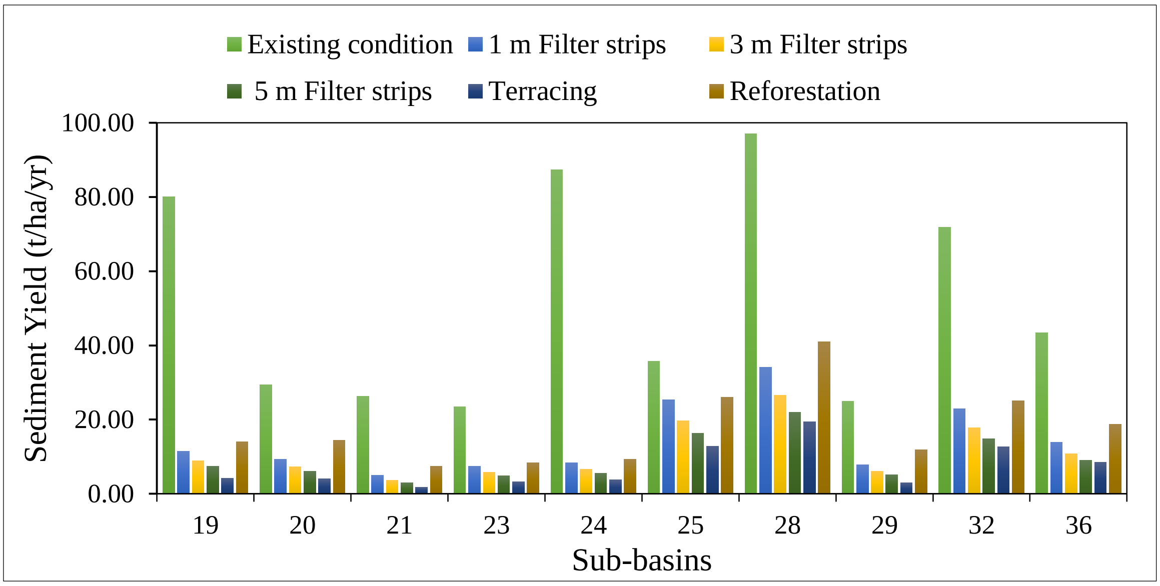

Figure 4.12. Comparison of best management practices in critical sub-basins

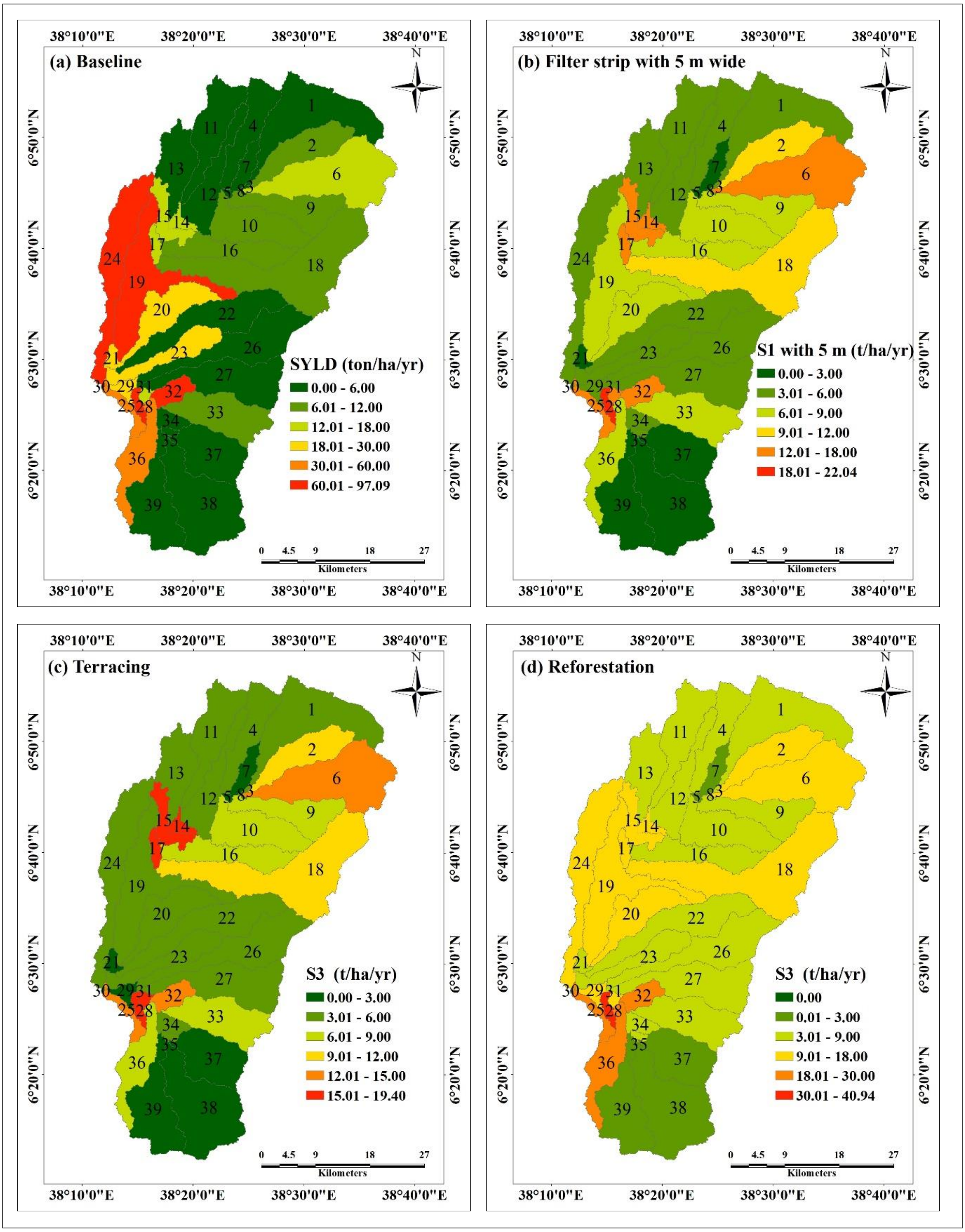

Figure 4.13. Comparison of best management practices sediment yield spatial distribution

5. CONCLUSIONS AND RECOMMENDATIONS

5.1 Conclusions

In this study, the impact of land use land cover (LULC) change on Gidabo watershed for the last 30 years was examined and best management practices were developed to alleviate sediment yield in the Gidabo watershed. The remotely sensed data of 1990, 2005, and 2019 were classified using ERDAS Imagine 2014 integrated with GIS data to analyze spatiotemporal LULC dynamics in the study area. The analysis of 1990, 2005, and 2019 LULC indicates, Gidabo watershed had experienced significant changes in the land use land cover over the past 30 years.

There were increasing in agricultural land, built-up area, and bare land whereas decreasing forest land, shrubland, and water body for the two consecutive periods (1990-2005 and 2005-2019). Agricultural land was increased by 5.79% but forest land and shrubland were decreased by 5.43% and 2.72% for the period 1990-2005. For the period 2005-2019 a slight increase in agricultural and a decrease in forest land with the high decrement of shrubland were obtained as compared with the first period. The result revealed that agricultural land was increased by 3.11% and forest land and shrubland were decreased 1.68% and 4.81% respectively. Rapid population growth in the area is the reason for the expansion of agricultural land which later causes a reduction in forest land and shrubland.

The impact of land use land cover dynamics on streamflow and sediment yield was evaluated using the hydrological SWAT model in the Gidabo watershed. A SWAT model was calibrated for the period 1990-2006 and validated for the period 2007-2014 for streamflow and sediment yield at multi-site stations of Aposto, Bedessa, and Measso (near dam outlet) in Gidabo watershed using SWAT-CUP. The performance of the SWAT model was evaluated using model performance indicators such as Coefficient of determination (R^2), Nash-Sutcliffe model efficiency (NSE), and percent bias (PBIAS) for streamflow and sediment yield simulation for calibration and validation were found to be in the acceptable range. This indicated the applicability of the SWAT model in simulating streamflow and sediment yield in Gidabo watershed. Thus, the model simulation result provides confidence for the further application of the model to analyze hydrologic response due to spatiotemporal watershed characteristics in Gidabo watersheds.

The changes in land use land cover resulted in streamflow and sediment yield changes. Comparison of simulated outputs of the model using 1990, 2005 and 2019 LULC indicated an increase of average annual streamflow by 1.16m^3/s (2.13%) and 2.04 m^3/s (3.62%) during the period 1990-2005 and 2005-2019 respectively. But, the mean monthly streamflow was increased for wet months while decreased in dry months. The land use land cover change impact on the annual average sediment yield in Gidabo watershed is much greater than its effect on the streamflow of the watershed. The LULC on sediment yield was increased by 44% during 1990-2005 and increased up to 47.38% during 2005-2019. The watershed was contributed the total annual sediment yield of 4.39 t/ha, 7.84 t/ha, and 14.89 t/ha with simulated LULC of 1990, 2005, and 2019 respectively. Generally, the expansion of agricultural land, bare land, and built-up area over forest land and shrubland which leads to increasing surface runoff and decreasing of lateral flow was highly responsible for increasing wet season streamflow and sediment yield.

Variation in topography, soil type, and land use land cover, and rainfall characteristics over the watershed results in spatial variability in surface runoff and sediment yield. Hence, out of 39 sub-basins, 10 sub-watersheds (19, 20, 21, 23, 24, 25 28, 29, 32, and 36) were identified as most critical sediment sources. Those sub-watersheds require attention for best management practices in the watershed to reduce the severity of sedimentation in Gidabo dam reservoir. Accordingly, three BMPs namely filter strips, terracing, and reforestation were simulated and tested using the SWAT model concerning sediment yield reduction. The result revealed that the terracing management option was the most effective conservation measure with 64.02% sediment yield reduction efficiencies. Implementing filter strips with 5m, 3 m, and 1 m wide indicated 59.12%, 55.97%, and 50.73% reduction respectively whereas, reforestation has given the least reduction of sediment yield that is 40.98% reduction. Furthermore, the simulation of best management practices (BMPs) by the SWAT model provides a great implication on the most effective practice for reducing sediment yield and the results would provide useful information for policymakers, practitioners, and water resource engineers to implement the most effective BMPs within the study area.

5.2 Recommendations

According to the research results, the following major recommendations are made:

- This study considered only historic land use land cover change but future researchers should include changes of future other variables like climate change because it has its impact on the hydrological response of the catchment.
- Data quality and availability are very important while using distributed hydrological models. In this study, metrological data missing and limitation of measured streamflow and sediment data at the outlet of the watershed were the biggest challenges. Without proper data, model implementation is impossible and very difficult. Therefore, the issue that concerns the local, regional, and federal authorities should be involved in integrated and coordinated data compilation.
- Non-tolerable sediment source areas of Gidabo watershed were identified and prioritized in this study for the future management plan of mitigating sedimentation issues in Gidabo dam reservoir. Hence, best sediment management practices should have to be encouraged in hot spot areas to reducing sediment loads that flow to the dam. Moreover, implementing terracing management options with other conservation measures has to be encouraged and should be implemented to increase the life span of the reservoir and for sustainable water supply for the irrigation project located downstream of the Gidabo dam.
- Financial and economic impact analysis of Gidabo dam reservoir sedimentation on sustainable irrigation water supply and cost analysis on the watershed management options is also recommended for future studies that help the decision-makers to take immediate action.

REFERENCES

Abbaspour, K. C., Vaghefi, S. A., and Srinivasan, R. (2017). A guideline for successful calibration and uncertainty analysis for soil and water assessment: A review of papers from the 2016 international SWAT conference. *Water (Switzerland)*, *10*(1). https://doi.org/10.3390/w10010006

Abbaspour, K., Vejdani, M., and Haghighat, S. (2007). SWAT-CUP calibration and validation uncertainty programs for SWAT. *Intl. Congress on Modelling and Simulation (MODSIM 07).*

Abebe, T., and Gebremariam, B. (2019). Modeling runoff and sediment yield of Kesem dam watershed, Awash basin, Ethiopia. *SN Applied Sciences*, *1*(5), 1-13. https://doi.org/10.1007/s42452-019-0347-1

Abraham, and Nadew. (2018). Impact of land use land cover dynamics on water balance, Lake Ziway watershed, Ethiopia. *Hydrology: Current Research*, *9*(4), 309.

Adeba, D., Kansal, M. L., and Sen, S. (2015). Assessment of water scarcity and its impacts on sustainable development in Awash basin, Ethiopia. *Sustainable Water Resources Management*, *1*(1), 71-87. https://doi.org/10.1007/s40899-015-0006-7

Adepoju, M. O., Millington, A. C., and Tansey, K. T. (2006). Land use/land cover change detection in metropolitan Lagos (Nigeria): 1984-2002. *American Society for Photogrammetry and Remote Sensing - Annual Conference of the American Society for Photogrammetry and Remote Sensing 2006: Prospecting for Geospatial Information Integration*, *1*, 8-14.

Aghsaei, H., Mobarghaee Dinan, N., Moridi, A., Asadolahi, Z., Delavar, M., Fohrer, N., and Wagner, P. D. (2020). Effects of dynamic land use/land cover change on water resources and sediment yield in the Anzali wetland catchment, Gilan, Iran. *Science of the Total Environment*, *712*, 136449. https://doi.org/10.1016/j.scitotenv.2019.136449

Akbari, S., and Singh, R. (2012). Hydrological modeling of catchments using MIKE SHE. *IEEE-International Conference on Advances in Engineering, Science and Management*, 335-340.

Alawamy, J. S., Balasundram, S. K., Hanif, A. H. M., and Sung, C. T. B. (2020). Detecting and analyzing land use and land cover changes in the Region of Al-Jabal Al-Akhdar, Libya using time-series Landsat data from 1985 to 2017. *Sustainability (Switzerland)*, *12*(11). https://doi.org/10.3390/su12114490

Arabi, M., Govindaraju, R. S., Hantush, M. M., and Engel, B. A. (2006). Role of watershed sub-divisions on modeling the effectiveness of best management practices using SWAT. *JAWRA Journal of the American Water Resources Association*, *42*(2), 513-528. https://doi.org/https://doi.org/10.1111/j.1752-1688.2006.tb03854.x

Arnold, J. G., Moriasi, D. N., Gassman, P. W., Abbaspour, K. C., White, M. J., Srinivasan, R., Santhi, C., Harmel, R. D., Van Griensven, A., Van Liew, M. W., Kannan, N., and Jha, M. K. (2012). SWAT: Model use, calibration, and validation. *Transactions of the ASABE*, *55*(4), 1491-1508.

Arnold, J. G., Williams, J. R., and Maidment, D. R. (1995). Continuous-time water and sediment-routing model for large basins. *Journal of Hydraulic Engineering*, *121*(2), 171-183. https://doi.org/10.1061/(ASCE)0733-9429(1995)121:2(171)

Bekele, D., Alamirew, T., Kebede, A., Zeleke, G., and Melesse, A. M. (2019). Land use and land cover dynamics in the Keleta watershed, Awash River basin, Ethiopia. *Environmental Hazards*, *18*(3), 246-265. https://doi.org/10.1080/17477891.2018.1561407

Betrie, G. D., Mohamed, Y. A., Griensven, A. Van, and Srinivasan, R. (2010). Sediment management modeling in Blue Nile Basin using SWAT model. *Hydrology and Earth System Sciences Discussions*, *7*(4), 5497-5524. https://doi.org/10.5194/hessd-7-5497-2010

Bewket, W., and Sterk, G. (2005). Dynamics in land cover and its effect on streamflow in the Chemoga watershed, Blue Nile basin, Ethiopia. *Hydrological Processes*, *19*(2), 445-458. https://doi.org/10.1002/hyp.5542

Bhatia, A. K., and Thawait, A. K. (2015). Impact assessment of BMP scenarios on sediment yield in the Mohgaon watershed. *International Journal of Engineering Research*, *4*(6), 23-27. https://doi.org/10.17577/ijertv4is060013

Bracmort, K. S., Arabi, M., Frankenberger, J. R., Engel, B. A., and Arnold, J. G. (2006). Modeling long-term water quality impact of structural BMPs. *Transactions of the ASABE*, *49*(2), 367-374.

Briak, H., Mrabet, R., Moussadek, R., and Aboumaria, K. (2019). Use of a calibrated SWAT model to evaluate the effects of agricultural BMPs on sediments of the Kalaya river basin (North of Morocco). *International Soil and Water Conservation Research*, *7*(2), 176-183. https://doi.org/10.1016/j.iswcr.2019.02.002

Burrough, P. A., and McDonnell, R. A. (1998). *Principles of geographical information systems*.

Chen, S. M., Wang, Y. M., and Tsou, I. (2013). Using artificial neural network approach for modeling rainfall-runoff due to typhoon. *Earth System Science*, *122*, 399-405. http://dx.doi.org/10.1007/s12040-013-0289-8

Choto, M., and Fetene, A. (2019). Impacts of land use/land cover change on streamflow and sediment yield of Gojeb watershed, Omo-Gibe basin, Ethiopia. *Remote Sensing Applications: Society and Environment*, *14*, 84-99. https://doi.org/10.1016/j.rsase.2019.01.003

Choubin, B., Soleimani, F., Pirnia, A., Sajedi-Hosseini, F., Alilou, H., Rahmati, O., Melesse, A. M., Singh, V. P., and Shahabi, H. (2019). Effects of drought on vegetative cover changes: Investigating spatiotemporal patterns. *Extreme Hydrology and Climate Variability: Monitoring, Modelling, Adaptation and Mitigation*, *2*, 213-222. https://doi.org/10.1016/B978-0-12-815998-9.00017-8

Chow, V., Maidment, D. R., and Mays, L. W. (1988). *Applied Hydrology*. McGraw-Hill.

Cunderlik, M. J. (2003). *Hydrologic model selection for the CFCAS project: Assessment of Water Resources Risk and Vulnerability to Changing Climatic Conditions*.

Desta, L., Volli, C., Asrat, W. A., and Yiteyew, A. (2005). *Community-Based Participatory Watershed Development: A Guideline. Federal Democratic Republic of Ethiopia Ministry of Agriculture and Rural Development, Addis Ababa, Ethiopia*.

Dibaba, W. T., Demissie, T. A., and Miegel, K. (2020). Watershed hydrological response to combined land use/land cover and climate change in highland Ethiopia: Finchaa catchment. *Water (Switzerland), 12*(6). https://doi.org/10.3390/w12061801

Dwarakish, G. S., and Ganasri, B. P. (2015). Impact of land-use change on hydrological systems: A review of current modeling approaches. *Cogent Geoscience, 1*(1). https://doi.org/10.1080/23312041.2015.1115691

Elfert, S., and Bormann, H. (2010). Simulated impact of past and possible future land-use changes on the hydrological response of the Northern German lowland Hunte catchment. *Hydrology*, *383*, 245-255. http://dx.doi.org/10.1016/j.jhydrol.2009.12.040

Elias, E., Seifu, W., Tesfaye, B., and Girmay, W. (2019). Impact of land use/cover changes on lake ecosystem of Ethiopia central rift valley. *Cogent Food and Agriculture*, *5*(1), 1595876. https://doi.org/10.1080/23311932.2019.1595876

Erle, E., and Pontius, R. (2007). Land-use and land-cover change. In *Earth. (Eds.).* (Cutler J.). Environmental Information Coalition, National Council for Science and the Environment.

Esa, E., Assen, M., and Legass, A. (2018). Implications of land use/cover dynamics on soil erosion potential in an agricultural watershed, northwestern highlands of Ethiopia. *Environmental Systems Research*, *7*(1). https://doi.org/10.1186/s40068-018-0122-0

FAO. (2002). *Major soils of the world land and water digital media series, Rome: CD-ROM 2002*.

Gashaw, T., Tulu, T., Argaw, M., and Worqlul, A. W. (2018). Modeling the hydrological impacts of land use/land cover changes in the Andassa watershed, Blue Nile Basin, Ethiopia. *Science of the Total Environment*, *619*(620), 1394-1408. https://doi.org/10.1016/j.scitotenv.2017.11.191

Gassman, P. W., Reyes, M. R., Green, C. H., and Arnold, J. G. (2007). The soil and water assessment tool: historical development, applications, and future research directions. *Transactions of the ASABE*, *50*(4), 1211-1250.

Getachew, H. E., and Melesse, A. M. (2012). The Impact of Land Use Change on the Hydrology of the Angereb Watershed, Ethiopia. *International Journal of Water Sciences*, 1. https://doi.org/10.5772/56266

Gianfagna, C. C., Johnson, C. E., Chandler, D. G., and Hofmann, C. (2015). Watershed area ratio accurately predicts daily streamflow in nested catchments in the Catskills, New York. *Journal of Hydrology: Regional Studies*, *4*, 583-594. https://doi.org/10.1016/j.ejrh.2015.09.002

Guzha, A. C., Rufino, M. C., Okoth, S., Jacobs, S., and Nóbrega, R. L. B. (2018). Impacts of land use and land cover change on surface runoff, discharge, and low flows: Evidence from East Africa. *Journal of Hydrology: Regional Studies*, *15*, 49-67. https://doi.org/10.1016/j.ejrh.2017.11.005

Heber Green, W., and Ampt, G. A. (1911). Studies on Soil Physics. *The Journal of Agricultural Science*, *4*(1), 1-24. https://doi.org/DOI: 10.1017/S0021859600001441

Hurni, H. (1985). Erosion-productivity-conservation systems in Ethiopia. *IV International Conference on Soil Conservation November 3-9, 1985 Maracay, Venezuela*, *January 1985*, 654-674.

Jin, X., Jin, Y., Yuan, D., and Mao, X. (2019). Effects of land-use data resolution on hydrologic modeling, a case study in the upper reach of the Heihe River, Northwest China. *Ecological Modelling*, *404*, 61-68. https://doi.org/10.1016/j.ecolmodel.2019.02.011

Jung, B. M., Fernandes, E. H., Möller, O. O., and García-Rodríguez, F. (2020). Estimating suspended sediment concentrations from river discharge data for reconstructing gaps of information of long-term variability studies. *Water (Switzerland)*, *12*(9). https://doi.org/10.3390/W12092382

Kassa, T. (2009). *Watershed hydrological responses to changes in land use and land cover, and management practices at Hare watershed, Ethiopia.* Ph.D. Thesis, University of Siegen, Germany, 229.

Kaul, H. a, and Sopan, I. (2012). Land use land cover classification and change detection using high-resolution temporal satellite data. *Journal of Environment*, *01*(04), 146-152.

Kidane, M., Bezie, A., Kesete, N., and Tolessa, T. (2019). The impact of land use and land cover (LULC) dynamics on soil erosion and sediment yield in Ethiopia. *Heliyon*, *5*(12), 2981. https://doi.org/10.1016/j.heliyon.2019.e02981

Koch, F. J., Van Griensven, A., Uhlenbrook, S., Tekleab, S., and Teferi, E. (2012). The effects of land-use change on hydrological responses in the Choke Mountain Range (Ethiopia) - A new approach addressing land-use dynamics in the model SWAT. *IEMSs 2012-Managing Resources of a Limited Planet: Proceedings of the 6th Biennial Meeting of the International Environmental Modelling and Software Society*, 3022-3029.

Lam, N. S. (1983). Spatial interpolation methods review. *The American Cartographer*, *10*, 129-149.

Lambin, E. F., Geist, H. J., and Lepers, E. (2003). *Dynamics of land use land cover*. https://doi.org/10.1146/annurev.energy.28.050302.105459

Maina, J., Wandiga, S., Gyampoh, B., and Charles, K. K. G. (2020). Assessment of land use and land cover change using gis and remote sensing: A case study of Kieni, Central Kenya. *Journal of Remote Sensing and GIS*, *9*(1), 1-5. https://doi.org/10.35248/2469-4134.20.9.270

Mallupattu, P. K., and Reddy, J. R. (2013). Analysis of land use/land cover changes using remote sensing data and GIS at an urban area, Tirupati, India. *The Scientific World Journal*, *2013*, 1-7. https://doi.org/10.1155/2013/268623

Mao, D., and Cherkauer, K. A. (2009). Impacts of land-use change on hydrologic responses in the Great Lakes region. *Journal of Hydrology*, *374*(1-2), 71-82. https://doi.org/10.1016/j.jhydrol.2009.06.016

Mather, P. (1995). Review of remote sensing and image interpretation (Third Edition). By Thomas M. Lillesand and Ralph W. Keifer. (New York: Wiley, 1994.). *International Journal of Remote Sensing*, *16*(3), 561-563. https://doi.org/10.1080/01431169508954421

Moges, D. M., and Bhat, H. G. (2018). An insight into land use and land cover changes and their impacts in Rib watershed, north-western highland Ethiopia. *Land*

Degradation and Development, *29*(10), 3317-3330. https://doi.org/10.1002/ldr.3091

Monteith, J. L. (1965). Evaporation and environment. *Symposia of the Society for Experimental Biology. 19*, 205-234.

Moriasi, D. N., Arnold, J. G., Van Liew, M. W., Bingner, R. L., Harmel, R. D., and Veith, T. L. (2007). Model evaluation guidelines for systematic quantification of accuracy in watershed simulations. *Transactions of the ASABE*, *50*(3), 885-900.

Morris, G. L., and Fan, J. (1998). *Reservoir sedimentation handbook : design and management of dams, reservoirs, and watersheds for sustainable use*. New York : McGraw-Hill.

MoWIE. (2019). *Environmental Impact Assessment Report for Gidabo Irrigation Project*.

Muttitanon, W., and Tripathi, N. K. (2005). Land use/land cover changes in the coastal zone of Ban Don Bay, Thailand using Landsat 5 TM data. *International Journal of Remote Sensing*, *26*(11), 2311-2323. https://doi.org/10.1080/0143116051233132666

Nadew, B., Chaniyalew, E., and Tsegaye, T. (2019). Runoff sediment yield modeling and development of management intervention scenarios, a case study of Guder watershed, Blue Nile Basin. *Hydrol Current Res*, *9*(4), 1-16. https://doi.org/10.4172/2157-7587.1000306

Nash, J., and Sutcliffe, J. (1970). River flow forecasting through conceptual models part-I: A discussion of principle. *Journal of Hydrology*, *10*, 282-290.

Negese, A. (2021). Impacts of Land Use and Land Cover Change on Soil Erosion and Hydrological Responses in Ethiopia. *Applied and Environmental Soil Science, 2021*, 15-17. https://doi.org/10.1155/2021/6669438

Neitsch, S., Arnold, J., Kiniry, J., and Williams, J. (2011). Soil and water assessment tool theoretical documentation version 2009. In *Texas Water Resources Institute*. https://doi.org/10.1016/j.scitotenv.2015.11.063

Neitsch, S. L., Arnold, J. G., Kiniry, J. R., Srinivasan, R., Williams, J. R., and Haney, E. B. (2012). Soil and water assessment tool theoretical documentation version 2012. *Texas Water Resource Institute TR-439.*, 1-650.

NMA. (2001). Initial national communication of Ethiopia to the united nations framework convention on climate change (UNFCCC). *Handbook of federal countries, 2005*, 136-148.

Oumer, H. A. (2009). *Land Use and Land Cover Change, Drivers and its impact: A comparative study from Kuhar Michael and Lenche Dima of Blue Nile and Awash Basins of Ethiopia.* MSc. Thesis, Cornell University, USA.

Parveen, S., Basheer, J., and Praveen, B. (2018). A literature review on land use land cover changes. *International Journal of Advanced Research*, *6*(7), 1-6. https://doi.org/10.21474/ijar01/7327

Raes, D., Willems, P., and GBaguidi, F. (2006). RAINBOW-A software package for hydro-meteorological frequency analysis and testing the homogeneity of historical data sets. *Proceedings of the 4th International Workshop on 'Sustainable Management of Marginal Drylands'*, 27-31.

Ramankutty, N., Graumlich, L., Achard, F., Alves, D., Chhabra, A., DeFries, R. S., Foley, J. A., Geist, H., Houghton, R. A., Goldewijk, K. K., Lambin, E. F., Millington, A., Rasmussen, K., Reid, R. S., and Turner, B. L. (2006). *Global Land-Cover Change: Recent Progress, Remaining Challenges*, 9-39. https://doi.org/10.1007/3-540-32202-72

Sarkar, A., and Kumar, R. (2012). Artificial neural networks for event-based rainfall-runoff modeling. *Water Resource and Protection*, *4*, 891-897. http://doi.org/10.4236/j warp.2012.410105

SCS. (1972). USDA Soil Conservation Service. In *National Engineering Handbook Section 4 Hydrology*.

Searcy, J. K., and Hardison, C. H. (1960). Double-mass curves. U.S. Geological Survey Water-Supply Paper 1541-B.

Shawul, A. A., Chakma, S., and Melesse, A. M. (2019). The response of water balance components to land cover change based on hydrologic modeling and partial least squares regression (PLSR) analysis in the Upper Awash Basin. *Journal of Hydrology: Regional Studies*, *26*, 100640. https://doi.org/10.1016/j.ejrh.2019.100640

Shirke, Y., Kawitkar, R., and Balan, S. (2012). Artificial neural network-based runoff prediction model for a reservoir. *Engineering Research and Technology*, *1*(3), 1-4.

Tedla, Y. B. (2011). *Estimation of catchment sediment yield using SWAT model: A Case of Gidabo Dam, Rift Valley Basin, Ethiopia*. M.Sc. Thesis, Addis Ababa University, Ethiopia.

Tesema, T. A., and Leta, O. T. (2020). Sediment yield estimation and effect of management options on sediment yield of Kesem Dam watershed, Awash Basin, Ethiopia. *Scientific African*, *9*, e00425. https://doi.org/10.1016/j.sciaf.2020.e00425

Thornes, J. (1990). *Vegetation and erosion : processes and environments*. Chichester, West Sussex, England ; New York, NY, USA : J. Wiley.

Tilahun, A., and Teferie, B. (2015). Accuracy assessment of land use land cover classification using Google Earth. *American Environmental Protection*, *4*(4), 193-198. https://doi.org/10.1 1648/j.ajep.20150404.14

UNESCO. (1976). An international classification and mapping of vegetation, ecology, and conservation. *Cartography*, *9*(3), 195. https://doi.org/10.1080/00690805.1976.10437920

Uniyal, B., Jha, M. K., Verma, A. K., and Anebagilu, P. K. (2020). Identification of critical areas and evaluation of best management practices using SWAT for sustainable watershed management. *Science of the Total Environment*, *744*, 140737. https://doi.org/10.1016/j.scitotenv.2020.140737

Vanlauwe, B., Asten, P. V, and Blomme, G. (2014). Challenges and opportunities for agricultural intensification of the humid highland systems of Sub-Saharan Africa. *Springer International Publishing*.

Vanmaercke, M., Zenebe, A., Poesen, J., Nyssen, J., Verstraeten, G., and Deckers, J. (2010). Sediment dynamics and the role of flash floods in sediment export from medium-sized catchments: A case study from the semi-arid tropical highlands in northern Ethiopia. *Journal of Soils and Sediments*, *10*(4), 611-627. https://doi.org/

10.1007/s11368-010-0203-9

Waidler, D., White, M., Steglich, E., Wang, S., Williams, J., Jones, C. A., and Srinivasan, R. (2011). Conservation practice modeling guide for SWAT and APEX. *Journal of Hydrology*, *50*(1-2), 30-49. http://linkinghub.elsevier.com/retrieve/pii/S0022169410006554%0A

Wang, S., Zhang, Z., McVicar, T. R., Zhang, J., Zhu, J., and Guo, J. (2012). An event-based approach to understanding the hydrological impacts of different land uses in semi-arid catchments. *Journal of Hydrology*, *416-417*, 50-59. https://doi.org/10.1016/j.jhydrol.2011.11.035

Welde, K., and Gebremariam, B. (2017). Effect of land use land cover dynamics on the hydrological response of watershed: A case study of Tekeze Dam watershed, northern Ethiopia. *International Soil and Water Conservation Research*, *5*(1), 1-16. https://doi.org/10.1016/j.iswcr.2017.03.002

Williams, J. (1969). Flood routing with variable travel time or variable storage coefficients. *Transactions of the ASABE*, *12*, 100-103.

Williams, J. (1975). *Sediment-yield prediction with Universal Equation using runoff energy factor*.

Williams, J., and Hann, R. (1972). Hymo, A problem-oriented computer language for building hydrologic models. *Water Resources Research*, *8*(1), 79-86. https://doi.org/10.1029/WR008i001p00079

Wolde, Z., Wei, W., Likessa, D., Omari, R., and Ketema, H. (2021). Understanding the impact of land use and land cover change on water-energy-food nexus in the Gidabo watershed, East African Rift Valley. *Natural Resources Research*. https://doi.org/10.1007/s11053-021-09819-3

Yesuf, H. M., Assen, M., Melesse, A. M., and Alamirew, T. (2015). Detecting land use/land cover changes in the Lake Hayq (Ethiopia) drainage basin, 1957-2007. *Lakes and Reservoirs: Research and Management*, *20*(1), 1-18. https://doi.org/10.1111/lre.12082

Yesuph, A. Y., and Dagnew, A. B. (2019). Land use/cover spatiotemporal dynamics, driving forces, and implications at the Beshillo catchment of the Blue Nile Basin, North Eastern Highlands of Ethiopia. *Environmental Systems Research*, *8*(1). https://doi.org/10.1186/s40068-019-0148-y

Zeleke, G., and Hurni, H. (2001). Implications of land use and land cover dynamics for mountain resource degradation in the Northwestern Ethiopian highlands. *Mountain Research and Development*, *21*(2), 184-191. https://doi.org/10.1659/0276474(2001)021[0184:IOLUAL]2.0.CO;2

Zhang, J., and Ross, M. (2015). Hydrologic modeling impacts of post-mining land-use changes on streamflow of Peace River, Florida. *Chinese Geographical Science*, *25*(6), 728-738. https://doi.org/10.1007/s11769-015-0745-2

APPENDIX

Appendix A

Appendix A.1. Average annual rainfall of stations in the study area

Year	Billate	Dilla	Kebado	Telamo Kentiso	Wonago	Yirgalem
1988	963.40	1537.80	1572.81	1317.55	1735.30	1261.28
1989	951.10	1241.50	1234.00	1062.77	1237.84	1040.81
1990	755.60	1208.10	1364.27	1096.42	1229.42	1012.28
1991	752.47	1212.18	1031.11	1204.44	1244.30	1232.42
1992	1076.26	1376.10	1447.13	1302.82	1560.60	1300.60
1993	796.70	1373.85	1473.10	1971.32	1412.57	2161.40
1994	818.60	1476.50	1622.80	2644.72	1530.50	2969.10
1995	617.20	1342.00	1511.70	1143.92	1436.80	1120.70
1996	1075.80	1709.74	1762.60	1501.13	1943.00	1472.20
1997	849.30	1601.60	1685.70	1404.81	1805.29	1389.96
1998	632.40	1346.90	1404.40	1571.31	1503.90	1658.80
1999	493.89	1181.88	1331.40	1068.12	1404.19	1075.70
2000	616.40	1145.40	1123.20	1064.07	1458.00	1071.76
2001	536.90	1366.10	1576.20	1534.43	2147.46	1573.90
2002	520.60	1101.40	1278.90	1048.14	1793.68	1045.42
2003	851.00	974.00	1150.70	879.41	1394.50	852.50
2004	813.80	1112.10	1146.00	871.68	933.01	853.23
2005	1000.70	1292.35	1275.00	1108.47	1284.38	1100.80
2006	1032.40	1491.00	1603.80	1405.19	1503.74	1412.90
2007	953.30	1660.70	1627.20	1468.85	1645.90	1482.20
2008	787.00	2781.10	1299.00	1138.39	2495.03	1207.30
2009	685.70	1095.40	1196.20	1065.90	1106.87	1066.60
2010	1082.30	1669.70	1654.10	1537.80	1654.62	1189.20
2011	856.94	2370.50	1414.30	1425.60	2174.76	846.10
2012	710.90	1279.32	1288.95	1078.88	1272.77	1181.64
2013	1245.36	1558.64	1240.30	1328.06	1498.66	1148.77
2014	833.80	1509.10	1484.18	1860.16	1516.58	1823.03
2015	674.10	1127.00	893.00	1168.60	1088.86	989.82
2016	682.60	1267.03	869.23	1662.56	1209.19	1308.53
2017	635.10	1417.70	1466.00	1550.71	1449.48	984.50
2018	1220.94	1586.20	1420.98	1506.01	1554.18	772.46

Appendix A.2. Weather generator input files and values

WGN	Jan	Feb	Mar	Apr	May	Jun	Jul	Aug	Sep	Oct	Nov	Dec
TMPMX	29.92	30.11	30.59	28.13	26.87	25.99	25.29	25.85	26.06	26.76	27.97	29.12
TMPMN	10.32	10.51	12.25	13.64	13.53	13.37	13.91	14.03	13.48	13.32	11.79	10.54
TMPSTDMX	1.70	4.28	2.69	2.36	1.80	1.82	1.96	2.32	1.68	2.12	1.64	1.56
TMPSTDMN	3.03	3.48	2.78	2.41	2.33	2.45	2.45	2.40	1.93	2.03	2.42	3.20
PCPMM	30.37	68.18	124.26	194.55	215.55	112.58	99.47	127.76	155.86	197.16	74.82	32.11
PCPSTD	3.23	6.98	8.22	9.32	9.81	7.08	7.11	7.91	7.13	8.90	6.08	3.29
PCPSKW	4.95	3.67	2.64	2.22	2.38	3.00	3.87	3.15	2.09	2.21	4.38	4.90
PR_W1	0.13	0.16	0.31	0.56	0.60	0.42	0.39	0.48	0.57	0.46	0.26	0.13
PR_W2	0.54	0.62	0.61	0.74	0.79	0.62	0.63	0.59	0.77	0.82	0.60	0.53
PCPD	7.03	8.48	13.71	20.42	23.00	15.77	16.00	16.87	21.39	22.42	11.90	6.58
RAINHHMX	3.84	5.00	8.43	11.75	12.04	9.29	8.67	9.51	9.08	10.81	7.24	3.50
SOLARAV	17.88	19.14	17.91	16.63	15.60	13.02	11.47	12.53	14.65	16.09	18.89	18.38
DEWPT	0.56	0.51	0.57	0.72	0.77	0.77	0.78	0.76	0.75	0.76	0.70	0.62
WNDAV	0.78	0.89	0.96	0.74	0.63	0.66	0.71	0.72	0.66	0.59	0.67	0.74

Where TMPMX =Average or mean daily maximum air temperature for month (°C), TMPMN =Average or mean daily minimum air temperature for month (°C).TMPSTDMX =Standard deviation for daily maximum air temperature for month (°C), TMPSTDMN =Standard deviation for daily minimum air temperature for month (°C), PCPMM =Average or mean total monthly precipitation (mm H_2O), PCPSTD =Standard deviation for daily precipitation for month (mm H_2O/day), PCPSKW =Skew coefficient for daily precipitation in month, PR_W1=Probability of a wet day following a dry day in the month, PR_W2=Probability of a wet day following a wet day in the month, PCPD =Average number of days of precipitation in month, SOLARAV =Average daily solar radiation for month (MJ/m^2/day), DEWPT =Average daily dew point temperature in month (°C), and WNDAV =Average daily wind speed in month (m/s).

Appendix A.3. LULC classification accuracy assessment

i. 1990 LULC

LULC Class	Agricultural	Bare Land	Built-up	Forest Land	Shrubland	Water Body	Total	User Accuracy (%)
Agricultural	30	2	0	0	2	0	34	88.24
Bare Land	1	18	1	0	0	0	20	90.00
Built-up	1	2	20	0	0	0	23	86.96
Forest Land	1	0	0	32	2	0	35	91.43
Shrubland	3	1	0	0	43	0	47	91.49
Water Body	0	0	0	1	0	20	21	95.24
Total	36	23	21	33	47	20	180	
Producer Accuracy (%)	83.33	78.26	95.24	96.97	91.49	100		
Overall Classification Accuracy = 90.56%								
Overall Kappa Statistics = 0.88								

ii. 2005 LULC

LULC Class	Agricultural Land	Bare Land	Built-Up	Forest Land	Shrubland	Water Body	Total	User Accuracy (%)
Agricultural	33	2	0	0	2	0	37	89.19
Bare Land	1	17	2	0	0	0	20	85.00
Built-Up	0	2	21	0	0	0	23	91.30
Forest Land	1	0	0	27	4	0	32	84.38
Shrubland	3	0	0	2	43	0	48	89.58
Water Body	0	0	0	1	0	19	20	95.00
Total	38	21	23	30	49	19	180	
Producer Accuracy (%)	86.84	80.95	91.30	90.00	87.76	100.00		
Overall Classification Accuracy = 88.89%								
Overall Kappa Statistics = 0.86								

Appendix A.4. Parameters used in a streamflow sensitivity analysis

Name	Min	Max	Description
CN2	35	98	SCS runoff curve number for moisture condition II
GW_DELAY	0	500	Groundwater delay.
ALPHA_BF	0	1	Baseflow alpha factor.
GWQMN	0	5000	Threshold depth of water in the shallow aquifer required for return flow to occur
GW_REVAP	0.02	0.2	Groundwater "revap" coefficient.
REVAPMN	0	1000	Threshold depth of water in the shallow aquifer for "revap" to occur
RCHRG_DP	0	1	Deep aquifer percolation fraction.
HRU_SLP	0	0.6	Average slope steepness.
CANMX	0	100	Maximum canopy storage.
ESCO	0	1	Soil evaporation compensation factor.
EPCO	0	1	Plant uptake compensation factor.
SURLAG	0	24	Surface runoff lag time in the HRU
SOL_K	0	2000	Saturated hydraulic conductivity.
SOL_Z	0	3500	Depth from soil surface to bottom of layer.
SOL_AWC	0	1	Available water capacity of the soil layer.
SLSUBBSN	10	150	Average slope length.
OV_N	0.01	10	Manning's "n" value for overland flow.
SLSOIL	0	150	Slope length for lateral subsurface flow.
CH_K2	-0.01	500	Effective hydraulic conductivity in main channel alluvium.
BIOMIX	0	1	Biological mixing efficiency

Appendix A.5. Parameters used in sediment yield sensitivity analysis

Name	Min	Max	Description
USLE_P	0	1	USLE equation support practice
SLSUBBSN	10	150	Average slope length.
HRU_SLP	0	0.6	Average slope steepness.
LAT_SED	0	5000	Sediment concentration in lateral flow and groundwater flow.
RSDIN	0	10000	Initial residue cover (kg/ha).
SPCON	0.0001	0.01	Linear parameter for calculating the maximum amount of sediment that can be retrained during channel sediment routing.
SPEXP	1	1.5	Exponent parameter for calculating sediment retrained in channel sediment routing.
USLE_K	0	0.65	USLE equation soil erodibility (K) factor.
CH_COV1	-0.05	0.6	Channel erodibility factor.
CH_COV2	-0.001	1	Channel cover factor.

Appendix A.6. Monthly average basin water balance value

LULC	1990					2005				2019			
Month	RF (mm)	SURQ (mm)	LATQ (mm)	ET (mm)	WY (mm)	SURQ (mm)	LATQ (mm)	ET (mm)	WY (mm)	SURQ (mm)	LATQ (mm)	ET (mm)	WY (mm)
Jan	49.65	5.23	3.52	22.83	28.62	5.83	3.34	23.16	29.05	6.50	3.36	22.36	29.69
Feb	60.04	7.05	3.93	28.83	24.16	7.65	3.76	28.93	24.57	8.62	3.75	27.82	25.60
Mar	104.46	5.91	5.72	55.17	27.64	6.65	5.55	54.89	28.27	8.27	5.42	53.18	29.80
Apr	186.81	16.75	10.73	71.13	49.90	18.04	10.41	71.15	51.31	21.58	10.12	70.20	54.82
May	195.74	20.02	15.73	74.70	81.64	21.34	15.40	74.67	83.11	24.88	14.87	73.76	85.93
Jun	106.82	8.37	11.77	54.16	78.24	9.12	11.56	54.15	78.70	10.85	11.15	53.82	79.10
Jul	105.10	8.21	8.49	51.36	68.08	9.05	8.27	51.14	68.37	10.80	8.06	50.69	68.84
Aug	126.09	11.19	8.88	52.98	64.17	12.27	8.55	52.32	64.64	14.38	8.42	51.21	65.73
Sep	159.34	13.95	10.61	61.11	69.29	15.29	10.21	59.90	70.28	18.00	10.00	58.08	72.28
Oct	171.51	19.16	14.85	68.19	93.83	20.68	14.39	66.71	95.42	23.58	14.00	64.37	97.62
Nov	54.16	3.65	8.43	60.15	70.83	4.09	8.24	58.47	71.37	5.04	7.96	55.04	71.48
Dec	45.93	4.70	4.44	43.04	46.76	5.33	4.29	42.03	47.41	5.99	4.21	39.01	47.66

Appendix B

Appendix B.1. Double mass curve

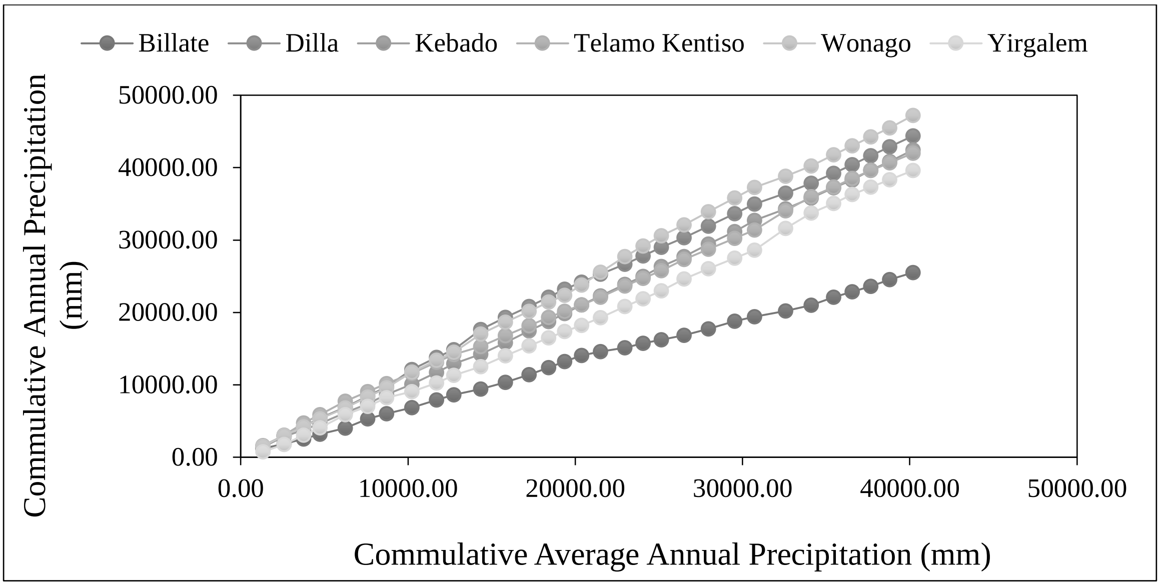

Appendix B.2. Homogeneity test plot

i. Billate

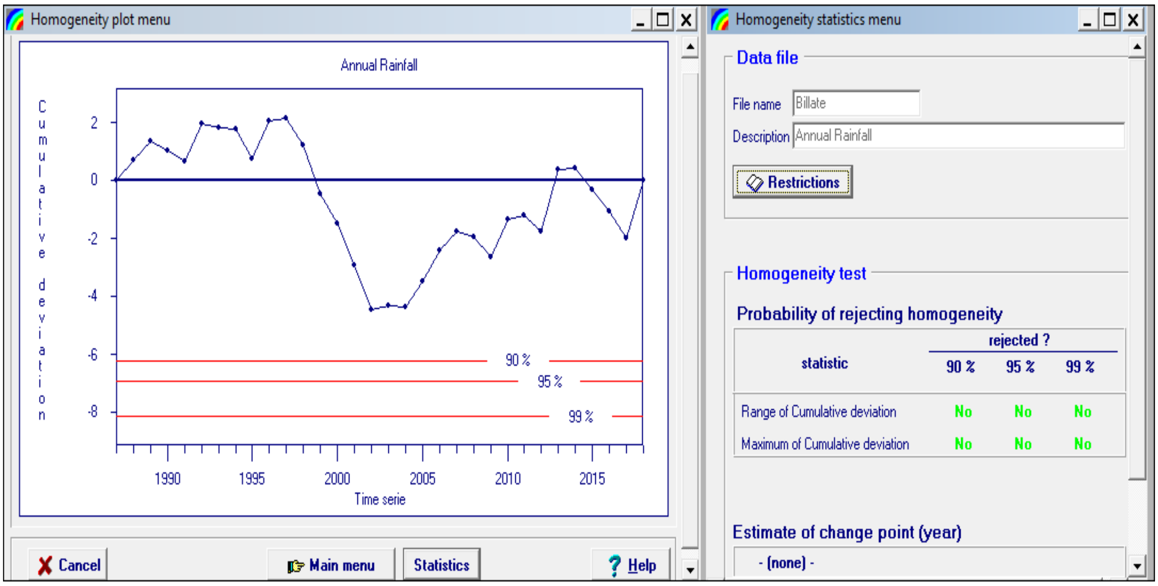

ii. Dilla

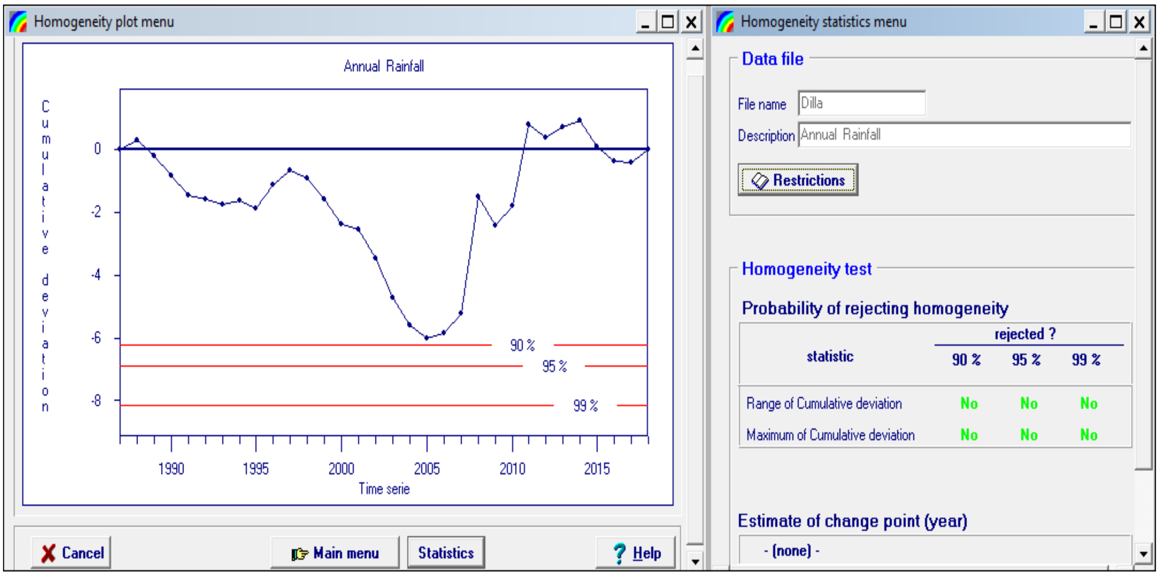

iii. Kebado

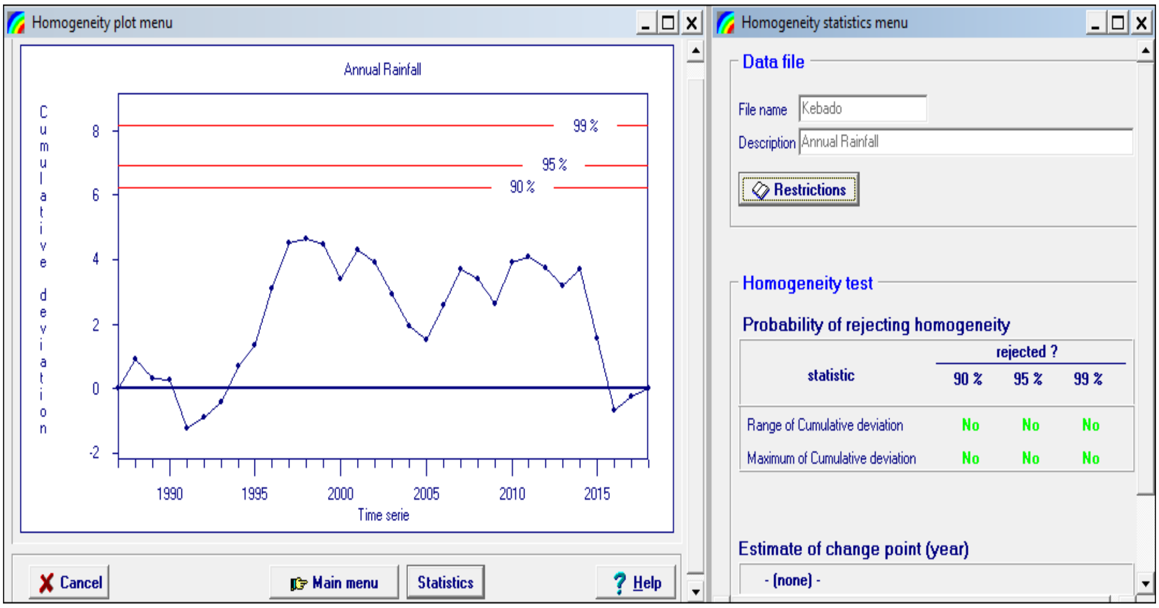

iv. Telamo Kentiso

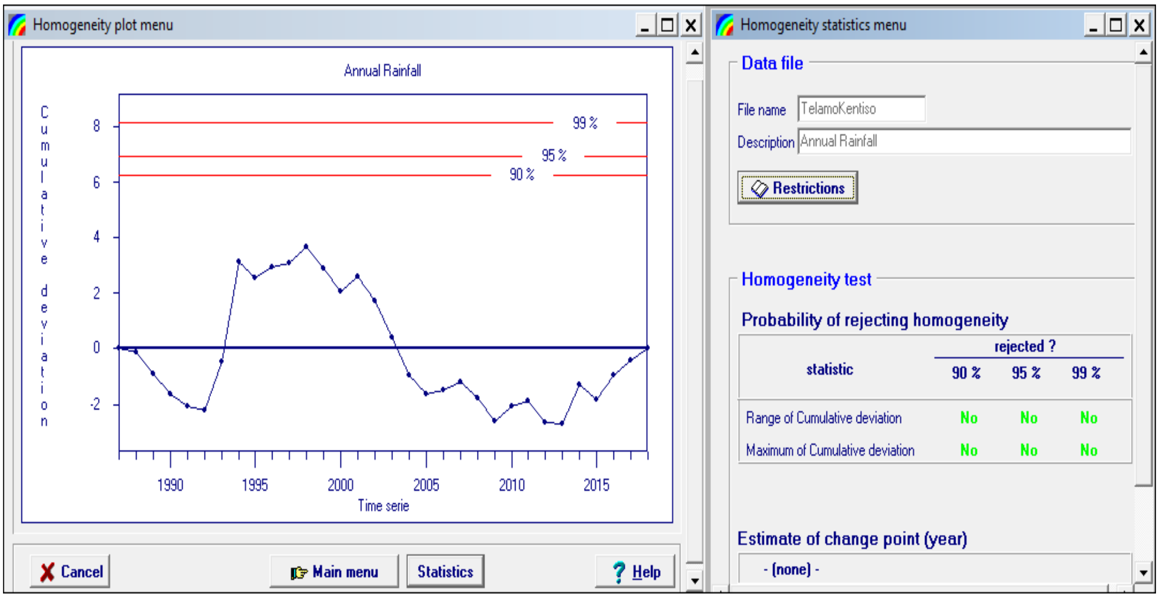

v. Wonago

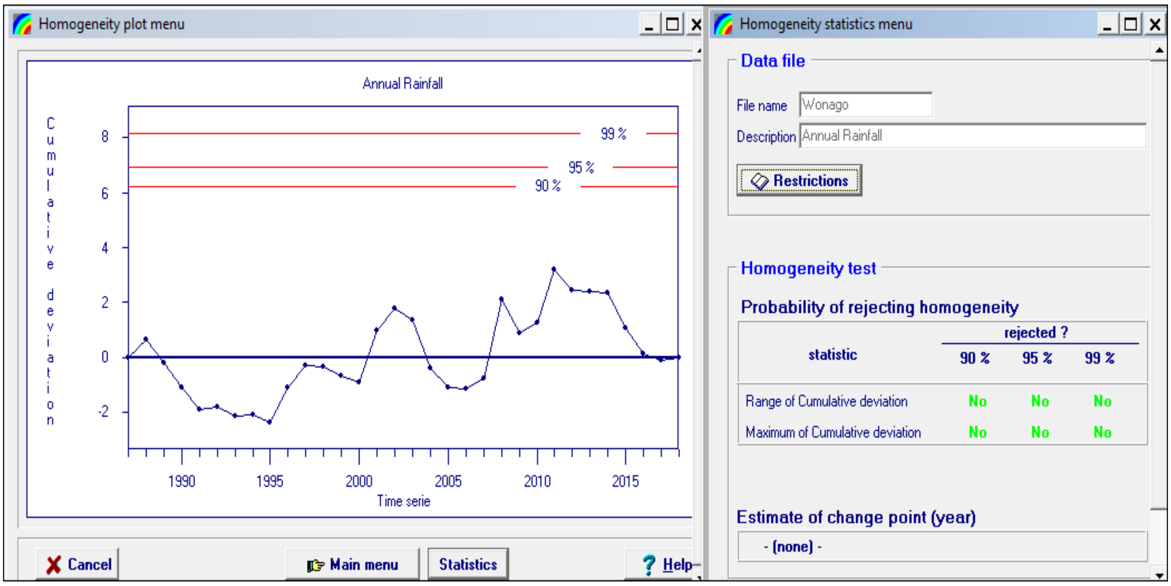

vi. Yirgalem

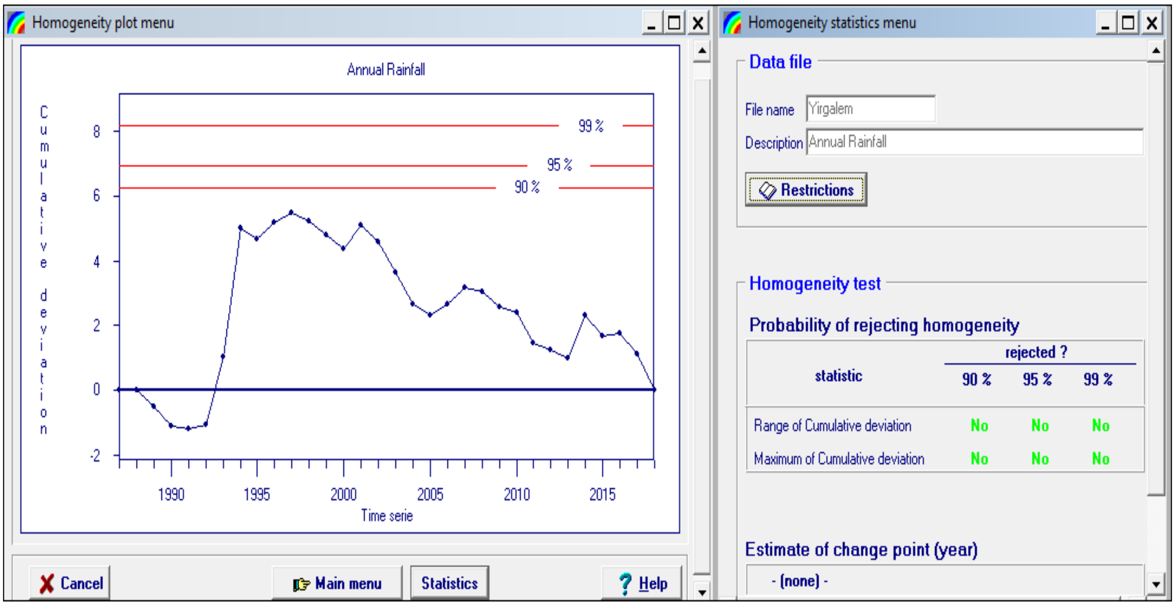

Appendix B.3. Streamflow calibration 95PPU plot

i. Aposto

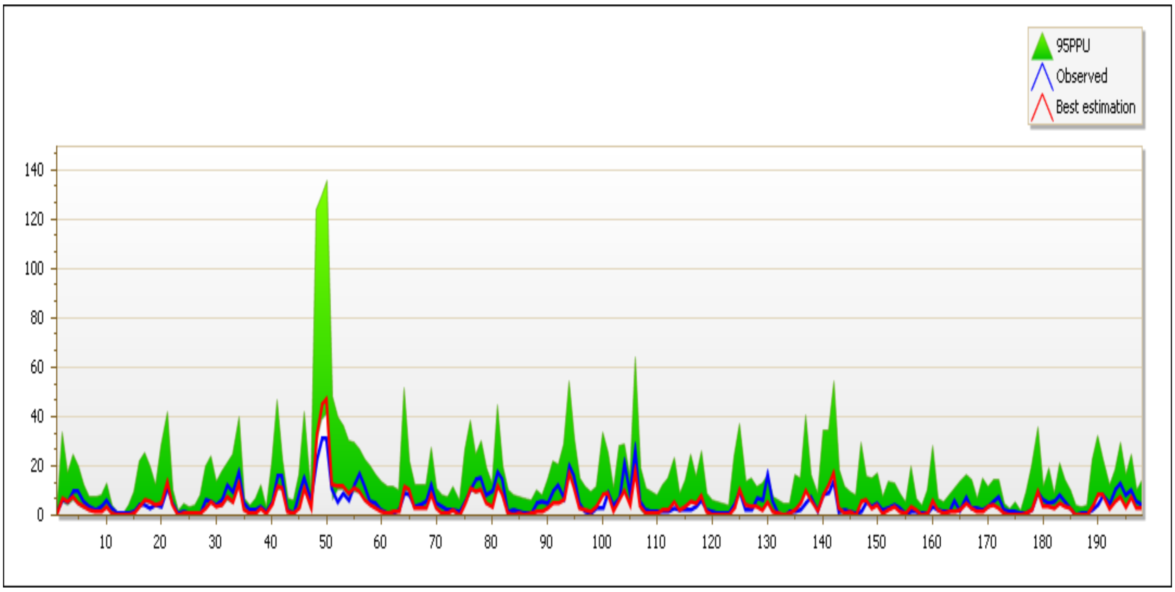

ii. Bedessa

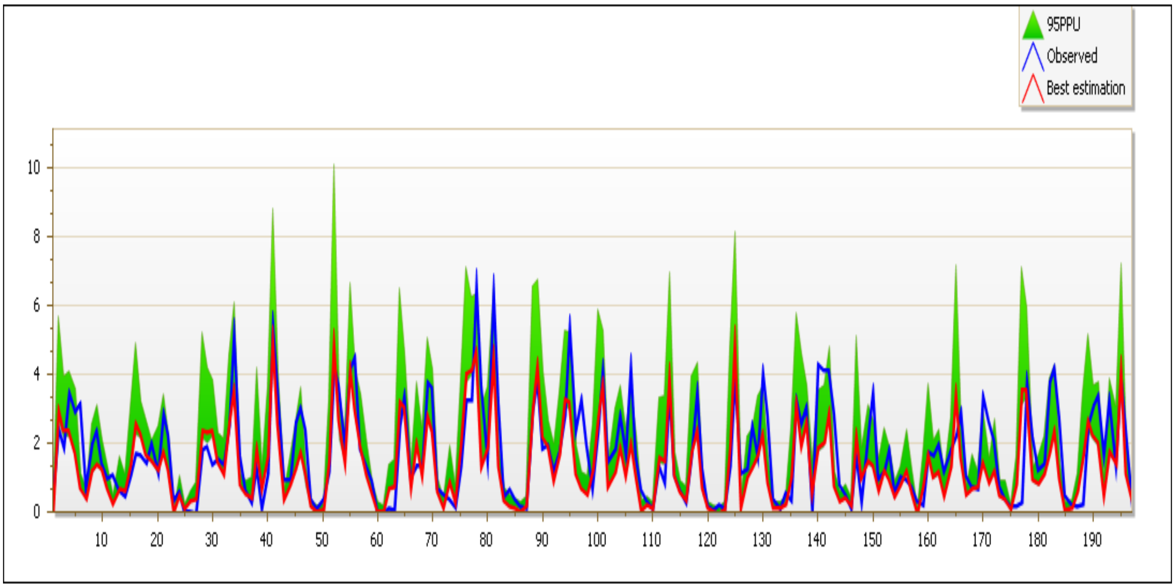

iii. Measso (near dam outlet)

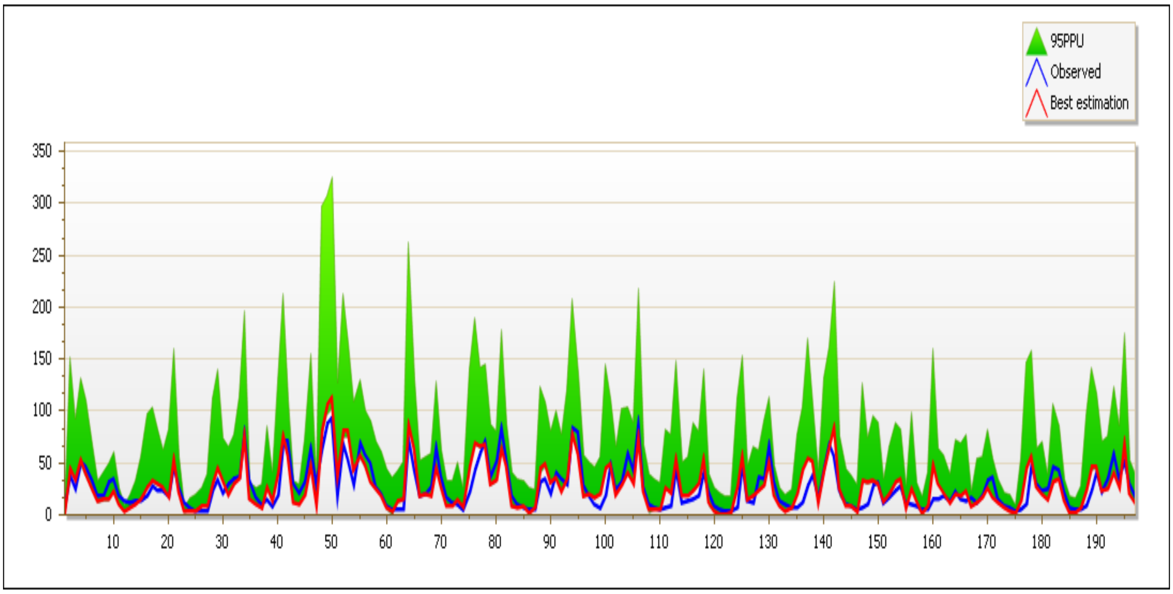

Appendix B.4. Streamflow validation 95PPU plot

i. Bedessa

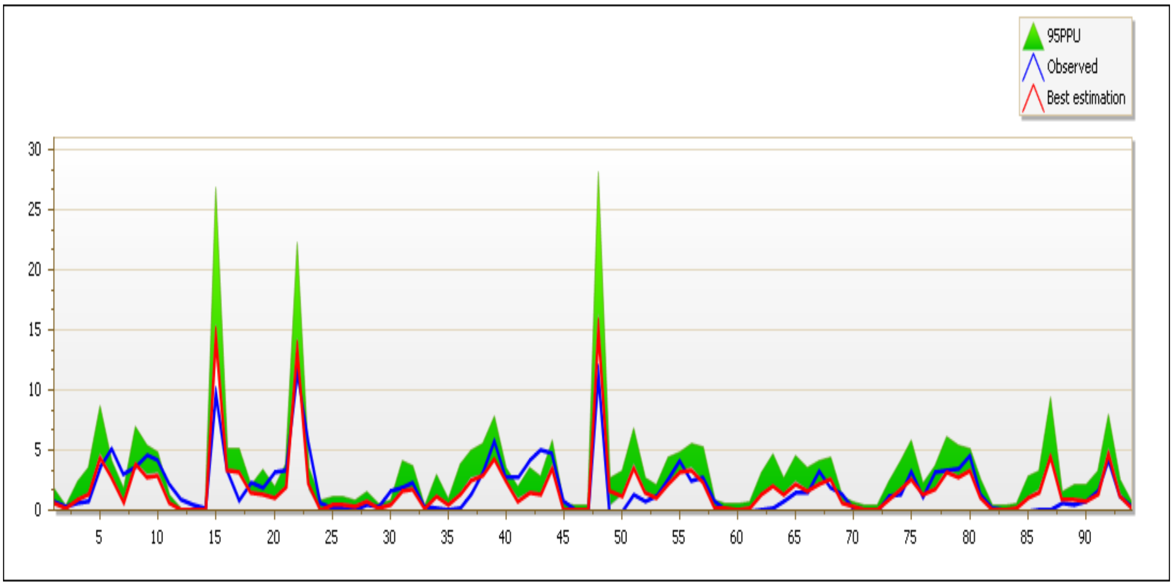

Appendix B.5. Sediment yield calibration 95PPU plot

i. Measso (near dam outlet)

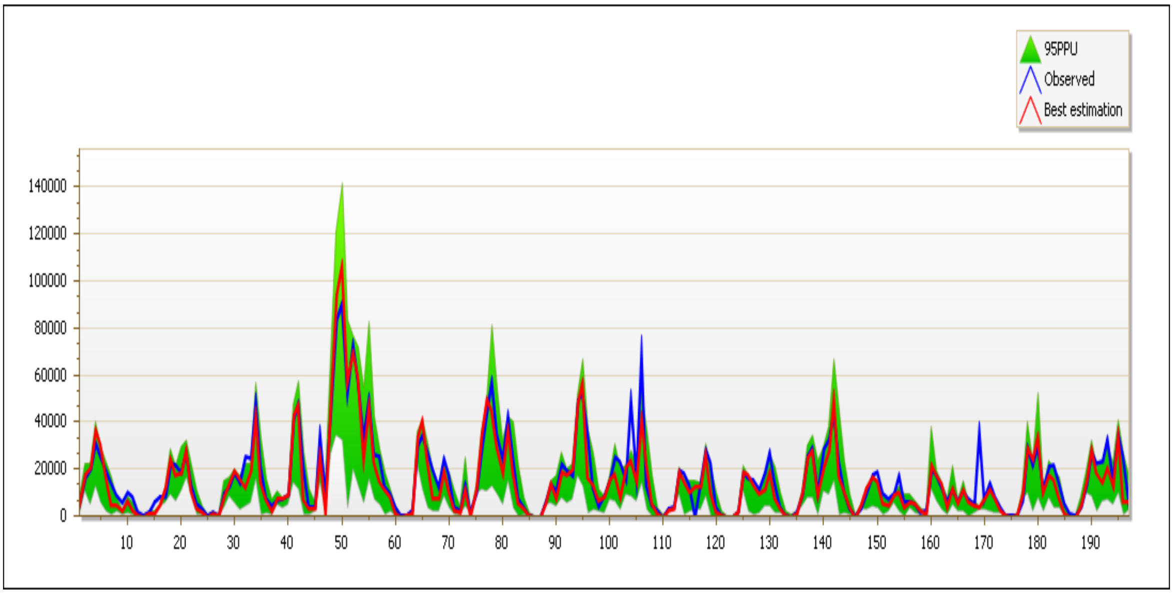

Appendix B.6. Sediment yield validation 95PPU plot

i. Aposto

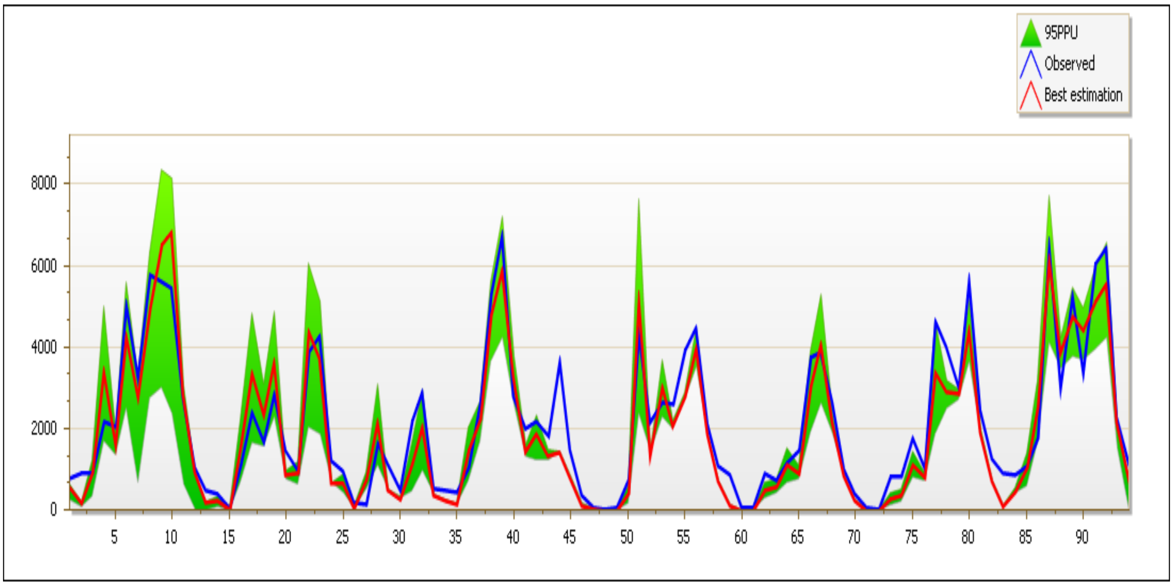

ii. Measso (near dam outlet)